Investigating relationships between thromboembolic risk and left atrial structure, function, and flow characteristics as assessed with advanced magnetic resonance techniques

Dr Marco Spartera, MD

St Peter's College
Division of Cardiovascular Medicine
Radcliffe Department of Medicine
Oxford Centre for Clinical Magnetic Resonance Research
University of Oxford



Thesis submitted for the degree Doctor of Philosophy in Medical Sciences at the University of Oxford

Trinity Term 2021

Declaration

The work in this thesis is my own. Dr Antonio Stracquadanio (AS), Dr Guilherme Pessao-Amorim (GPA), and Dr. Victoria Young (VY) contributed to blinded data analysis. Dr Aaron T Hess (ATH) coded the Matlab-based in-house software used for post-processing analyses (MATLAB R2015 8.6.0.267246; Mathworks, Nattick, USA, published at https://doi.org/10.5287/bodleian:ey4ovzdbB). Research nurses Mrs Rachel Teal and Mrs Lauren Quinn screened stroke patient in the Stroke Unit at the John Radcliffe Hospital. Radiographers Mrs Alison Fletcher (AF) and Mr Peter Manley (PM) contributed to scanning a subset of research participants in my presence.

Abstract

Atrial fibrillation (AF) is associated with alterations in left atrial (LA) blood flow characteristics which, in turn, increase the risk of LA thrombus formation and, consequently, of cardioembolic stroke. Anticoagulation is highly effective in preventing ischaemic stroke in patients with AF and stroke risk factors. More recently, it has been suggested that a cardioembolic aetiology may also underlie a proportion of ischaemic strokes that occur in sinus rhythm (SR) in the context of an atrial myopathic process caused by increased exposure to clinical risk factors, before the onset of AF. To date, it is still unclear whether LA myopathy is linked to increased embolic stroke risk and whether this association is causally determined.

I used advanced cardiovascular magnetic resonance (CMR) methods to investigate the relationship between LA characteristics and ischaemic stroke risk beyond AF, as well as the relative effect of AF and clinical stroke risk factors on LA function and flow characteristics.

First, I developed an application for measuring left atrial (LA) four-dimensional (4D; i.e. on the *x, y, z* axes over time) involving a MATLAB-based software and post-processing protocols. Reproducibility of LA flow characteristics derived by using this novel application was then assessed in volunteers and in patients with stroke risk factors. LA 4D Flow parameters have an overall good reproducibility and acceptable temporal variability with same-day scan-rescan coefficients of variation (CVs) of 6% for peak velocity, 5% for mean velocity, 7% for vorticity, 9% for vortex volume, and

10% for stasis. From this work, LA peak velocity and vorticity emerged as the parameters with the best technical and inter/intra-observer reproducibility and the least temporal variability.

Next, LA flow characteristics were assessed in 37 patients with persistent AF before and after cardioversion and compared to those of patients in SR with a similar (moderate) stroke risk (N=35) and those obtained in low-risk controls in SR (N=23). Restoration of SR after cardioversion led to improvement in LV systolic function and in all LA 4D flow parameters. In the presence of SR, there were no differences in LA flow characteristics between groups with similar stroke risk, regardless of the history of AF; both, however, were similarly impaired when compared to low-risk controls. From this work, I demonstrated for the first time that patients at moderate stroke risk in SR display altered LA flow characteristics in association with an LA dysfunction and reduced LV diastolic function, regardless of a history of AF.

Finally, in 134 patients with median (Q1-Q3) CHA_2DS_2VASc of 3 (2-4), LA vorticity was significantly and independently associated with prevalent embolic brain infarcts defined as large non-cortical or cortical brain infarcts. LA vorticity, a measure of the rotational tendency of LA flow, is linked to shear stress, the reduction of which leads to biomechanical platelet activation. By contrast, the presence of embolic brain infarct was not associated with other LA parameters, such as LA volume, function, and flow velocities. After adjusting for age, rhythm during CMR, history of AF, and CHA_2DS_2VASc, a SD reduction in LA vorticity remained associated with a 2-fold higher risk of embolic brain infarcts. These results remained statistically significant in the subgroup of patients in SR without a diagnosis of AF (N=66, $P<0.05$) and after

adjusting for LV/LA structural and functional parameters. Notably, neither LA vorticity nor any other LA flow parameter was associated with lacunar (non-embolic) brain infarcts.

Taken together, these findings indicate that LA flow parameters have a potential for refining stroke risk stratification, and thus the selection of patients who would benefit from anticoagulation. Further studies in large prospective cohorts are now needed to assess whether LA 4D flow parameters predict incident cardioembolic events, and whether prescription of anti-thrombotic therapy based on a risk scores including these parameters would lead to a cost-effective improvement in patient management.

List of Publications, Prizes, and Awards

Manuscripts during D. Phil. studies

1. **M Spartera**, G Pessoa-Amorim, A Stracquadanio, A Von Ende, A Fletcher, P Manley, S Neubauer, V M Ferreira, B Casadei, AT Hess & RS Wijesurendra. Left Atrial 4D Flow MRI: Reproducibility and Temporal Variability. Left atrial 4D flow cardiovascular magnetic resonance: a reproducibility study in sinus rhythm and atrial fibrillation. *Journal of Cardiovascular Magnetic Resonance* 23, 29 (2021).

2. **M Spartera**, G Pessoa-Amorim, A Stracquadanio, G Harston, S Mazzucco, V Young, J Kennedy, A Von Ende, A Fletcher, P Manley, S Neubauer, V M Ferreira, AT Hess, B Casadei & RS Wijesurendra. Reduced Left Atrial Rotational Blood Flow Is Independently Associated with Embolic Brain Infarct: A Potential Novel Mechanism of Cardioembolic Risk in Sinus Rhythm.
   Finalist Early Career Award (Translational) at *SCMR conference* 2021.
   Manuscript in preparation.

3. **M Spartera**, G Pessoa-Amorim, A Stracquadanio, A Von Ende, A Fletcher, P Manley, S Neubauer, V M Ferreira, AT Hess, RS Wijesurendra & B Casadei. Impact of Atrial Fibrillation and Stroke Risk Factors on Left Atrial Blood Flow Characteristics. Abstract presented at *ESC Congress 2020*.
   Manuscript in preparation.

4. **M Spartera**. New Valves, Old Diagnostic Problems - Time to embrace novel approaches? *International Journal of Cardiology* 2018 Jun 7. Invited

Editorial.

5. Raman B, Ariga R, **Spartera M**, Sivalokanathan S, Chan K, Dass S, Petersen SE, Daniels MJ, Francis J, Smillie R, Lewandowski AJ, Ohuma EO, Rodgers C, Kramer CM, Mahmod M, Watkins H, Neubauer S. Progression of myocardial fibrosis in hypertrophic cardiomyopathy: Mechanisms and clinical implications. *Eur Heart J Cardiovasc Imaging*. 2018 Oct 24.

Faculty presentations during D. Phil.

1. ECMO: when to start weaning based on echocardiography. "Euroecho", Vienna 2019 (Invited faculty presentation)

2. Thinking Outside the Heart - a Sobering Case of Heart Failure. "ESC congress", Paris 2019 (faculty presentation)

3. Flushing out the diagnosis in rapidly progressing tricuspid regurgitation. "ESC congress", Munich 2018 (faculty presentation)

4. Cardiac Amyloidosis: more than a Zebra sign. "Cardiology for Non-Clinician Scientists and Allied Healthcare Professionals" (Oxford, UK), 25th August 2017. (Invited faculty presentation)

Prizes and Awards During D. Phil.

2021 Early Career Award finalist (translational) - *Society for Cardiovascular Magnetic Resonance (SCMR)* 2021

2019	£ 22,500 Pump Priming funding for LOSE-AF trial (co-applicant) by Oxford BHF Centre of Research Excellence
2019	£ 300 from the St Peter's College Foundation Graduate Award
2018	£ 150 from the St Peter's College Foundation Graduate Award
2017	€ 20,000 research scholarship of Italian Society of Cardiology for 4D Flow research
2017	Best poster presentation- European Society of Cardiology (ESC) 2017

Table of Contents

Declaration ..... ***ii***

Abstract ..... ***iii***

List of Publications, Prizes, and Awards ..... ***vi***

Table of Contents ..... ***ix***

List of Figures and Tables ..... ***xiii***

Abbreviations ..... ***xv***

Chapter 1 ..... ***1***

Introduction ***1***

1.1 Overview & rationale for study design 1

1.2 Aims 4

1.3 Clinical implications 5

1.4 Embolic stroke 6

1.4.1 Aetiologic classification and advent of ESUS construct 9

1.5 Prevention of embolic stroke 11

1.5.1 Atrial Fibrillation 11

1.5.2 PFO and large vessel atherosclerosis 14

1.5.3 ESUS 16

1.5.4 Anticoagulation for patients in sinus rhythm 17

1.6 Imaging biomarkers and mechanisms of cardioembolic stroke 19

1.7 Overview of Thesis 35

Chapter 2 ..... ***36***

Methods and Technical Development ***36***

2.1 Ethical Considerations 36

2.2 Study Participants 36

2.3 Consent process and ethical considerations 37

2.4 Research Assessment 38

2.5 Data Blinding for Analysis 39

2.6 CMR Protocol 40

2.6.1 Cine imaging 41
2.6.2 Left Atrial 4D Flow 47

Chapter 3 53

Left atrial 4D flow MRI: a reproducibility study in sinus rhythm and atrial fibrillation 53

3.1 Abstract 53
3.1.1 Background 53
3.1.2 Methods 53
3.1.3 Results 54
3.1.4 Conclusions 54
3.2 Introduction 55
3.3 Methods 57
3.3.1 Design 57
3.3.2 CMR imaging protocol 58
3.3.3 LA 4D Flow processing 61
3.3.4 Blinding 63
3.3.5 Statistical analysis 64
3.4 Results 66
3.4.1 Reproducibility and temporal variability in the whole cohort 72
3.4.2 Assessment of sources of variability in LA flow characteristics 81
3.5 Discussion 88
3.5.1 Reproducibility and temporal variability 88
3.5.2 Suitability for potential clinical application 90
3.5.3 Limitations 92
3.6 Conclusion 95

Chapter 4 96

Impact of Atrial Fibrillation and Stroke Risk Factors on Left Atrial Blood Flow Characteristics 96

4.1 Abstract 96
4.1.1 Background 96
4.1.2 Methods 96
4.1.3 Results 97
4.1.4 Conclusions 97
4.2 Introduction 98
4.3 Methods 99

4.3.1 Study design 99
4.3.2 Recruitment of the study population 100
4.3.3 Cardiovascular magnetic resonance 100
4.3.4 Power Calculation and Statistical Analysis 101
4.4 Results 102
4.4.1 CMR findings at the baseline scan 106
4.4.2 Effects of cardioversion in individuals with persistent AF 110
4.4.3 Comparison between groups in SR 118
4.5 Discussion 126
4.5.1 LA flow characteristics and predisposition to thrombus formation 129
4.5.2 Limitations 130
4.6 Conclusion 130

Chapter 5 131

Reduced left atrial rotational blood flow is independently associated with embolic brain infarct: a potential novel mechanism of cardioembolic risk in sinus rhythm 131

5.1 Abstract 131
5.1.1 Background 131
5.1.2 Methods 131
5.1.3 Results 132
5.1.4 Conclusions 132
5.2 Introduction 133
5.3 Methods 134
5.3.1 Design 134
5.3.2 Patient Population 135
5.3.3 CMR protocol 136
5.3.4 Brain MRI protocol 138
5.3.5 Sample Size Determination 140
5.3.6 Statistical Analysis 141
5.4 Results 142
5.4.1 Clinical characteristics 142
5.4.2 Brain and cardiac magnetic resonance 143
5.4.3 Predictors of embolic brain infarcts 150
5.5 Discussion 157

5.5.1 Pro-thrombotic LA flow pattern and pathophysiologic rationale for novel therapeutic targets 158
5.5.2 CMR imaging parameters as biomarkers of stroke risk in SR 160
5.5.3 Limitations 162
5.6 Conclusions 163
Chapter 6 164
General conclusions 164
Bibliography 166

List of Figures and Tables

Figure 1. Schema of Left Atrium (LA)-related mechanisms of thromboembolic risk. 2
Figure 2. Gaps in knowledge identified from the schema of the mechanisms of Left Atrium (LA)-related mechanisms of thrombo-embolic risk presented in Figure 1. 3
Figure 3. Pathophysiologic classification of ischemic stroke. 7
Table 1: Association between cardiac Imaging biomarkers and stroke. 20
Figure 4. Relationship between LA size and incident stroke. 22
Figure 5. Outcome of participants stratified according to tertiles of total left atrial emptying fraction. 24
Figure 6. Left Atrial 4D Flow parameters in Atrial Fibrillation. 32
Figure 7 Representative cases of Left Atrial vortex patterns. 34
Figure 8 : Representative myocardial contours in a patient during CMR. 43
Figure 9 Strain and strain rate profile for the left ventricle (LV) and left atrium (LA). 45
Figure 10: Representative cases of left atrial 4D Flow in study participants with sinus rhythm and atrial fibrillation. 50
Table 2: 4D Flow protocols used in the reproducibility study. 59
Table 3: Baseline clinical characteristics. 67
Figure 11: Comparison in LA flow characteristics in SR and AF at baseline. 69
Table 4: Baseline LA flow characteristics 70
Figure 12: Variability assessment of LA 4D Flow parameters. 72
Table 5. Reproducibility in the whole cohort 73
Table 6. Inter-rater Correlation Coefficient (ICC). 75
Figure 13: Intra- and Inter-observer Bland-Altman plots. 77
Figure 14: Rescan and Interval-scan Bland-Altman plots. 78
Table 7. Reproducibility and temporal variability of flow patterns 80
Table 8. Coefficient of Variations for rescan and interval-scan variability by rhythm at the time of the scan. 82
Table 9. Coefficient of Variations for interval-scan variability by heart rate paired changes between baseline and interval-scan. 84
Table 10. Coefficient of Variations for interval-scan variability by blood pressure paired changes between baseline and interval-scan. 85

Table 11. Inter-correlation among LA flow parameters stratified by rhythm 87
Table 12. Scan-rescan coefficient of variation for left atrial 4D Flow parameters according to each CMR protocol..... 94
Table 13: Baseline characteristics of the study groups. 103
Table 14 – Medications at the time of baseline scan. 105
Table 15 – Baseline CMR characteristics 107
Figure 15: LA flow characteristics at baseline. 109
Table 16 – Clinical risk in AF patients (Group 1) who recovered SR (AF-SR) or remained in AF (AF-AF) at follow-up and in SR controls (Group 2). 111
Table 17 – CMR characteristics and medications in Group 1 patients who were successfully cardioverted at follow-up (AF-SR) versus those who remained in AF (AF-AF)..... 112
Table 18 – Characteristics and CMR data in Group 1 patients who reverted to SR (AF-SR) and those who were still in AF (AF-AF) at follow-up 115
Figure 16: LV and LA CMR parameters in patients with persistent AF before and after cardioversion. 116
Figure 17: LA flow patterns assessed with pathlines. 117
Figure 18: LV and LA parameters in the 3 groups in SR. 119
Table 19 – Haemodynamics and CMR parameters for all Groups in SR 120
Table 20 – Correlation coefficients between LA flow and structural/functional parameters in the whole population in SR at the time of the scan. 122
Figure 19: Relationships between LA emptying fraction, LV diastolic function, and LA flow. 123
Table 21 – Relationships between LA emptying fraction, LV diastolic function, and LA flow after adjustment for covariates in SR groups 125
Figure 20: LA 4D flow characteristics in SR and AF. 128
Figure 21: Left atrial 4D Flow CMR and embolic brain infarcts. 137
Table 22. Clinical and CMR characteristics by brain MRI outcome 144
Table 23. Medication use at the time of the scan stratified by brain outcome 145
Table 24: Brain imaging characteristics by brain outcomes 146
Table 25: Brain imaging vascular territory distribution 147
Table 26. CMR characteristics by brain MRI outcome 149
Table 27. Predictors of LNCCIs in the whole population 151
Figure 22: Relationship between Left Atrial (LA) vorticity and embolic brain infarcts. 153
Figure 23: Relationship between Left Atrial (LA) vorticity and embolic brain infarcts in subgroups.. 154
Figure 24: Percentage of embolic brain infarcts for LA vorticity tertiles. 155
Table 28. Relationship between CMR parameters and Small Non-Cortical Infarcts 156

Abbreviations

4D FLOW	= four-dimensional flow
AF	= atrial fibrillation
ACA	= anterior cerebral artery
ANOVA	= analysis of variance
BA	= Bland-Altman
BMI	= body mass index
BPM	= beats per minute
CEA	= carotid endarterectomy
CI	= confidence interval
CMR	= cardiovascular magnetic resonance
CO	= cardiac output
CT	= computed tomography
CV	= within-subject coefficient of variation
DAPT	= dual antiplatelet therapy
DBP	= diastolic blood pressure

DCCV = direct current cardioversion

DWI = diffusion-weighted imaging

ECG = electrocardiogram

EDV = end-diastolic volume

EF = ejection/emptying fraction

ESUS = embolic stroke of undetermined sources

ESV = end-systolic volume

FLAIR = fluid-attenuated inversion recovery

FOV = field of view

HLA = horizontal long axis

GLSR-E = left ventricular early diastolic strain rate

GRAPPA = generalised auto calibrating partially parallel acquisition

HR = heart rate

ICC = inter-rater correlation coefficient

Q1-3 = first-third quartiles

LA = left atrium/atrial

LAEF = left atrial emptying fraction

LAA = left atrial appendage

LAAO = left atrial appendage occlusion

LGE = late gadolinium enhancement

LLPV = left lower pulmonary vein

LUPV = left upper pulmonary vein

LV = left ventricle/ventricular

LVH = left ventricular hypertrophy

MCA = middle cerebral artery

NOAC = non-vitamin K oral anticoagulants

OR = odds ratio

ORA = oxford university research archive

PA-TDI = P-wave to A′ duration on tissue doppler imaging

PCA = posterior cerebral artery

PFO = patent foramen ovalis

REC = research ethics committee

RLPV = right lower pulmonary vein

RUPV = right upper pulmonary vein

SBP = systolic blood pressure

SD = standard deviation

SD-TTP = standard deviation of the time to peak strain

SEC = spontaneous echocardiographic contrast

SR = sinus rhythm

SSFP = steady-state free precession

T = tesla

TOAST = Trial of ORG 10172 in Acute Stroke Treatment

TOE = trans-oesophageal echocardiography

TE = echo time

TIA = transient ischaemic attack

TR = repetition time

VLA = vertical long axis

Chapter 1

Introduction

1.1 Overview & rationale for study design

Atrial fibrillation (AF), the most common sustained arrhythmia[1, 2], is strongly associated with stroke[3, 4] and premature death[5]. The vast majority (>80%) of strokes are ischaemic rather than haemorrhagic[6]. AF is the presumed cause of about 15-25% of all ischaemic strokes[7, 8], and has also been indicated as a possible cause of a proportion of ischaemic strokes of undetermined cause, due to subsequent demonstration of asymptomatic (silent) AF with prolonged cardiac monitoring in such cases[9].

Data from multiple large observational cohorts[10] support the association between AF and stroke. The fact that oral anticoagulation consistently reduces stroke risk in AF patients in randomized controlled trials[1, 11-14] also suggests a direct causal relationship. Nevertheless, the precise mechanisms of stroke in the context of AF may be less straightforward than traditionally thought[15]. Several emerging strands of evidence support the hypothesis that the link between AF and ischaemic stroke is not entirely explained by the rhythm abnormality, and could instead reflect the presence of an underlying abnormal atrial substrate in patients with AF, potentially regardless of rhythm[15] (**Figure 1**). In fact, whilst patients with

subclinical AF detected by implanted cardiac devices have an increased risk of ischaemic stroke[16], only a small minority (~15%) of patients experienced an AF episode in the 30-day period prior to the presumed embolic stroke[17]. Additionally, one would theoretically expect that if AF causes stroke, rhythm control strategies aiming at reducing the number of AF episodes would translate to reduced stroke risk. On the contrary, a number of large randomized clinical trials have failed to show any meaningful reduction in stroke risk with a rhythm-control strategy compared to rate-control, despite the former strategy resulting in a significant reduction in AF recurrence[18, 19]. Recent data from CMR studies have also highlighted that signs of atrial myopathy such as reduced total LA emptying fraction (LAEF) and increased LA fibrosis (as assessed with late gadolinium enhancement) are associated with incident ischemic cardiovascular events regardless of AF[20, 21].

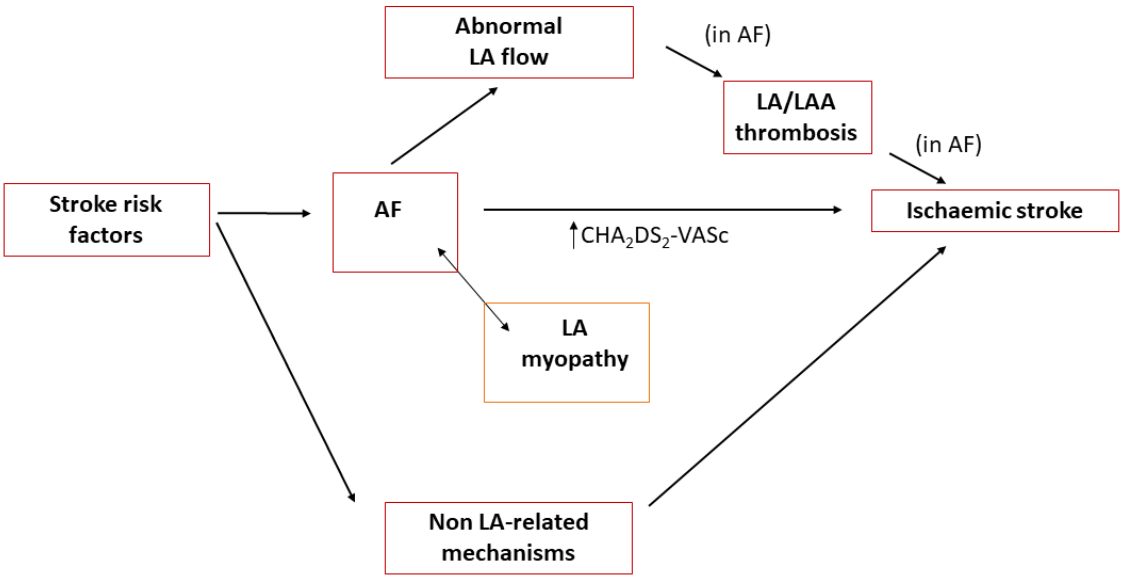


Figure 1. Schema of Left Atrium (LA)-related mechanisms of thromboembolic risk. *Left Atrium (LA); Left atrial appendage (LAA); Atrial Fibrillation (AF). This schema was modified from Kamel et al[15].*

To date, the potential mechanisms behind the association between LA myopathy and increased stroke risk remain unclear (**Figure 2**). For instance, LA remodelling could be a marker of extra-cardiac stroke risk factors, such as large-artery atherosclerosis[22] or small vessel disease[23], as suggested by the association between LA dysfunction and lacunar brain infarcts[23]. Altered LA features may also be a consequence of subclinical episodes of paroxysmal AF, with only the latter responsible for the increased stroke risk[24]. Alternatively, a cardiomyopathic process, brought about by ageing and exposure to cardiovascular risk factors, may lead to both cardiac dysfunction and adverse LA flow characteristics in the absence of AF[25], as suggested by the findings that anticoagulation reduces ischaemic stroke in high-risk patients in SR[26, 27].

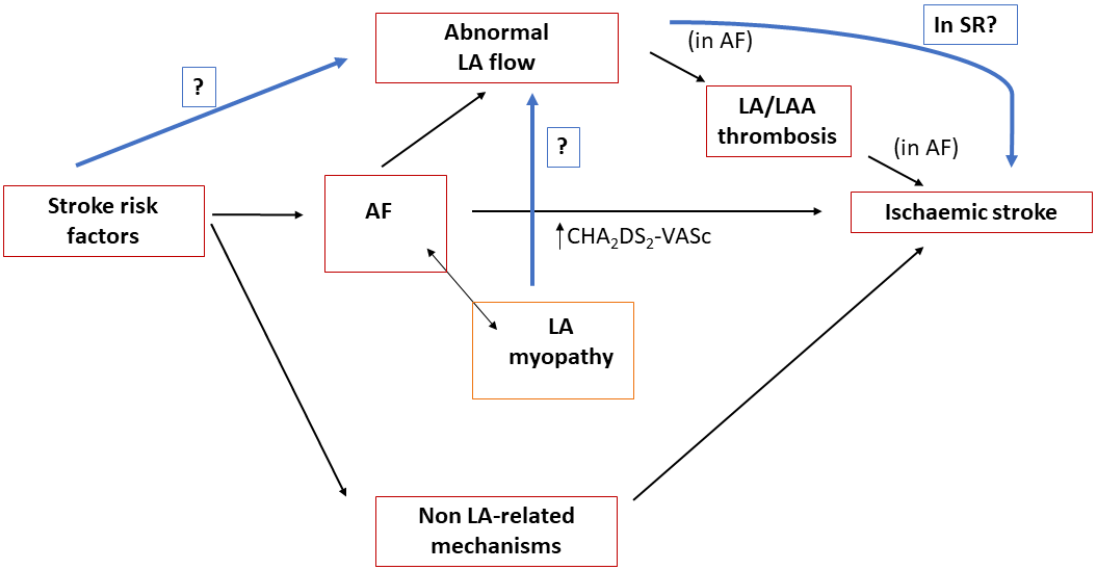


Figure 2. Gaps in knowledge identified from the schema of the mechanisms of Left Atrium (LA)-related mechanisms of thrombo-embolic risk presented in Figure 1. *Left Atrium (LA); Left atrial appendage (LAA); Atrial Fibrillation (AF).*

To date, there are no studies systematically investigating whether stroke risk factors and LA dysfunction are associated with abnormal LA blood flow characteristics regardless of AF. Further, it is unclear whether LA flow parameters are associated with brain infarcts in patients in SR regardless of a diagnosis of AF (**Figure 2**).

The main limitation to perform such studies has traditionally been the relatively complex LA three-dimensional anatomy with difficulties for standard imaging techniques to comprehensively evaluate the overall LA flow profile[28]. Recently, a proof of principle study by Markl et al.[28] showed, for the first time, that it is possible to quantitatively assess blood flow velocities within the LA by the use of 4D Flow CMR, although the in-house post-processing software and protocol used have not been made publicly available and no data on the reproducibility of LA 4D Flow parameters was present in the literature.

1.2 Aims

The work included in this thesis aims to (1) develop and make publicly available post-processing protocols for the application of 4D Flow CMR to the LA;(2) assess the reproducibility and temporal variability of LA 4D Flow parameters in patients and healthy volunteers (3) assess the effect of restoration of SR in AF patients, as well as the effects of clinical stroke risk factors on cardiac parameters (4) evaluate the association between LA 4D Flow parameters and brain infarct.

1.3 Clinical implications

My results may have important clinical implications. Although AF is strongly associated with stroke risk, the annual rate of incident stroke varies widely from very low (<1%) to high (>15%) in different subgroups[29]. Therefore, refining stroke risk stratification is a major goal in current clinical practice. To date, CHA_2DS_2-VASc score[29, 30] is the main clinical score used for risk stratification. It is a scoring system which relies almost exclusively on upstream clinical risk factors by apportion of one point each for congestive heart failure (C), hypertension (H), age ≥65 (A), age ≥75 (a further point, i.e. A2), diabetes (D), prior thromboembolic disease (S2, two points), vascular disease (VA), and female sex category (Sc). Although originally developed to stratify the stroke risk of patients with non-valvular AF[15, 31], higher scores are also linked to higher risk of incident ischaemic stroke in SR[30]. Furthermore, although many studies have confirmed that CHA_2DS_2-VASc is independently associated with stroke risk not only in populations at high cardiovascular risk (i.e. with heart failure[32] or coronary artery disease[33]), but also in the general population without AF[34], the CHA_2DS_2-VASc score has modest predictive power for the end-point of ischemic stroke, with C statistics ranging between 0.6 and 0.7[31, 32].

Incorporation of imaging biomarkers of risk, directly measuring pathophysiologically relevant embolic mechanisms, may improve our risk predictive capacity thus allowing better targeting of preventive treatment[35].

The majority of the remainder of this introductory Chapter introduces the concept of embolic stroke and currently available preventive strategies, and it

reviews prior research studies investigating potential mechanisms of cardioembolic risk using different imaging modalities.

1.4 **Embolic stroke**

Stroke is a major health condition with an incidence of at least 100,000 per year[36] in the United Kingdom, and a 30-day mortality of approximately 23%[37]. Of those who survive a stroke, approximately 50% suffer from disability[38], and around 1 in 4 will experience another stroke (i.e. recurrence) within five years[36]. Alongside its serious clinical impact, stroke represents an enormous economic burden for society and national healthcare systems, resulting in total estimated costs of around £7bn per year in England alone[39].

In older adults, there are mainly three ischemic stroke subtypes where an aetiologic mechanism can be identified: atherothrombotic stroke, small vessel disease, and cardioembolic stroke[40]. About 25% of ischaemic strokes is attributed to large vessel atherosclerosis, ~25% to small vessel disease (lacunar strokes), and ~20% to cardioembolic sources (**Figure 3**)[41]. In up to one third of strokes, it is not possible to clearly identify a cause, and thus they are defined as cryptogenic[42]. Finally, other stroke subtypes (e.g. arterial dissection, vasospasm, vasculitis, etc.) are more rare (~5%)[41] and usually more relevant in early adulthood[43].

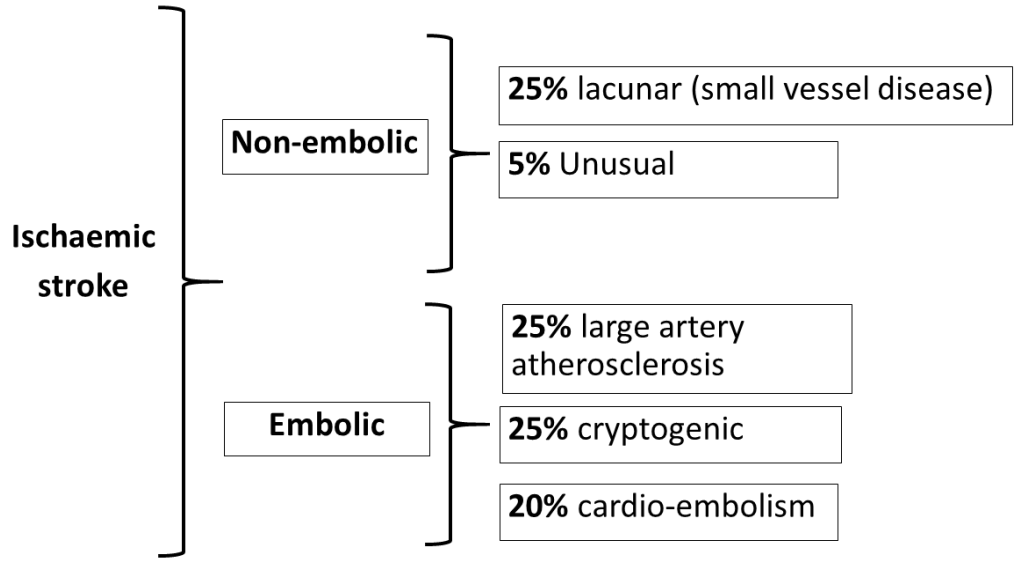


Figure 3. Pathophysiologic classification of ischemic stroke. *Pathophysiologic mechanisms of ischaemic stroke with breakdown figures per subtypes in North American and European studies. Modified from Hart et al.[41] & Ntaios et al.[44]*

Overall, the majority of ischaemic strokes are due to embolism, so called 'embolic strokes' (**Figure 3**)[44]. The vast majority of embolic strokes are due to thrombosis-related embolism with air/fat embolisms being considered more rare mechanisms[45, 46].

One embolic mechanism involves clots originating from any of the brain-supplying arteries, namely the aortic arch, intracranial and extracranial carotid, vertebrobasilar arteries (so called 'arteriogenic' embolism) either because of atherosclerotic plaques, or because of dissected cervical arteries[44]. Another major source of embolic strokes are the cardiac chambers usually as a result of thrombus formed in the context of LV dysfunction, LV non-compaction cardiomyopathy, AF and other atrial arrhythmias, valvular disease, paroxysmal embolus from pervious foramen ovalis (PFO), or due to non-thrombotic mechanisms such as from septic

vegetations, myxoma, papillary fibroelastoma, sarcoma, and other cardiac tumors[44]. Pragmatically, in the clinical practice, the following sources of embolic strokes are usually the subject of targeted investigations aiming to include or exclude such mechanisms[47]:

a) Cardioembolic[47]: AF and sustained atrial flutter, PFO (particularly relevant in early adulthood), severe LV dysfunction with LV Ejection Fraction (EF) <30%, recent myocardial infarct (<4 weeks), valvular vegetations and infective endocarditis, cardiac tumours (e.g. atrial myxoma, fibroelastoma, etc.), prosthetic cardiac valve, mitral stenosis, intra-cardiac thrombus.
b) Non-cardioembolic[47]: extracranial or intracranial atherosclerosis causing ≥50% luminal stenosis in arteries supplying the area of ischaemia.

Atherothrombotic sources are common[48] and culprit atherosclerotic plaques are usually found in large arterial vessels such as those forming the circle of Willis, the internal carotid and the vertebral arteries[49], which are at risk of thrombus formation and subsequent embolization to downstream brain vessels[43]. This is pathophysiologically distinct from the non-embolic lacunar strokes due to small vessel disease, a condition characterised by hypertension-related damage of the arterial wall occurring in the distribution territory of the small calibre vessels of the brain (e.g. the brainstem and the basal nuclei) with evidence of thickening of the media, micro-aneurisms and rupture, and ischemic lacunar lesions[43]. A detailed overview of the cardioembolic mechanisms involved is given in paragraph 1.5.

Currently, ischaemic strokes are classified into different subtypes according to aetiologic classifications, which generally rely on diagnostic tests and clinical history/examination to identify major sources of stroke[50]. This is particularly important for secondary prevention, as clinical management may change according to the cause of an ischemic stroke. For instance, the presence of a significant extracranial carotid stenosis supplying the territory of brain infarct prompts revascularisation, whereas evidence of AF-related LA thrombus prompts anticoagulation[51]. The most widely-used classification, Trial of ORG 10172 in Acute Stroke Treatment (TOAST)[52, 53], was first developed to improve standardization in multicentre randomized clinical trials, and has subsequently been used in various other types of research (e.g. genetic, epidemiologic, risk factors studies, etc.)[54]. According to the TOAST classification, strokes can be classified into 1) large-artery atherosclerosis, 2) cardio-embolism, 3) small-vessel occlusion, 4) stroke of other determined aetiology, and 5) stroke of undetermined aetiology[52, 53]. Such classification depends on the clinical interpretation of the patient's neurological examination, brain imaging, standard ECG monitoring, echocardiography, and ultrasound of extra- and intra-cranial arteries. Accordingly, cardioembolic strokes account for around 20-25% of all ischaemic strokes[55] and AF is the most important contributing factor[4, 7, 8, 56].

1.4.1 Aetiologic classification and advent of ESUS construct

Although the TOAST classification carries a value for the standardisation of patients' risk and prognostication[57], causal relationships are not straightforward to

demonstrate[54]. Traditionally, about one third of all strokes cannot be allocated to any specific category after diagnostic testing (i.e. cryptogenic strokes)[55]. However, the fact that the 'cryptogenic' aetiological entity also includes multiple possible stroke aetiologies or incomplete diagnostic work-up, prompted further work towards creating a positively defined aetiological construct. Hence, in 2014, the new construct of Embolic Stroke of Undetermined Sources (ESUS) was generated, defined as a subset of cryptogenic strokes which displays an estimated prevalence of 17%[41]. ESUS is effectively a subset of cryptogenic strokes[41]. A total of 300,000 incident cases annually in North America and Europe are defined as ESUS: a non-lacunar brain infarct without occlusive atherosclerosis or cardioembolic sources[41].

The criteria for diagnosis of ESUS[41] are therefore: (1) the detection of a brain infarct with embolic features at brain imaging (i.e. brain infarct that is 'large non-cortical or cortical'); (2) absence of atherosclerosis causing ≥50% luminal stenosis in arteries supplying the area of brain infarct; (3) absence of major-risk cardioembolic source of embolism; (4) absence of other specific rarer cause of stroke identified (e.g. arteritis, dissection, migraine/vasospasm, drug misuse).

Notably, the brain imaging criterion of '*large non-cortical or cortical infarcts*' (LNCCI) is paramount for the diagnosis of ESUS. LNCCI are in fact more likely to be embolic in origin[41, 58] and are associated with worse neurological symptoms[58] and cognitive decline[59]; by contrast, smaller non-cortical lesions are more likely to be vascular in origin[60]. Lacunar infarcts, age-related and hypertension-related manifestation of small vessel disease and cerebral amyloid angiopathy[61], are defined neuroradiologically[47] as a subcortical infarct smaller than or equal to 1.5 cm

on brain imaging (≤2.0 cm on MRI diffusion-weighted images) in its largest dimension and in the distribution of the small penetrating cerebral arteries. Brain imaging can be by computed tomography (CT) or MRI; however, CT usually needs delayed imaging (i.e. greater than 24–48 h after stroke onset) for evaluation of brain infarcts[47]. Therefore, LNCCI is a neuroimaging construct[41, 59, 60, 62] which can result from a number of heterogenous mechanisms such as cardiac embolism (e.g. AF, LV disease, PFO) or atherosclerotic plaques affecting large vessels[63].

Proposed diagnostic assessment for ESUS[47] include brain imaging (CT or MRI), 12-lead ECG, echocardiography, cardiac monitoring for ≥24 h, imaging of both the extra- and intracranial arteries supplying the area of the brain infarct (catheter, MR, or CT angiography, or cervical duplex plus transcranial doppler ultrasonography). The fact that, after a full diagnostic evaluation, ~17% (and up to 20-25%) of LNCCI still remain of undetermined cause, suggests that some pathophysiologic mechanisms of embolic stroke are currently still unknown. Importantly, these unknown mechanisms may overlap with currently recognized mechanisms whilst a potential embolic source should not be automatically presumed as exclusive[44, 63].

1.5 Prevention of embolic stroke

1.5.1 Atrial Fibrillation

Oral anticoagulation (OAC) is recommended in all AF patients with CHA_2DS_2-VASc score ≥2 in men and ≥3 in women[64] irrespective of the clinical pattern or burden of AF (i.e. paroxysmal, persistent, permanent, first detected)[64]. Further, in

AF patients at risk of stroke, it is recommended to continue OAC long-term even after successful rhythm control management[64]. Such international guidelines are based on several randomized control trials in patients with AF showing the efficacy of anti-thrombotic treatment in preventing stroke risk. A meta-analysis[65] of 29 trials including 28,044 participants (mean age of 71 years with a mean follow-up for events of 1.5 years), showed that adjusted-dose warfarin (6 trials, 2900 participants) and antiplatelet agents (8 trials, 4876 participants) reduced stroke by 64% (95% CI, 49% to 74%) and 22% (CI, 6% to 35%), respectively. Notably, in 12 trials, N=3003 AF patients with previous stroke or TIA who were assigned to placebo had an average stroke rate of 13% per year whereas in primary prevention trials the stroke rate was 4.1% per year[65]. Although there was a modest effect of antiplatelet agents on stroke risk, adjusted-dose warfarin therapy was substantially more efficacious (relative risk reduction, 39% [CI, 22% to 52%] in 12 trials, 12 963 participants)[65].

Bleeding risk is relevant[66] when continuing long term OAC, thus ability to discriminate risk is vital. In fact, of 54 321 AF patients (median age of 73 years; 56% male; mean CHA_2DS_2-VASc score of 2.9) on oral anticoagulation (either rivaroxaban, dabigatran, apixaban, or warfarin), a total of 2418 patients (4.5%) experienced a major bleeding event over all available follow-up[66]. Non-vitamin K oral anticoagulants (NOAC) are similar or superior to warfarin in terms of efficacy with a safer bleeding risk profile[12-14].

The observation that the majority of the intracardiac thrombus formation generally occurs within the left atrial appendage (LAA), particularly in non-

rheumatic heart disease[67, 68], generated the rationale for testing LAA occluders devices (LAAO) as a potential preventive treatment to reduce stroke risk. The WATCHMAN LAAO device was tested in two randomized trials, the PROTECT-AF and the PREVAIL trials[69]. The first trial, PROTECT-AF, demonstrated that the efficacy of percutaneous closure of the LAA was non-inferior to that of warfarin therapy, but there was a higher rate of periprocedural complications raising concerns about safety[70]. Following on several concerns raised by the U.S. Food and Drug Administration regarding patient selection criteria (e.g., 33% of included patients had a $CHADS_2$ score of 1) and acute safety events, a second trial was recommended[69] leading to the PREVAIL (Prospective Randomized Evaluation of the Watchman LAA Closure Device in Patients with Atrial Fibrillation Versus Long Term Warfarin Therapy) trial. The combined 5-year outcomes of the PREVAIL and PROTECT AF trials, demonstrate that LAAO with Watchman plus anti-platelet provide a stroke prevention in nonvalvular atrial fibrillation that is comparable to warfarin, with additional reductions in major bleeding, particularly haemorrhagic stroke, and mortality[69]. Notably, the LAAO led to effective prevention of haemorrhagic stroke despite a trend towards a higher incidence of ischaemic stroke in the device group (as a result of peri-procedural events)[69]. In these trials, anti-thrombotic therapy with LAAO was managed as follows: a) warfarin with a goal international normalized ratio between 2.0 to 3.0 and aspirin (81 mg) for 45 days after the procedure; b) following transoesophageal echocardiography demonstrating adequate LAA closure (no peri-device leak > 5mm width), warfarin was discontinued, and clopidogrel (75 mg) and aspirin (81 to 325 mg) were instituted for 6 months; and finally, c) clopidogrel was discontinued and aspirin

(325 mg) was continued indefinitely. Overall, international guidelines give a Class IIb recommendation for implantation of LAAO devices for patients with AF and contraindications for long-term OAC (e.g. intracranial bleeds).

1.5.2 PFO and large vessel atherosclerosis

When a PFO is found, this has implications in terms of preventive strategies. Three randomized, open-label trials tested PFO closure combined with antiplatelet therapy versus antiplatelet therapy alone: Gore REDUCE, CLOSE, RESPECT trials[71-73]. These trials showed a consistent benefit for PFO closure over medical therapy alone thus providing solid clinical data to support PFO closure in practice for young and middle-aged patients with a PFO who have had a cryptogenic ischemic stroke[71-73]. Notably, in this selected subgroup of patients (median age ~45 years, with minimal clinically evident atherosclerotic disease), during a median follow-up of 3-5 years, clinical ischaemic stroke were reduced to 0-1.4% of the patients in the PFO closure group whilst in the antiplatelet-only group 5.4-5.9% of the patients experienced a recurrent stroke[72, 73]. This protective effect of PFO closure was noted in spite of a higher rate of AF in the PFO closure group than in the antiplatelet-only group: 4.6-6.6% vs. <1%[72, 73]. Patients in the PFO closure group were treated with one 300-mg dose of clopidogrel before or immediately after the procedure, if not already on clopidogrel, followed by 75 mg daily for 3 days, and then resumed or started the chosen antiplatelet therapy option (with % similar to control arm)[72]. The underlying mechanism of stroke in patients with PFO is presumed to be paradoxical embolism of a clot from deep veins and anticoagulation might be also an effective

treatment option to antiplatelet drugs and PFO. There is currently no clinical trial testing PFO closure versus anticoagulation. Notably, older trials[74-76] of PFO closure versus medical therapy had failed to demonstrate effectiveness of PFO closure; this may be attributed to the fact that the medical therapy group included anticoagulation as alternative option to anti-platelets as well as discontinuation of antithrombotic therapy was permitted after PFO closure[74-76]. In these negative older trials, analyses of subgroups provided crucial insight to design the new Gore REDUCE, CLOSE, RESPECT trials[71-73]. In fact, it was postulated that PFO closure may have provided a greater benefit in patients with a substantial (grade 3) right-to-left shunt and an atrial septal aneurysm, and that PFO closure may be superior to antiplatelet therapy rather than anticoagulation[74].

In stroke patients with significant carotid vessel atherosclerosis ipsilateral to the brain infarct, carotid endarterectomy (CEA) is recommended as the best treatment option to prevent recurrences of stroke. In fact, it has been shown in randomized controlled trials of secondary prevention that patients with stenosis of more than 50% benefit from CEA as compared to medical therapy and that patients with severe stenosis (≥70 percent) had a durable benefit from endarterectomy at eight years of follow-up[77-79]. Patients with a stroke who had stenosis of 70 to 99 % in the symptomatic carotid artery, had a life-table estimates of the cumulative risk of any ipsilateral stroke at 2 years of 26% on medical therapy and 9% in the CEA patients[77-79]. Further, among patients with moderate stenosis (50 to 69 percent), the 5-year rate of any ipsilateral stroke (failure rate) was 15.7% among patients treated surgically and 22.2% percent among those treated medically[77-79]. Finally,

among patients with less than 50 percent stenosis, there was no significant difference between patients treated with endarterectomy (14.9%) versus those in the medically treated group (18.7%, P=0.16)[77-79]. More recent evidence from primary prevention randomized trials showed that non-symptomatic patients with at least 60% stenosis, had reduced long-term (10 years) risk of incident stroke (occurring in 13.4% of patients, 10.8% without peri-operative strokes) than patients treated medically (17.9%)[80]. Medical therapy involved mainly aspirin and ~11% used anticoagulant. Notably, the effect of CEA was only on ischaemic strokes that were not classified as cardioembolic. Further, CEA also reduced contralateral stroke which may be explained through mechanisms involving the circle of Willis[80].

1.5.3 ESUS

The fact that emboli are mainly made of thrombotic material, prompted the rationale to design randomised trials testing whether OAC are more effective than anti-platelets for secondary prevention of embolic strokes of undetermined source[41]. Despite a strong rationale, rivaroxaban[81] and dabigatran[82] showed no superiority to aspirin with regard to the prevention of recurrent stroke after an initial embolic stroke of undetermined source with an annualized rate of recurrence of ~5% in both intervention and control groups.

Pre-specified analysis of subgroups revealed that Rivaroxaban was associated with a reduced risk of recurrent stroke among patients with ESUS and moderate or severe LA enlargement (diameter >4.6 cm)[27], although this constituted only ~5% of the population.

Research assessing the role of carotid disease in ESUS showed that of the 4644 ESUS patients (38.1% women), a carotid plaque was much more often found ipsilaterally to the qualifying ischemic stroke (estimated as ~5% of the whole cohort imaged) than contralaterally (estimated as <2% of the whole cohort), supporting a possible aetiological role for non-stenotic carotid disease in ESUS albeit in a small proportion of patients[83]. Further, ESUS patients with evidence of carotid atherosclerosis did not behave differently from those without carotid disease in terms of prevention of recurrent stroke between those allocated to rivaroxaban and those allocated to aspirin although aspirin was safer, consistent with the overall trial results[83].

Finally, pooled data set derived from 3 prospective stroke registries[22] revealed that of the 800 patients with ESUS, the 3 most prevalent potential embolic sources were left ventricular disease, arterial disease, and atrial cardiopathy with a major overlap among them. This has been proposed as a reason to design randomized controlled trials of combination of anticoagulation and aspirin for the prevention of stroke recurrence in patients with ESUS[22].

1.5.4 Anticoagulation for patients in sinus rhythm

In the COMPASS trial, in patients with stable cardiovascular disease in SR at the time of recruitment, low-dose rivaroxaban in combination with aspirin was associated with large, significant reductions in ischaemic strokes with a sub analysis showing a reduction in cardioembolic strokes and embolic strokes of undetermined source[84]. Unfortunately, this trial did not investigate systematically the

prevalence/incidence of AF with long-term ECG monitoring in the trial population, thus it is not possible to tease out the mechanisms behind the beneficial effects of rivaroxaban.

Further research exploring the pathophysiological mechanisms of stroke is much needed in order to (a) generate relevant imaging and blood biomarkers to improve risk stratification and (b) identify new therapeutic targets for primary and secondary prevention[85]. An appealing hypothesis is that the additional beneficial effects in SR patients observed in the COMPASS trial may come from tackling embolic strokes arising from cardiac thrombi, and possibly from a diseased LA chamber. Recent studies have demonstrated that markers of atrial cardiopathy such as natriuretic peptides might be helpful in secondary prevention of ischaemic stroke by identifying a subset of patients without known atrial fibrillation who may benefit more from anticoagulants than antiplatelet agents[86]. Consistent with this hypothesis, in the COMPASS trial, the prognostic benefit was mainly driven by a lower incidence of ischemic stroke in both rivaroxaban groups compared to aspirin-alone group, whilst rates of myocardial infarct were not significantly different between groups[26]. Again, this raises the suspicion that subclinical (silent) AF and/or atrial cardiopathy could be implicated in the pathophysiology of a larger proportion of strokes than it is currently thought.

However, caution is needed as there is also clinical-trial evidence showing no superiority of anticoagulation versus antiplatelet therapy in SR, reminding us of the importance of patient selection[87].

1.6 Imaging biomarkers and mechanisms of cardioembolic stroke

A number of heart conditions can lead to thrombus formation locally and embolic obstruction of brain vessels thus causing an ischaemic stroke[88]. Regardless of the cause, once the brain arteries are obstructed, there will be cellular hypoxia and disruption of the normal neuronal metabolism which is dependent on a constant supply of oxygen and glucose[43]. Subsequently, excitatory neurotransmitters accumulate in the synaptic cleft thus causing a rapid influx of calcium and superoxide anion, and eventually resulting in necrosis[43].

The most common predisposing conditions for cardioembolic stroke are AF, severe left ventricular dysfunction, acute myocardial infarct, and valvular disease[88]. The proposed mechanism for intra-cardiac thrombus formation is described by the Virchow's triad of endothelial/endocardial damage, increased blood stasis, and hypercoagulability[89, 90]. In recent years, important research efforts have been made to find imaging biomarkers of stroke risk that are supposedly more tightly linked to the pathophysiological mechanism described by the Virchow's triad. In **Table 1**, there is a list of published studies evaluating the relationship between stroke events and relevant cardiac imaging parameters.

Table 1: Association between cardiac Imaging biomarkers and stroke.

Parameters	Association with stroke in AF	Association with stroke independently/regardless of AF	Association with stroke independently of clinical risk scores
LEFT ATRIUM			
LA size	Echo[91]	Echo[92-99]	Echo[91, 92, 96, 97]
LA strain	Peak LA strain (Echo)[100] Reservoir strain (Echo)[101] Reservoir strain (CMR) [102]	-	Reservoir strain (Echo)[101] Reservoir strain (CMR) [102]
Total atrial conduction time (PA-TDI)	Echo[101]	-	Echo[101]
LA mechanical dyssynchrony (SD-TTP)	CMR[103]	-	CMR[103]
LA spontaneous echo contrast	Echo [104-107]	Echo [108]	-
LAA size	Echo[109]	-	-
LAA morphology	CT[110]	Echo [111]	Echo, CT[110, 111]
LAA peak velocity	Echo[112-114]	Echo [115]	Echo, CT[116, 117]
LA emptying fraction (LAEF)	-	CMR[20]	CMR[20]
LA fibrosis (late gadolinium enhancement)	CMR[118]	CMR[21, 119]	CMR[21, 119]
LA velocities/ flow patterns/ vortex volume/ vorticity	-	-	-
LEFT VENTRICLE			
LV function	Diastolic (Echo)[123, 124]	Systolic (Echo)[120-122] Diastolic (Echo)[123, 125, 126]	-
LV hypertrophy/geometry	-	Echo, CMR[127-131]	-

Echocardiography (Echo); Cardiovascular Magnetic Resonance (CMR); Computed Tomography (CT); Left atrial (LA); Left Atrial Appendage (LAA); Sinus Rhythm (SR); Atrial Fibrillation (AF); P-wave to A' duration on Tissue Doppler Imaging (PA-TDI); Standard Deviation of the Time To Peak strain (SD-TTP)

Studies on the LA structure and function have demonstrated that traditional cardiovascular risk factors such as age, obesity, hypertension, and diabetes can lead to the remodelling of the LA[132], with consequent alterations in both structure (i.e. LA enlargement and fibrosis) and function, key features of atrial myopathy[133]. This process could represent on its own an important pathophysiological substrate for thrombus formation and embolization[134]. Further, such LA myopathy is also linked to increased risk of developing AF[134], which is strongly associated with embolic stroke. These are believed to be the pathophysiological mechanisms behind the relationship between LA myopathy and incident cerebrovascular accidents[135].

LA size is probably the most studied of all LA imaging parameters. There is robust evidence from echocardiographic studies showing that increased LA size is associated with increased risk of incident stroke regardless of AF[92-99] and independently of current clinical stroke risk stratification[91, 92, 96, 97]. Epidemiological evidence from the Framingham Heart Study showed that, in subjects 50 years of age and older, increased LA size was significantly associated with incident ischaemic stroke[93] (**Figure 4**). After multivariable adjustment for age, hypertension, diabetes, AF, smoking, LV hypertrophy (by ECG criteria), it was demonstrated that for every 10-mm increase in LA size, the relative risk of stroke at 8-years follow-up was 2.4 in men (95% CI, 1.6 to 3.7) and 1.4 in women (95% CI, 0.9 to 2.1)[93].

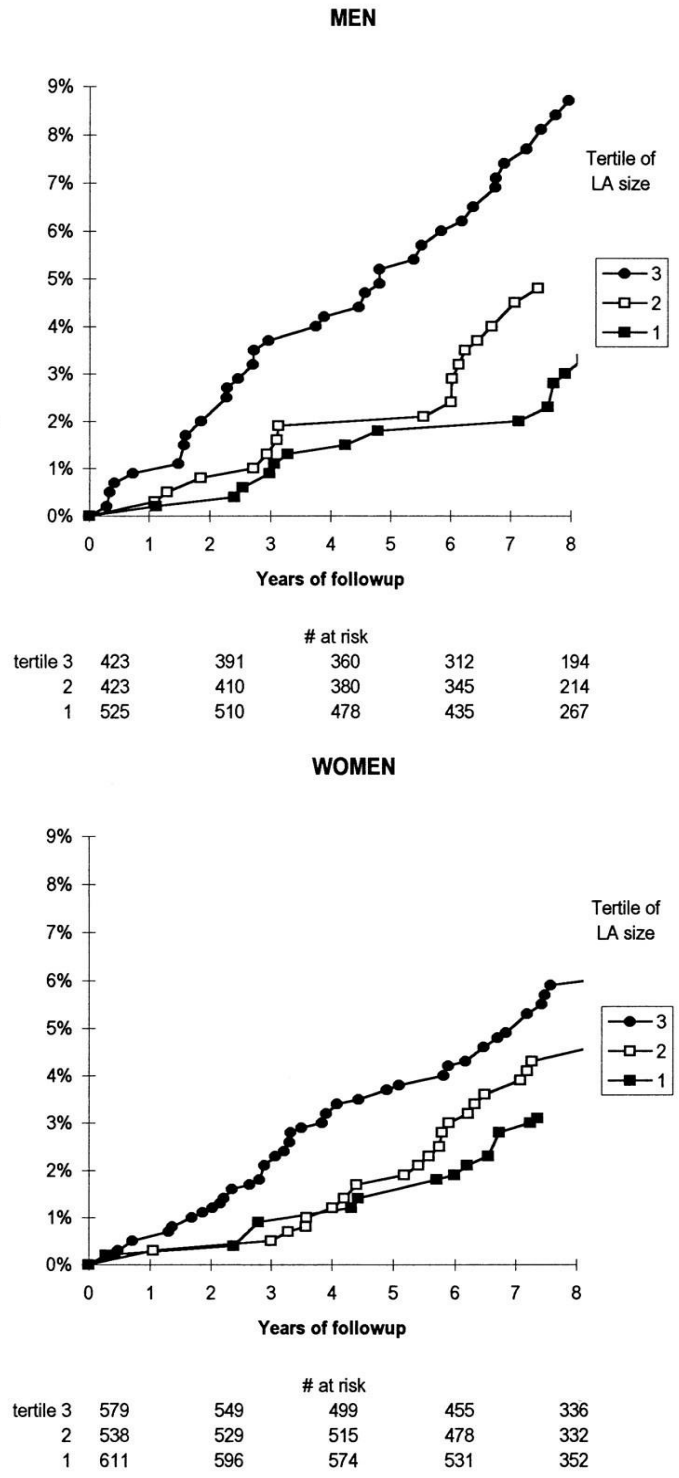


Figure 4. Relationship between LA size and incident stroke. *Age-adjusted cumulative incidence of stroke by tertile of left atrial (LA) size stratified by gender. Reproduced with permission from Benjamin et al.[93].*

Although there was evidence of an association between LA size and ischaemic stroke, it was not clear whether this association would be reproduced in a population free of known cardiovascular disease studied with a more comprehensive (CMR-based) assessment of the LA size and function (rather than the historical echo-derived LA diameter). Recently published data from the Multi-Ethnic Study of Atherosclerosis (MESA) study assessed relationships between indices of LA remodelling (i.e. LA emptying fraction [LAEF] and LA volumes by CMR cine, as well as peak longitudinal LA strain by feature-tracking CMR) and incident ischaemic stroke events at 11.6 ± 3.5 years in a population of 5,004 participants without known cardiovascular disease at enrolment (**Figure 5**). Notably, LA size was associated with incident stroke risk; however, this association did not hold after multivariate adjustment for interim risk factors and LV mass. Although LA dilatation was not an independent imaging biomarker in this cohort, in multivariate analysis, LAEF was associated with stroke events, after adjusting for interim AF, cardiovascular risk factors, and LV mass. The incorporation of LAEF into risk prediction tools (clinical risk factors and LV mass) led to a small (but statistically significant) increase in predictive accuracy (C statistic of 0.76 vs. 0.73; $p = 0.039$)[20].

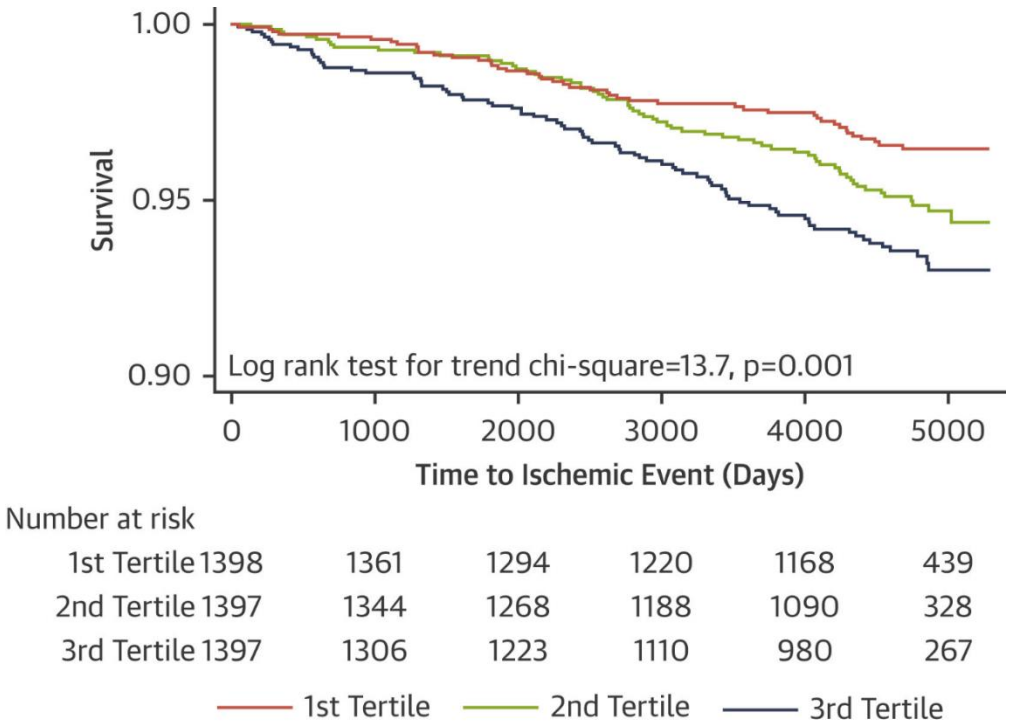


Figure 5. Outcome of participants stratified according to tertiles of total left atrial emptying fraction. *Kaplan-Meier survival curves showing the ischaemic-stroke-free survival of participants with different level of left atrial emptying fraction. LAEF = left atrial emptying fraction. Reproduced with permission from Habibi et al.* [20]

Further, advances in imaging post-processing tools allowed analysis of LA function beyond global function (as in the case of LAEF)[20, 136]; and it is now possible to analyse the different phases of atrial function, namely the LA reservoir, conduit and booster function[137], using echocardiographic speckle tracking or CMR tissue tracking, among other techniques. The role of LA phasic function in the stratification of stroke risk seems to be particularly relevant in AF patients[101]. Out of 1361 individuals with a first diagnosis of AF, the 7% who developed a stroke during the average 7.9 years of follow-up, displayed reduced LA reservoir (14.5% vs. 18.9%, P

= 0.005) and conduit strains (10.5% vs. 13.5%, P= 0.013), and increased P-wave to A' duration on tissue Doppler imaging (PA-TDI) (166 ms vs. 141 ms, P < 0.001) as compared with non-stroke group, despite similar LV size and function, and similar LA volumes. After adjustment for CHA_2DS_2-VASc score, age, and anticoagulant use, LA reservoir strain and PA-TDI were the only parameters which held statistical significance in their association with the risk of incident ischaemic stroke[101]. This observation may imply that an alteration of LA compliance can be relevant in the pathophysiology of cardiac embolism and can be used to refine risk stratification in AF patients[101]. By contrast, measurement of LA phasic function in SR participants in MESA study (measured using feature-tracking CMR in a population free of known cardiovascular disease), showed no significant differences between patients who developed a stroke versus those who did not. For instance, LA reservoir strain was 30.6±12.2 % in stroke patients vs 30.8±14.8 % in those without a stroke (P=0.805)[20]. Overall, these results imply that the pathophysiology of cardiac embolism in AF and in SR may be different.

More sophisticated imaging such as CMR late gadolinium enhancement (LGE) of the LA now allows indirect measurement of LA fibrosis thus giving new insights on the relationship between atrial myopathy and ischemic stroke. Accordingly, increased LA LGE burden is associated with increased risk of developing atrial arrhythmias[138] but it also seems to be sufficient by itself to generate LA stasis (assessed by spontaneous echo contrast) and LAA thrombus[139]. This is relevant as LA LGE has been shown to relate to cerebrovascular accidents both in AF[118] and in SR[119] although these studies are still preliminary. Specifically, in

1,228 patients with AF, more severe LA LGE was associated with major cardiovascular events at 5-years follow-up which was primarily driven by the stroke component of the composite endpoint analysed[118]. Further, in a population of 111 patients recruited after an ischaemic stroke, patients with a cryptogenic stroke had a higher burden of LA fibrosis by LGE than those with large artery/small vessel disease (18 ± 16% vs 10.5 ± 16%, p = 0.03); notably, the LGE burden observed in cryptogenic strokes was similar to that observed in the context of AF (25 ± 21%, p = 0.22)[21]. Finally, there is preliminary evidence that N=10 patients with ESUS have more atrial fibrosis by LGE than N=10 controls (16.8 ± 5.7% vs 10.6 ± 5.7%, p = 0.019). For every quartile increase in LGE, there was an Odds Ratio (OR) of 3.17 (95% CI 1.05-9.52, p = 0.041, CHA_2DVASc score adjusted)[119]. Although interesting, more robust evidence is needed in support of the relationship between LA LGE and stroke risk, particularly in SR.

Although thrombus formation can occur in both the LA and LAA, the latter is the most common site for LA thrombus formation, particularly in non-rheumatic disease. In fact, in a series of AF patients with rheumatic heart disease, surgical direct inspection revealed that, out of 51 patients with evidence of left atrial thrombi at the time of surgery, 21 patients (41%) had thrombi both within the atrial cavity and within the LAA, whilst 11 (21%) had thrombi solely in the left atrial appendage, and 19 patients (37%) had thrombi solely detected in the left atrial cavity[67]. Similarly, an analysis of 668 atrial thrombi detected by echocardiography, autopsies, and surgical inspection in AF patients[68] (446 thrombi in rheumatic AF and 222 thrombi in non-rheumatic AF) revealed that 43% thrombi were localized

in the LA cavity in rheumatic AF, but only 9-10% in non-rheumatic AF[68]. The fact that the LAA is such an important site for thrombus formation may reflect the role played by the LAA in the modulation of LA pressure and function[140]. LAA morphology seems to play an important role the pathophysiology of embolic stroke[110, 111]. CT classification of LAA anatomy into "cactus", "cauliflower," "chicken wing", and "windsock" types showed that a "cauliflower" LAA is a risk feature for prevalent stroke in AF patients undergoing ablation (OR 3.8; 95% CI 1.5–10.0; P = 0.005), even after adjustment for CHA_2DS_2-VASc score (OR 3.3; 95% CI 1.2–9.0; P = .017) [110]. Moreover, in patients without AF, a Trans-Oesophageal Echocardiography (TOE) defined 'complex' LAA morphology (i.e. any type other than chicken-wing) was associated with cryptogenic strokes even after adjusting for CHA_2DS_2-VASc score [111].

Beyond anatomical considerations, there is robust evidence showing that, in AF patients, lower LAA peak velocities (measured at LAA junction with the LA wall in proximity to the LAA orifice by TOE) are associated with incident cardioembolic events[112]. In particular, LAA peak velocities < 20 cm/s were associated with appendage thrombus (P <0.01) and subsequent cardioembolic events (P <0.01)[112]. Notably, there is preliminary evidence that the relationship observed between LAA velocities and embolic events seems to hold true also in stroke patients without AF[115]; specifically, stroke patients in SR were shown to display lower LAA flow velocities than controls without stroke (17.7 ± 8.2 cm/s versus 27.5 ± 8 cm/s, P <0.05), even without significant differences in LAA size[115]. As per LA LGE, more robust evidence is needed in support of LAA relationship with stroke risk,

particularly in SR patients without AF. So far, after ~20 years from the observation of a relationship between LAA flow and stroke risk in SR, no study has reproduced these results.

Traditional imaging techniques allow only two-dimensional sampling of the LAA flow velocities. Nonetheless, low LA flow velocities can be indirectly and qualitatively assessed using Spontaneous Echocardiographic Contrast (SEC) by echocardiography[141], where, in presence of low flow velocities and other prothrombotic conditions (i.e. high haematocrit), erythrocytes tend to form aggregates that reflect echoes and are visualized as a 'smoky' trace inside the LA chamber[141]. SEC seems to be due to erythrocyte aggregation linked to activation of the coagulation cascade, elevated vWF[142-145], and platelet activation[146]. Notably, lower LAA peak velocity and increased LA size are significantly associated with the grade of spontaneous echo contrast (P = 0.0001) in AF[147]. But is SEC related to stroke events? Out of 272 consecutive AF patients undergoing TOE, the 59% of patients displaying LA SEC at baseline had an embolic event rate significantly higher than the one observed in those patients without LA SEC (12%/year vs 3%/year, respectively, P=0.002) and by multivariate analysis, LA SEC was the only positive predictor of risk in this study (OR of 3.5, p=0.03)[105]. Similarly, in a population of 382 patients with AF, SEC was also significantly associated with thromboembolism (increasing the embolic rate per year of 2.9 times compared to patients without SEC; P = 0.06)[107]. Further, therapy with warfarin has been demonstrated to reduce the rate of stroke among patients with SEC from 8.2% per year to 4.5% per year[107]. The role of SEC as a biomarker of stroke risk has been suggested to extend also to

patients in SR regardless of AF. In a large retrospective study of a selected group of patients from a referred TOE population, out of 1,288 TOE studies, the 2% who had evidence of LA SEC despite being in normal SR had a significantly higher prevalence of past cerebrovascular events compared to SR controls with LA dilatation but without SEC (83% vs 56%, P=0.02)[108]. The high prevalence of previous cerebrovascular events in the overall cohort, probably reflects the population referred for a TOE in this study. LA SEC was again associated with increased LA size; however, even after adjusting for LA size, SEC was significantly associated with cerebrovascular accidents (P=0.03)[108]. Overall, as per LAA flow, after ~20 years from the publication of a relationship between LA SEC and stroke risk in SR, no study has reproduced these results.

The role of the left ventricle (LV) in cardioembolic strokes has also been studied extensively, and its potential pathophysiological role is mainly explained by LV dysfunction causing blood flow stasis (both in the LV and the LA) and promoting pro-thrombotic arrhythmias[122]. Such association with stroke risk seems to hold not only in cases of severe LV systolic dysfunction[121], but also in patients with moderately impaired LV systolic function (i.e. 41-50%) with a 4-fold increase in stroke risk[122], and even in the context of a diastolic impairment in SR[123, 126].

On a similar note, LV hypertrophy (LVH), which is linked to LV diastolic dysfunction, is independently associated with an increased risk of stroke[128]. Notably, in patients with cryptogenic strokes, severe LV diastolic dysfunction was associated with a cardioembolic pattern of brain lesions[123], thus suggesting that diastolic dysfunction could promote intra-cardiac thrombus formation and

subsequent embolization, probably due to the increased LA pressures and the consequent atrial remodelling[148]. Similarly, other studies have demonstrated the association between LVH and increased risk of cerebrovascular events (a) in a population of 2363 initially untreated hypertensive patients where those with echocardiography-assessed LVH displaying 64% increase in the risk of cerebrovascular events (relative risk 1.64; 95% confidence interval (CI): 1.07–2.68)[127], and (b) in 5098 participants initially free of cardiovascular disease, those with LV mass assessed by CMR was positively associated with the incidence of stroke (hazard ratio 1.2 per 10% increment, P=0.01)[130], as well as (c) in 40,138 adult patients from the general population echocardiography-assessed LV mass showed an independent association with all-cause mortality, myocardial infarct and stroke both in women (hazard ratio 1.26, 95% CI: 1.13–1.40, P<0.001) and in men (hazard ratio 1.19, 95% CI: 1.09–1.30, P<0.001)[131]. Further, the fact that LV mass reduction induced by antihypertensive treatment significantly reduced the risk of stroke (OR 0.76, 95% CI: 0.64–0.89, P<0.001) in a large meta-analysis of 12,809 hypertensive patients but did not change the risk of myocardial infarct or heart failure, may imply that LVH is a relevant pathophysiologic mechanism of stroke risk[129] even if it has to be stressed that this is still non-randomized evidence. LVH is linked to LV diastolic dysfunction[129] and, in principle, assessment of LV diastolic function may generate better biomarkers of stroke risk. In patients with type 2 diabetes, LV diastolic dysfunction (assessed with the ratio between MV E wave peak to E′ peak at TDI) was revealed to be a strong predictor of myocardial infarct and stroke, with superior predictive value to LV systolic function parameters such as global longitudinal strain and LV Ejection Fraction (LVEF)[125]. Interestingly, severe LV diastolic

dysfunction by echocardiography was significantly associated with cryptogenic stroke displaying brain lesion patterns mimicking cardioembolic brain infarcts[123].

However, the association between LV function and stroke may not reflect causal relationships, as they are in conflict with the evidence from a clinical trial showing no superiority of anticoagulation versus antiplatelet therapy in SR patients with chronic heart failure[87], suggesting that LV dysfunction may be a risk biomarker rather than a cause of stroke. Overall, although a number of imaging studies have explored numerous biomarkers of stroke risk, these preliminary findings have not yet been reproduced in large-scale studies to be able to demonstrate a meaningful increase in C-statistics on top of clinical predictive tools.

The advent of 4D Flow CMR allows a comprehensive non-invasive assessment of cardiovascular flow in a way that was not possible with previous technology[28, 149]. Markl et al. pioneered its application to the LA[28, 149]. In a proof-of-principle study, they measured in vivo 3D blood flow velocities in 60 AF patients and 15 SR controls (**Figure 6**)[28] thus demonstrating feasibility of the following measures of LA and LAA 4D flow: peak velocity, mean velocity, and stasis (expressed as the percentage of very-low velocities <0.1 m/s within one cardiac cycle). The authors thus proved that AF was associated with worse LA flow profile as compared to SR controls, and that in AF patients, increased CHA_2DS_2-VASc score was associated with significantly reduced LA velocities and elevated stasis ($P<0.043$)[28]. Further, in a subset of 30 AF patients, 4D flow metrics were compared with Doppler TOE; TOE-based LAA peak velocities modestly but significantly correlated with 4D

flow–based LA velocities (r=0.41) and stasis (r=−0.39), both P<0.05[28]. Details on 4D Flow technique are provided in the technical development Chapter 2.

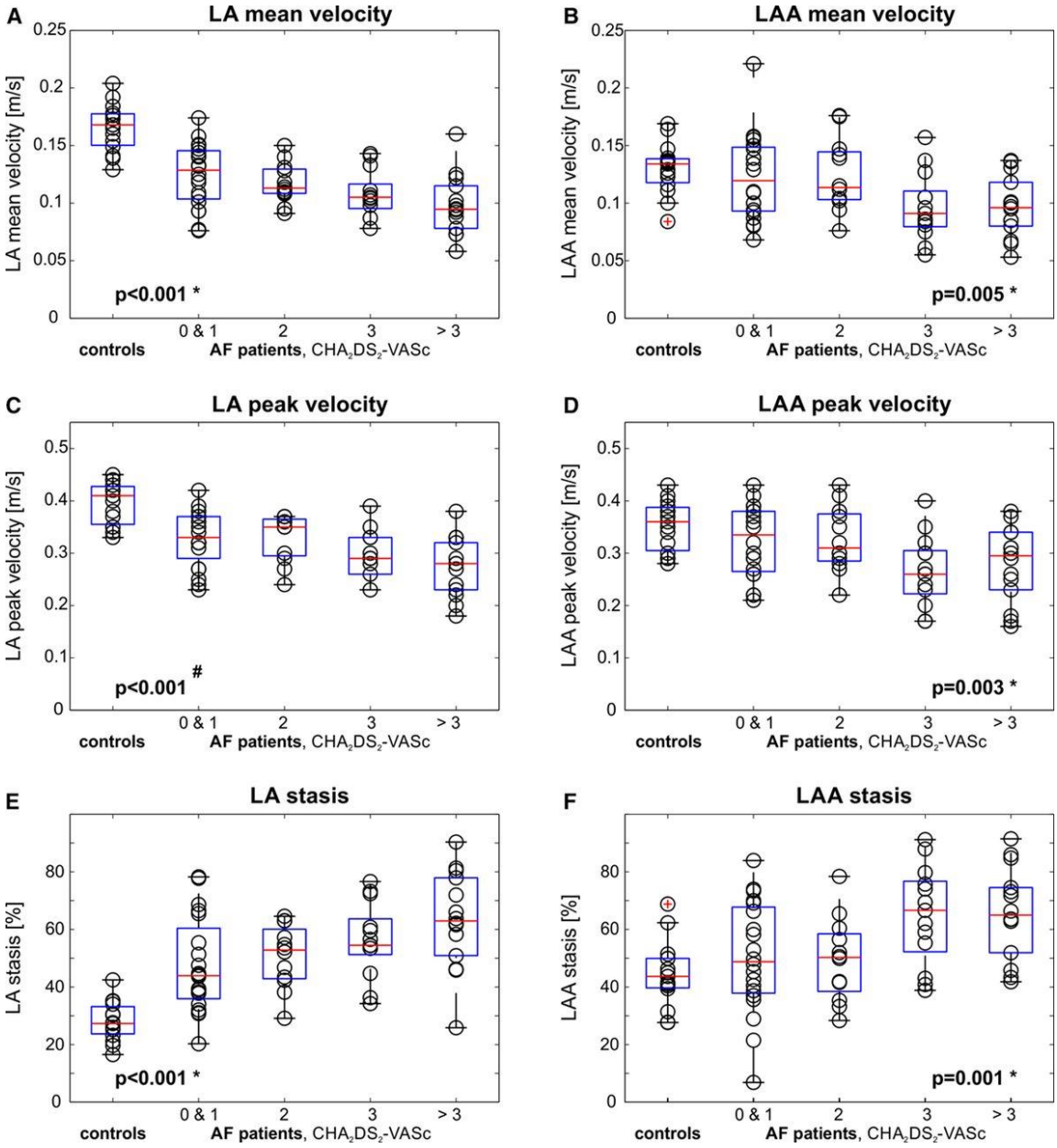


Figure 6. Left Atrial 4D Flow parameters in Atrial Fibrillation. *Comparisons of left atrial (LA) and left atrial appendage (LAA) 4D flow parameters between healthy controls and AF patients with different stroke risk as assessed by CHA_2DS_2-VASc scores. Boxplots indicate median and interquartile range. P values are from 1-way analysis of variance (ANOVA; *normal distribution) or Kruskal–Wallis test (#non-normal distribution). AF indicates atrial fibrillation. Reproduced with permission from Markl et al.[28].*

Apart from measurement of absolute velocities within the LA, a 4D flow dataset records velocity fields that allow analysis of flow patterns within the LA both qualitatively and quantitatively[150]. It has been shown that in humans, normal LA blood flow patterns are typically vortical and this seems to be linked to asymmetries and curvatures of the looped heart rather than purely mechanistic parameters such as LA dilation/function[150]. Intracardiac vortex patterns are widely present across dynamic species within the vertebrate line[12] and are important drivers of cardiogenesis and determinant of the final cardiac shape[32] via shear stress-induced epigenetic mechanisms. In addition to its phylogenetic functions, vortex rings have been associated with biomechanical platelet activation[151, 152] via alteration of shear stress forces. Similarly, abnormal cardiac flow patterns have also been linked to thrombus formation within other regions of the cardiovascular system such as within the LV of patients after acute myocardial infarct[153] as well as within abdominal aortic aneurysms[154]. Garcia et al.[155] demonstrated that it is possible to measure LA vortex size in vivo using λ2 method (**Figure 7**) and that vortex size was increased in SR patients with history of paroxysmal AF as compared to SR controls without AF. Interestingly, LA vortex size was inversely correlated with peak pulmonary vein inflow velocities ($P < 0.05$), positively correlated with LA volume ($P < 0.05$), positively related to CHA_2DS_2-VASc risk score, and increased across all phases of the cardiac cycle even if the most elevated size was noticed during diastole[155].

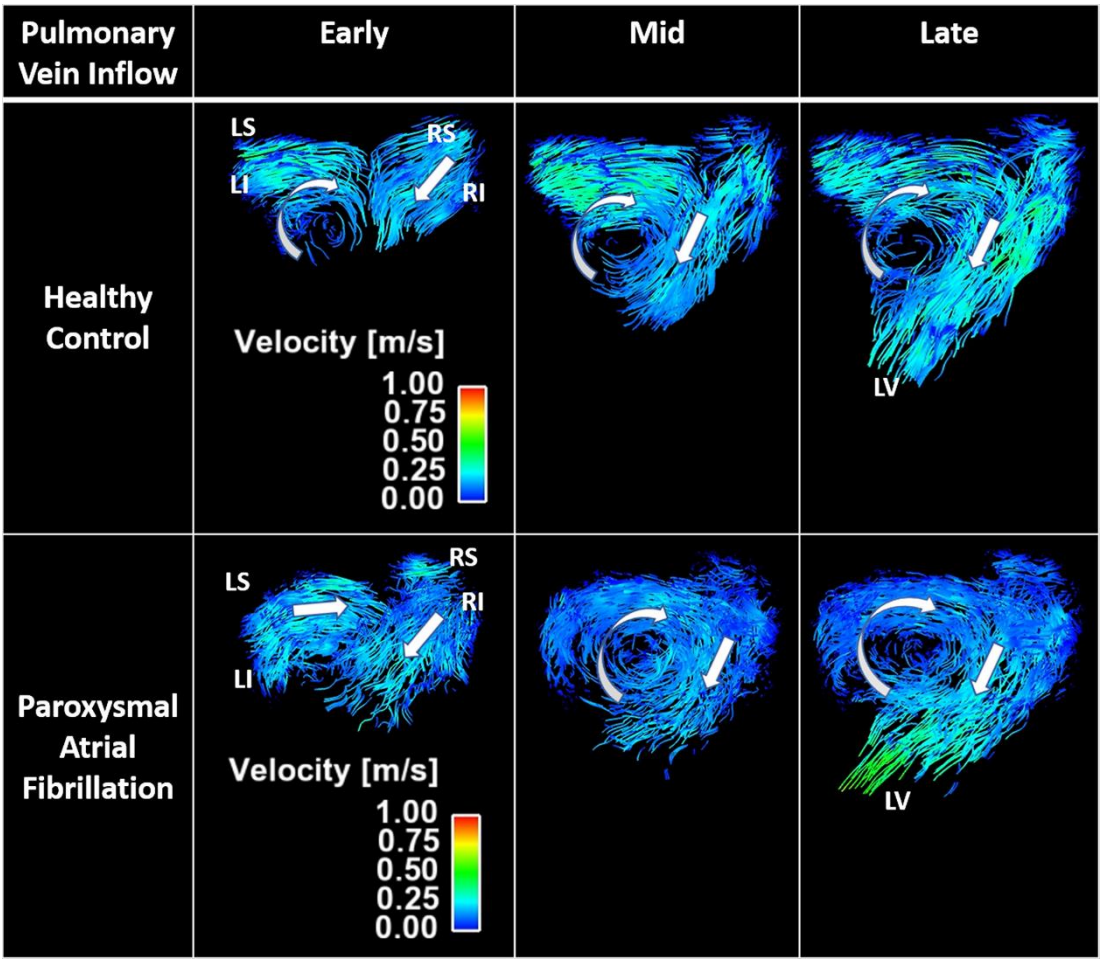


Figure 7 Representative cases of Left Atrial vortex patterns. *4D flow pattern comparison using particle traces between a healthy control subject and a patient in Sinus Rhythm at the time of the scan but with a positive history of paroxysmal atrial fibrillation. Left atrial vortex is disrupted in patients with atrial fibrillation with fragmentation and increased vortex size. LS: left superior; LI: left inferior; RS: right superior: RI: right inferior; LV: left ventricle. Reproduced with permission of Garcia et al.*[155]

Currently, there are no studies exploring the relationship between stroke risk and LA 4D Flow parameters in SR patients without a diagnosis of AF. Building on the above-mentioned preliminary studies, the next step towards clinical application of this novel technique is to create standardized post-processing tools and protocols which are to be tested systematically in terms of reproducibility and in terms of independent associations with stroke and brain infarct.

1.7 Overview of Thesis

This Thesis consists of related CMR studies, each specifically designed to answer a distinct (although related) scientific question (Chapter 4, Chapter 5) as well as technical development work (Chapter 2, Chapter 3). A detailed description of methods is contained in Chapter 2.

Building on in-house (already available) 4D flow acquisition protocols, technical development work was undertaken to create in-house software to analyse an LA 4D Flow dataset as well as create a 'contouring' protocol (Chapter 2Chapter 2). Further, measured LA 4D Flow parameters were tested for reproducibility and temporal variability in a dedicated study, both in patients with AF and in those with SR. The results of these investigations are contained in Chapter 3. LA flow profile assessment directly quantifies one aspect of the pathophysiological basis for intra-cardiac thrombus formation; however, it is not clear to what extent the AF rhythm contributes to the pro-thrombotic changes observed within the LA versus the clinical risk factors affecting LA/LV function. Results of the mechanistic study exploring the effects of a rhythm of AF and of stroke risk factors on LA flow profile are contained in Chapter 4. Chapter 5 describes a study investigating the relationship between embolic or non-embolic brain infarcts and LA flow parameters. Finally, the overall conclusions of this Thesis and future research directions are detailed in Chapter 6.

Chapter 2

Methods and Technical Development

2.1 Ethical Considerations

An overarching research protocol has been written in order to create 3 pre-defined observational cohorts (corresponding to those described in Chapters 3, 4, and 5) and address the aims of this Thesis. Research procedures received a favourable opinion from the Yorkshire & The Humber - Leeds East Research Ethics Committee (REC reference: 18/YH/0096) of the National Research Ethics Service (NRES) representing the NRES Directorate within the National Patient Safety Agency and Research Ethics Committees in England. The study also received approval from Oxford University Hospitals NHS Foundation Trust with University of Oxford as sponsor (Principal Investigator: Prof. Barbara Casadei). All patients gave written informed consent for all study procedures.

2.2 Study Participants

Full details of recruitment strategies for study participants within each study cohort is reported in the relevant chapters below. Briefly, the study protocol allows recruitment of (a) patients admitted to the stroke unit at the John Radcliffe Hospital, Oxford University Hospital (OUH) NHS Foundation Trust (Oxford, UK) with a

diagnosis of ischaemic stroke; (b) patients (and family members) attending the John Radcliffe Hospital, OUH NHS Foundation Trust (Oxford, UK) for a clinical appointment; (c) controls contacted from a pool of participants who had previously given consent to be contacted in the future following expressions of interest and/or recruitment to previous research studies, as well as (d) individuals interested after hearing about the study by word of mouth.

The CHA_2DS_2VASc score[156] and its components[156] were calculated from the information collected via a questionnaire administered to all participants. Clinical management of patients was at the discretion of the responsible physician. Study participants were offered a 7-day ECG monitor to assess rhythm.

2.3 Consent process and ethical considerations

Inclusion and exclusion criteria for each study are provided in detail in Chapters 3, 4, and 5. Eligible participants were provided with a patient information leaflet and invited to take part in the study. Patients who gave written informed consent were then enrolled into the study. Fourteen young healthy volunteers were recruited under an ethically approved departmental technical development protocol and provided verbal consent (as specified in the SOP No: OCMR_007 version 1).

For potential participants who were unable to consent as result of the stroke, a designated member of the research team appropriately trained in Good Clinical Practice and in the Mental Capacity Act, discussed the study with a consultee who was required to provide advice regarding patient's participation. A 'personal

consultee' was generally someone engaged in caring for the participant (not professionally or for payment) or was interested in his/her welfare, plus was prepared to be consulted. If no appropriate person was identified who was willing to act as a 'personal consultee', there was an option for the researchers to resort to a 'nominated consultee', i.e. a person independent of the project appointed in accordance with the Department of Health's guidance on nominating a consultee for research involving adults who lack capacity to consent. In accordance with the Mental Capacity Act 2005, such patients were enrolled in the study providing that the researcher had discussed the study with a consultee, and where possible the patient. A formal consent/advice process with the patient or a consultee occurred in all cases before any research procedures were undertaken.

In case a potential participant was unable to sign the consent form with his/her dominant hand (as a consequence of the stroke) but was otherwise able to consent, he/she was invited to personally sign and date, with his/her non-dominant hand and in the presence of a witness, the latest approved version of the informed consent form, before any study specific procedures were performed.

The consent process took ~20 min and a copy of the signed consent form was given to the participants. The original signed form is kept at the study site; a further copy is in the medical notes.

2.4 **Research Assessment**

All subjects underwent a focused clinical assessment (usually on the day of scanning). This included history for:

- Inclusion and exclusion criteria
- Collection of medical history focused to conditions relevant to clinical stroke and bleeding risk
- Drug history
- MRI safety questionnaire

The following study procedures were also performed:

- Blood pressure measurement (averaged for 3 measurements in a recumbent position if irregular rhythm)
- Heart rate (averaged for 3 measurements in a recumbent position if irregular rhythm)
- Height (cm) and weight (kg) using calibrated scales
- CMR and brain MRI protocol (with optional within-session rescan protocol and up to 2 optional follow-up scans)
- Offer to wearing 7-day continuous research ECG monitoring to evaluate presence of AF

2.5 Data Blinding for Analysis

All imaging assessments (including determination of LA and LV function, 4D flow parameter analysis, and flow visualisation) were conducted by investigators blinded to all clinical information, including rhythm at the time of the scan. Details about blinded analysis for each study are specified in Chapters 3, 4, and 5. Briefly,

study identification codes were mixed in Excel and then anonymised using Circle software; operators not involved with scanning participants placed contours on the anonymised datasets. After appropriate training, a blinded observer contoured all the dataset derived from cine imaging and from the 4D Flow sequence; as well as annotating all the qualitative data regarding flow patterns using the Ensight software, according to a dedicated in-house post-processing protocol (see below). Relevant data were extracted from Circle software and 4D Flow MATLAB software and imported in an Excel spreadsheet by blinded observers who sent the anonymized final dataset to me.

In the next two paragraphs of this chapter, I will give details on the research CMR protocol used in this Thesis together with the technical development of the post-processing software and protocol created for the purpose of this work. Finally, the brain MRI protocol will be covered in detail in Chapter 5.

2.6 CMR Protocol

Research participants underwent CMR scanning on 3 Tesla (3T) MRI systems (Verio syngo MR B17 or MAGNETOM Prisma VE11C, both Siemens, Germany) which included the following:

(1) Long axis cine with 4-chambers and 2-chambers view orientation to assess LV and LA volumes and function

(2) Three-dimensional time-resolved phase-contrast cardiovascular magnetic resonance (4D flow CMR) for assessment of LA flow characteristics

Care was taken with positioning of ECG electrodes to ensure good ECG signal quality in order to minimize the risk of mis-triggering during acquisitions. All images were acquired with the subject in the supine position. All image analysis was conducted offline using the following post-processing software: cvi42 software (v.5.3.4, Circle Cardiovascular Imaging Inc, Calgary, ON, Canada), Ensight (ANSYS 2019 R1, Canonsburg, Pennsylvania, USA), and a Matlab-based in-house software designed by ATH and MS and coded by ATH (MATLAB R2015 8.6.0.267246; Mathworks, Nattick, USA).

2.6.1 Cine imaging

Cardiac volumes and function were acquired using steady state free precession (SSFP) imaging where scan parameters were typically as follows: voxel size 1.6×1.6×8.0 mm, FOV=360mm, TR/TE 54.53-54.91/1.23ms, flip angle 50°, GRAPPA=3, 45 reference lines, segments=78, concatenations=1. Pilot images were initially acquired and used to plan and acquire horizontal long axis (HLA or 4-chamber view) and vertical long axis (VLA or 2-chamber view).

The CMR protocol included ECG-gated balanced steady-state free precession (SSFP) cine imaging in four-chamber and two-chamber axis orientations of the LV, for the evaluation of LVEF, and end diastolic and end systolic volume (LVEDV and LVESV, respectively), as well as LAEF and LA maximal and minimal volumes (LAmax and LAmin, respectively), and for derivation of LV and LA longitudinal strain and strain rate parameters by feature tracking, as described previously[157-159]. Briefly, CMR

cines were generally acquired with retrospective gating, including use of arrhythmia sorting as required. LV short axis epicardial and endocardial borders were manually contoured at end diastole and end systole (see Figure 8). LV end systolic (ESV) and end diastolic (EDV) volumes were used to calculate stroke volume (SV) as SV = EDV - ESV. Ejection fraction (EF) and cardiac output (CO) were calculated as EF = SV / EDV and CO = SV x HR, respectively. LV mass was calculated by subtracting the endocardial volume from the epicardial volume in end-diastole, based on prior knowledge of myocardial specific gravity (1.05 g/cm^3). LAmax and LAmin were determined with the biplane area-length method[157] and used to calculate LAEF, where $\text{LAEF} = \frac{(\text{LAmax} - \text{LAmin})}{\text{LAmax}}$. LA volume (ml) reported in this Thesis corresponds to LAmax. LV and LA endocardial contours were contoured in end-diastole and end-diastole, using a point-and-click approach. Epicardial contours for the LV were contoured in end-diastole. End-diastole was defined as the first frame of acquisition. For LV contours, end-systole was defined as the frame in which the LV cavity had the smallest volume. For LA contours, end-systole was defined as the frame immediately before the opening of the mitral valve.

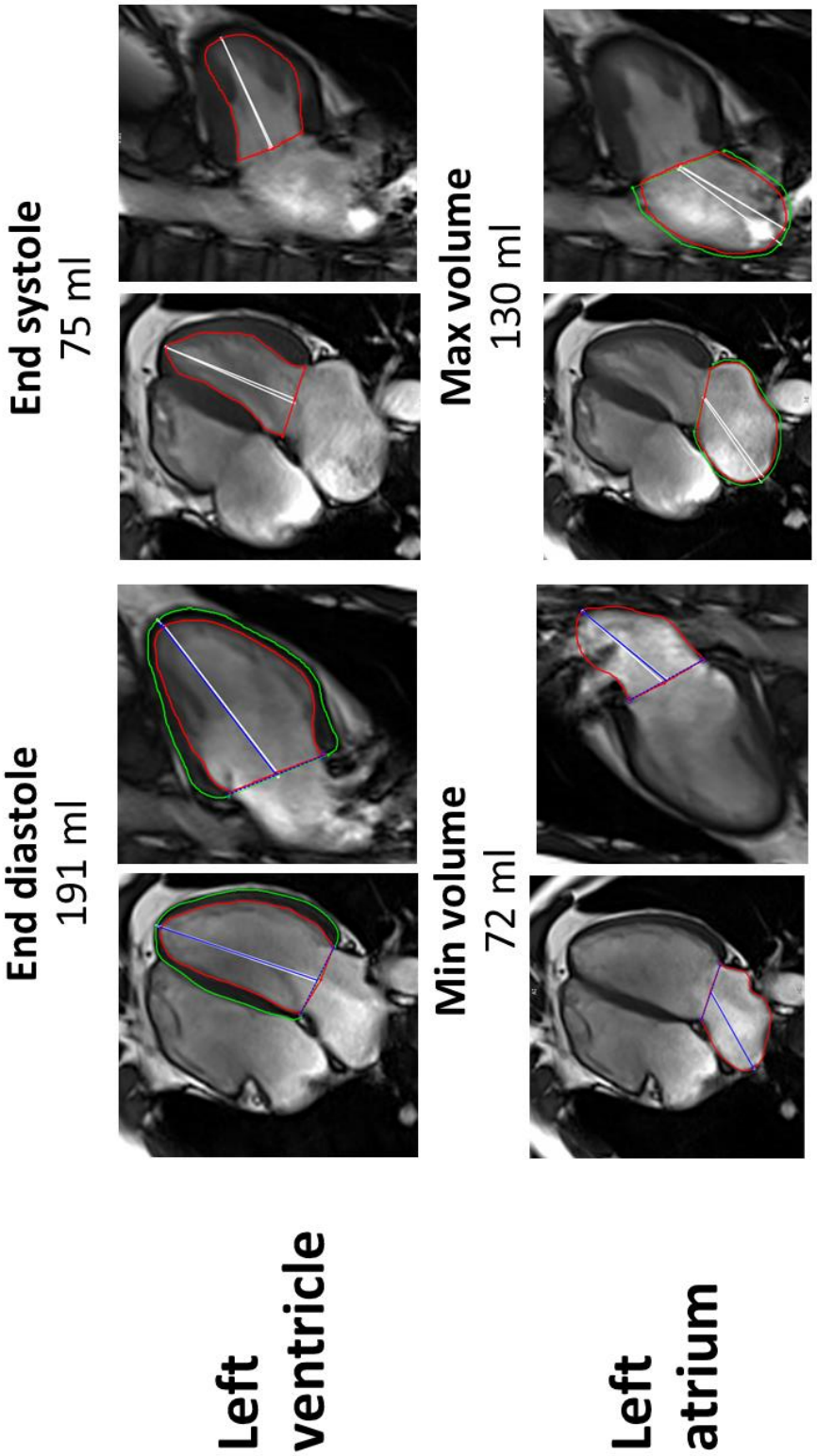


Figure 8 : Representative myocardial contours in a patient during CMR. *A blinded observer drew manually endocardial (red) and epicardial (green) contours as shown.*

The final contours were saved as DICOMs in CVI42. LV and LA cine contours for function were loaded in the Tissue Tracking module of CVI42, which has been previously used for LV and LA[160]. After importing the relevant sequences, the software automatically performed a feature tracking analysis giving as output strain and strain rate curves & values. The software calculated averaged values from the endocardial and epicardial borders (i.e. global) which were reported in the final database. The quality of tracking was manually reviewed by superimposing a color-coded map of longitudinal strain between the endocardial and epicardial parameters in the cine sequences. Contours were then manually adjusted by blinded observers in the areas in which the software failed to track motion wall correctly. The updated contours were saved separately from the original ones as DICOM in CVI42.

For the purpose of data extraction, CVI42 automatically creates a report of the general and segmental analysis of all parameters collected for both LV and LA strain analysis. This report was saved for each study. The parameters derived from the global analysis of longitudinal strain were extracted from this report and used for statistical analysis.

Global LV and LA strain and strain rate curves were also saved. The following parameters of deformation imaging were therefore derived for the LV (**Figure 9**):

- LV longitudinal systolic strain (automatically extracted by the software as the peak global longitudinal strain). Global longitudinal strain (expressed in %) is an established measure of LV systolic function[125].

- LV global longitudinal early diastolic strain rate (automatically extracted by the software as the peak global longitudinal strain rate during diastole). Early diastolic global longitudinal strain rate (GLSR-E) was defined as the peak of the curve describing the rate (1/s) of myocardial longitudinal deformation during early diastole[159], as a measure of LV relaxation and diastolic function[159].

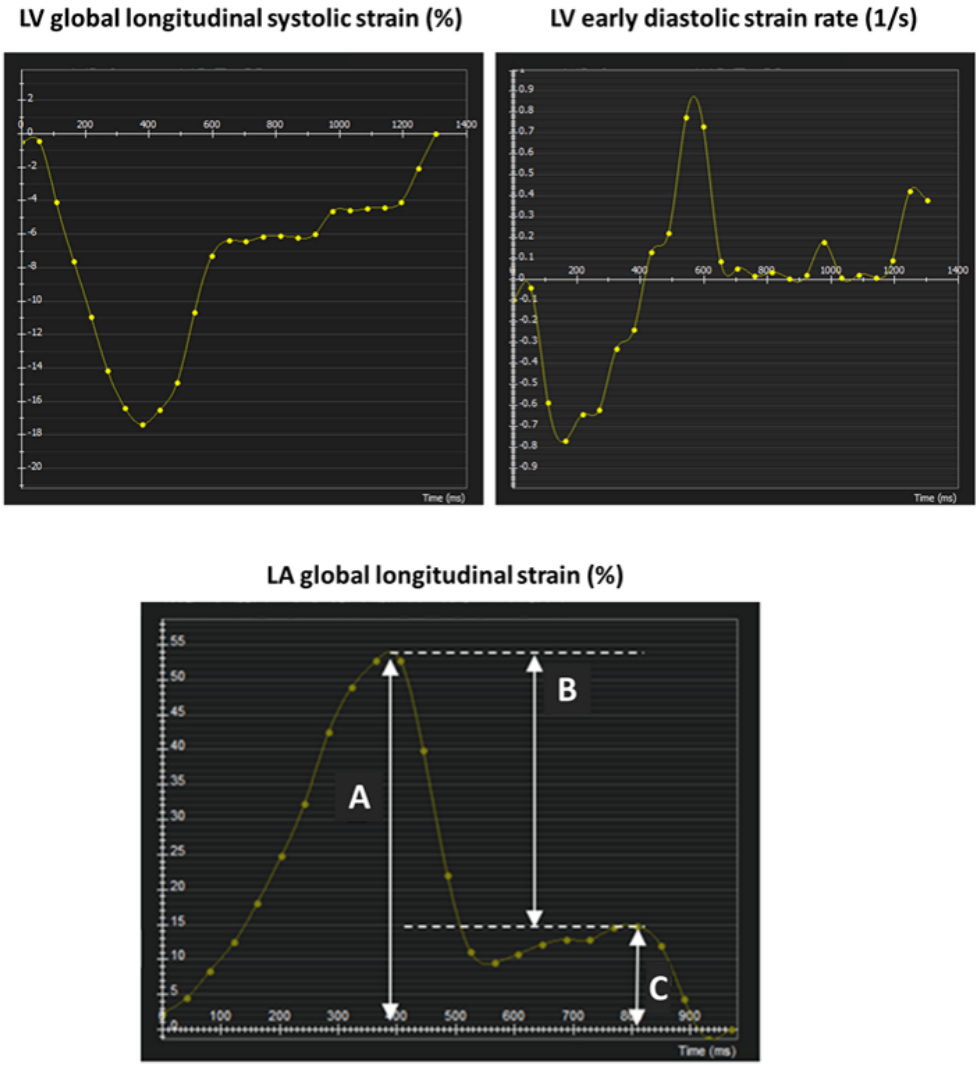


Figure 9 Strain and strain rate profile for the left ventricle (LV) and left atrium (LA). *Example of strain and strain rate curves from a study participant in sinus rhythm. A: LA global peak longitudinal reservoir strain; B: LA global longitudinal conduit strain; C: LA global longitudinal booster strain.*

LA strain values were used to assess atrial function in the 3 phases of the atrial cycle as previously described[158] (see **Figure 9**): (A) LA reservoir strain (a marker of atrial distensibility) was the peak of the longitudinal strain curve during ventricular systole; (B) LA conduit strain (a marker of passive atrial conduit function during early ventricular diastole) was estimated as the difference between LA reservoir strain and LA booster strain; and (C) LA booster strain (reflecting the atrial 'kick' during late ventricular diastole) was the end-diastolic peak of the longitudinal strain curve. All images were analysed using cvi42 software (Circle Cardiovascular Imaging Inc, Calgary, ON, Canada).

LA feature tracking parameters were derived from the global LA longitudinal strain curves (see **Figure 9**):

- LA global longitudinal reservoir strain (automatically extracted as the peak global longitudinal strain) – (A in **Figure 9**)
- LA global longitudinal conduit strain (which will be calculated as the difference between the LA global longitudinal reservoir strain and the LA global longitudinal booster strain) - (B in **Figure 9**)
- LA global longitudinal booster strain (manually extracted as the strain value at the time point immediately before atrial contraction , i.e. at the end of the plateau in the LA strain curve during LV diastole) - (C in **Figure 9**)

2.6.2 Left Atrial 4D Flow

The 4D Flow protocol included ECG-gated time-resolved 3D phase-contrast MRI with 3-directional velocity encoding ('4D flow') imaging to allow in vivo assessment of blood flow velocities in the LA. The 4D flow MRI data were acquired during free breathing using navigator gating of diaphragmatic motion, with pulse sequence parameters as follows: flip angle =6-7°, spatial resolution/voxel size 2.4×2.4×2.5-3.0×3.0×3.0 mm, temporal resolution = 39.52-48.88 ms, reconstructed to 20-30 time frames, TE = 2.39-3.66 ms, imaging acceleration (GRAPPA technique) with an acceleration factor of R=3, total acquisition time = 5-20 min depending on heart rate and navigator efficiency, velocity encoding sensitivity = 110-120 cm/s. The field-of-view (FOV) was axial and adjusted to encompass the entire left atrium in each subject.

All 4D flow were acquired with Maxwell term correction[161], DICOM tools from the OXSA toolbox were used[162], and data were corrected for velocity aliasing[163], and eddy currents[164] using Matlab-based in-house software designed by ATH and MS (MATLAB R2015 8.6.0.267246; Mathworks, Nattick, USA), available on the Oxford University Research Archive (ORA) platform (https://doi.org/10.5287/bodleian:ey4ovzdbB). A three-dimensional time-averaged phase contrast angiogram was generated to facilitate better orientation in the context of the atrial anatomy and interpretation of the flow data[165]. To isolate the atrial velocity data, data analysis included 3D segmentation of the minimum LA volume (directly on magnitude images in the 4D Flow dataset) using cvi42 software.

Two sets of parameters were derived from 4D flow dataset: (A) absolute velocities and (B) directionality of flow and LA flow patterns.

The absolute atrial velocities for each voxel inside the segmented LA were determined as described previously[28] (see **Figure 10**). Briefly, for each voxel, the peak & mean velocities (m/s) were determined; stasis was calculated as the ratio of the total number of cardiac time frames (n) with a velocity below the threshold of 0.1 m/s (n stasis) to the total number of frames (NTot) [28, 149]: stasis = $\frac{\text{n stasis}}{\text{NTot}}$. Global LA stasis was defined as the average proportion of stasis across all LA voxels and it is expressed as a proportion from 0 to 1, where 0 is the lowest amount of stasis and 1 is the highest[28, 149].

Regarding flow patterns, a 4D velocity field within the LA was used to generate 3D pathlines and to evaluate atrial flow patterns during both ventricular systole and diastole using the Runge-Kutta method[166, 167] with Ensight software (ANSYS 2019 R1, Canonsburg, PA, USA), see **Figure 10**. Pathlines were emitted at each time-frame from probe planes positioned at each of the pulmonary veins (starting at the beginning of the cardiac cycle), allowing derivation of flow patterns inside the atrium during both ventricular systole and diastole (based on mitral valve opening time derived from the magnitude images). Flow patterns were evaluated after quality control steps were applied, as previously described[168]. Normal flow within the LA is characterized by the presence of a vortex[150, 166, 169] (i.e. pathlines with a circular/elliptic trajectory see **Figure 10**). Atypical flow patterns observed were classified visually into *short-ranged* vortex (pathlines failing to reach the mitral valve plane during one averaged cardiac cycle, see **Figure 10**), and into *other*

patterns. Further, for all scans, after flow denoising using divergence free wavelets[170], the volumes of the largest vortex rings inside the LA were calculated automatically using the lambda2 (λ2) method[166]. In each case, a specific lambda threshold for vortices was defined as half the mean λ2 value over the cardiac cycle[155]. LA vortex volume (ml) is reported as the mean of LA vortex volumes throughout the cardiac cycle alongside peak LA vortex volumes (ml) within systole and diastole. Finally, we also applied a measure of tendency of the blood flow to rotate using the volume-averaged magnitude of vorticity (units radians/sec)[171, 172], after flow denoising [170]. LA vorticity is reported as the area under the vorticity-time curve over the entire cardiac cycle (in radians or rad), see **Figure 10**.

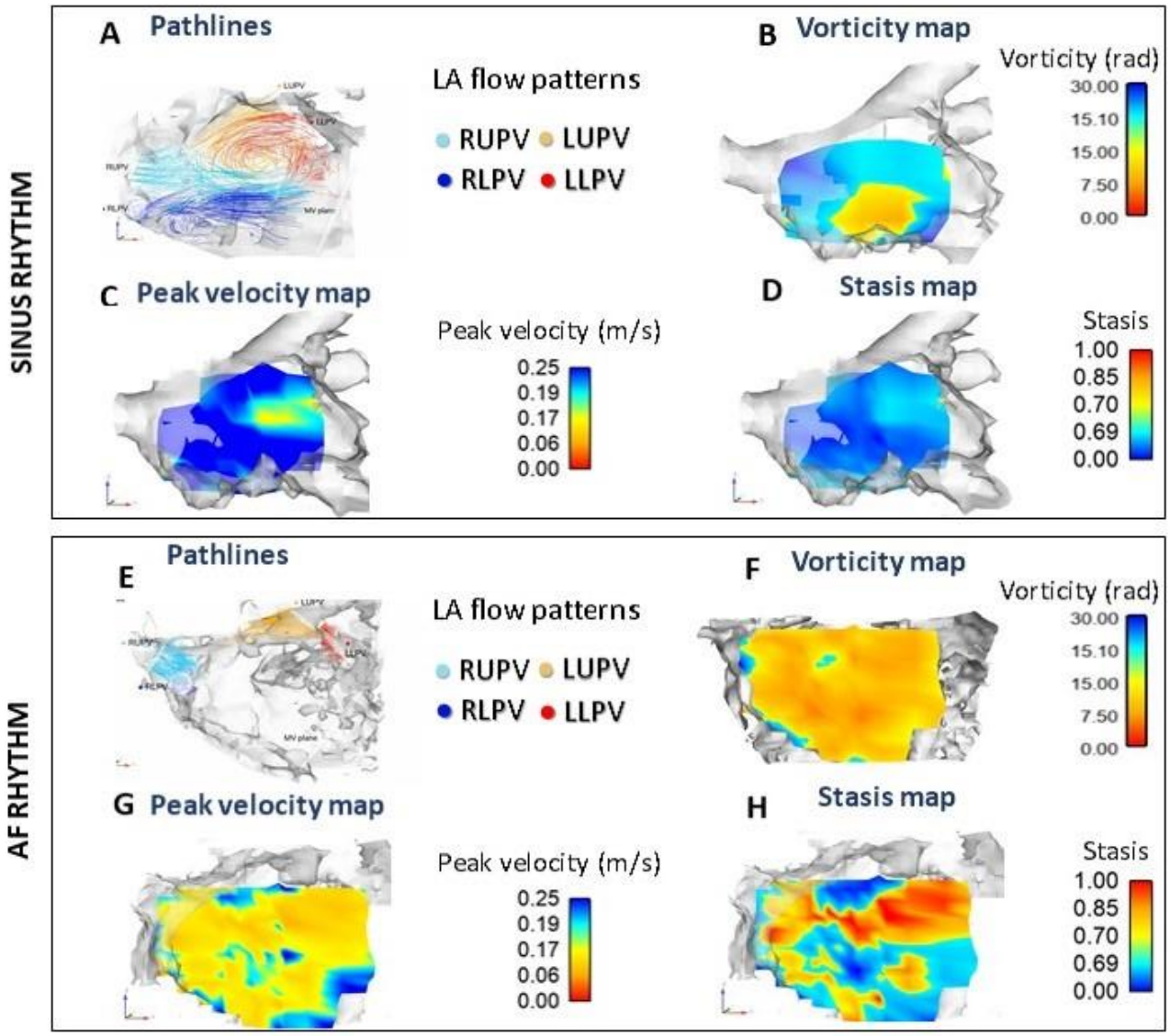


Figure 10: Representative cases of left atrial 4D Flow in study participants with sinus rhythm and atrial fibrillation. *Map legends are colour-coded such that hot colours represent deranged 4D flow values. 4D Flow imaging in a SR participant (70 year-old male with BMI 30 kg/m2 and CHA_2DS_2-VASc = 1) shows a typical vortex (with pathlines emitted from pulmonary veins). Similar imaging in a patient with AF (67 year-old male with BMI 26 kg/m2 and CHA_2DS_2-VASc = 3) shows a short-range vortex. Right Upper (RU); Left Upper (LU); Right Lower (RL); Left Lower (LL); Pulmonary Vein (PV).*

I drafted an in-house post-processing protocol for LA 4D Flow as follows: 3D segmentation was performed in the axial orientation on 4D Flow 'magnitude images' derived from the 4D flow dataset with the use of a dedicated CVI42 post-processing software (Short 3D function). Contouring included all LA slices between the Pulmonary Artery bifurcation (*top slice)* and the coronary sinus (*bottom slice)*. Care was taken to adjust the contours throughout the cardiac cycle so that the contours are consistently within the LA chamber. The resulting 3D mask was exported as *.cvi42wsx file which was subsequently used in MATLAB to isolate the velocity within the LA volume.

The visualization of flow patterns with pathlines involves the following steps:

A. Open Ensight (ANSYS 2019 R1, Canonsburg, PA, USA)
B. Load the .case file (generated after MATLAB processing of 4D Flow dataset)
C. Apply the angiogram generation script (Angiogram.enc) from the command window
D. Place the plane tool at the junction between PVs and LA wall and create a clip plane (i.e. PV tag)
E. Emit twenty-five pathlines (5x5 grid, Emission time start = 0, Total time limit = Full Cycle Duration, Time Delta = time at frame n. 1) from all the PV tags at each time frame. For each case, the time of mitral valve opening is used to determine the systolic and diastolic phases
F. Set the view in the Y plane (coronal view) and animate the generated pathlines

Overall, the acquisition of 4D Flow sequence may take 5-20 min depending on heart rate and navigator efficiency. After appropriate training, contouring of the LA in cvi42 software takes on average ~5 min. Subsequently, contours are extracted from cvi42 software and loaded in our in-house MATLAB software for calculations (this operation takes ~10 min) to generate the output with quantitative results. Further, after MATLAB processing, the case can be loaded in Ensight software for the visualization of flow patterns (this operation takes on average ~10 min).

Chapter 3

Left atrial 4D flow MRI: a reproducibility study in sinus rhythm and atrial fibrillation

3.1 Abstract

3.1.1 Background

4D Flow CMR allows sophisticated quantification of LA blood flow, and could yield novel biomarkers of propensity for intra-cardiac thrombus formation and embolic stroke. As reproducibility is critically important to diagnostic performance, we systematically investigated technical and temporal variation of LA 4D Flow in AF and SR.

3.1.2 Methods

Eighty-six subjects (64 in SR, 22 in AF) with wide-ranging stroke risk (CHA2DS2VASc 0-6) underwent LA 4D Flow assessment of peak and mean velocity, vorticity, vortex volume, and stasis. Eighty-five (99%) underwent a second acquisition within the same session, and 74 (86%) also returned at 30 (27-35) days for an interval scan. We assessed variability attributable to manual contouring (intra- and inter-observer), and subject repositioning and reacquisition of data,

both within the same session (same-day scan-rescan), and over time (interval scan). Within-subject coefficients of variation (CV) and bootstrapped 95% CIs were calculated and compared.

3.1.3 Results

Same-day scan-rescan CVs were 6% for peak velocity, 5% for mean velocity, 7% for vorticity, 9% for vortex volume, and 10% for stasis, and were similar between SR and AF subjects (all $p>0.05$). Interval-scan variability was similar to same-day scan-rescan variability for peak velocity, vorticity, and vortex volume (all $p>0.05$), and higher for stasis and mean velocity (interval scan CVs of 14% and 8%, respectively, both $p<0.05$). Longitudinal changes in heart rate and blood pressure at the interval scan in the same subjects were associated with significantly higher variability for LA stasis ($p=0.024$), but not for the remaining flow parameters (all $p>0.05$). SR subjects showed significantly greater interval-scan variability than AF patients for mean velocity, vortex volume, and stasis (all $p<0.05$), but not peak velocity or vorticity (both $p>0.05$).

3.1.4 Conclusions

Peak velocity and vorticity are the most reproducible and temporally stable novel LA 4D Flow biomarkers, and are robust to changes in heart rate, blood pressure, and differences in heart rhythm.

3.2 Introduction

Stroke is the second most common cause of death and the third most common cause of disability worldwide[173]. AF is a strong risk factor for embolic stroke mainly as it causes pro-thrombotic alterations in atrial blood flow and consequent thrombus formation within the LA[90, 147, 174, 175]. Pooled evidence from echocardiography, autopsies, and surgical inspection of the LA reveals that intracardiac thrombus formation generally occurs within the LAA, particularly in non-rheumatic heart disease [67, 68]. Overall, as many as 40% of all ischaemic strokes may be due to embolism from the LA/LAA, encompassing not only patients with AF prior to or at the time of the stroke, but also those with AF detected sub-clinically on subsequent cardiac monitoring, as well as a proportion of patients with embolic stroke of unknown origins with signs of atrial myopathy[15].

Prediction of ischaemic stroke risk in clinical practice relies almost exclusively on scoring systems based on upstream clinical risk factors, such as the CHA_2DS_2VASc score[29], which apportions one point each for congestive heart failure (C), hypertension (H), age ≥65 (A), age ≥75 (a further point, i.e. A2), diabetes (D), prior thromboembolic disease (S2, two points), vascular disease (VA), and female sex category (Sc). Although higher scores are linked to higher risk of incident ischaemic stroke, this and other similar clinical prediction tools are limited by a modest predictive capacity both in AF and in SR patients[29, 30]., Hence, the ability to assess parameters such as LA blood flow characteristics comprehensively (i.e. absolute flow velocities, the degree of stasis, and vortical flow patterns) both in AF

and in SR is very attractive, since these features contribute directly to the downstream pathophysiologic substrate for thrombus formation and may be mechanistically relevant to the risk of embolic stroke[90].

ECG-gated time-resolved phase-contrast MRI with 3-directional velocity encoding (4D Flow) is an established CMR technique that allows comprehensive in-vivo visualisation and quantification of cardiovascular flow velocities[176]. Recent proof-of-principle studies have shown that peak and mean velocity and stasis measurements derived from LA 4D Flow are associated with clinical stroke risk in patients in SR with history of AF[28, 155] and low blood flow velocities have been linked to activation of the coagulation cascade[90, 147]. Furthermore, assessment of the pattern of blood flow within the LA[150] may also be relevant to embolic risk, since loss of normal vortical flow has been found in patients in SR with a history of paroxysmal AF at higher stroke risk [155] and is associated with platelet aggregation and thrombus formation[151, 152]. Together, these observations raise the intriguing possibility that parameters derived from 4D Flow could eventually be used as imaging biomarkers to improve embolic risk stratification in clinical practice, particularly in patients in SR. Nevertheless, it is currently unclear whether LA 4D Flow parameters can be measured in a reproducible fashion. Hence, the first step to clinical application is systematic evaluation of reproducibility and temporal variation, as these directly impact on diagnostic performance and hence the feasibility and power calculations for larger-scale studies. Although analysis of LA 4D flow parameters by MRI is more time-consuming than the collection of simpler measurements, such as LA volume and emptying fraction, direct assessment of a key

component of the Virchow's triad would be highly attractive if able to identify patients in SR or with a low AF burden (e.g., not identified by short-term ECG monitoring [177]) who would benefit from anticoagulation. In the present study, we aimed to evaluate and compare the reproducibility of a number of LA flow characteristic parameters[28, 155], both within the same session and over time. We included subjects with AF or SR and a wide range of clinical stroke risk, to provide information on reproducibility across a heterogeneous and clinically-relevant population.

3.3 Methods

This study was undertaken in a single tertiary centre (University of Oxford, Radcliffe Department of Medicine, Oxford, UK). The study protocol was approved by a local Research Ethics Committee, and all patients gave written informed consent.

3.3.1 Design

Patients (in AF or SR) were prospectively non-consecutively recruited from a number of sources at our institution, including outpatient clinics, the waiting list for electrical cardioversion, clinical CMR referrals, a pool of control subjects who had participated in other research studies, and through word of mouth. Young healthy volunteers in SR (N=14, 16%) were recruited under an ethically approved departmental technical development protocol and provided verbal consent (as specified in the protocol).

Subjects were recruited with a wide range of clinical stroke risk, as assessed by the CHA_2DS_2VASc score[29]. Patient medical records were screened to document stroke risk factors where available, and a research questionnaire designed to collect this information was administered to all participants.

3.3.2 CMR imaging protocol

CMR examinations were performed by one of three operators (AF, PM, or MS) on one of two 3 Tesla MRI systems (Verio syngo MR B17 and MAGNETOM Prisma VE11C, both Siemens, Germany). Details are reported in Chapter 2. Briefly, at the baseline scan, the CMR protocol included retrospectively ECG-gated time-resolved balanced steady-state free precession (SSFP) cine imaging in horizontal long axis ('four-chamber') and vertical long-axis ('two-chamber'), for the evaluation of LVEF and volumes, and LAEF and volumes as previously described[157, 178]. All images were analysed using cvi42 software (v.5.3.4, Circle Cardiovascular Imaging Inc, Calgary, AB, Canada).

Additionally, the 4D Flow sequence was undertaken twice during the same baseline session with removal of the subject from the scanner and performing repeat isocentre positioning (scan 1a and scan 1b) for determination of 'same-day scan-rescan' variability. The same 4D Flow sequence was also undertaken again at an interval of approximately 1 month in the same scanner (scan 2) for determination of 'interval scan-rescan' variability. In 4 subjects (5%) in whom 'same-day scan-rescan' variability had not been determined at scan 1, this was done during scan 2 instead. The 4D Flow protocol included retrospectively ECG-gated

time-resolved 3D phase-contrast MRI with 3-directional velocity encoding ('4D flow') imaging to allow in vivo assessment of blood flow velocities in the LA. In two cases (2%), a prospectively triggered 4D flow sequence was used instead.

The 4D flow MRI data were acquired during free breathing using navigator gating of diaphragmatic motion, with the following sequence protocols (A, B, C, and D) with breakdown figures of participants that were investigated with each protocol (Table 2).

Table 2: 4D Flow protocols used in the reproducibility study.

Protocols	**Scanner system**	**Acquisition**	**N of participants (% out of 86 total)**
Main study protocols			
A	Verio syngo	Retrospective	33 (38%)
B	MAGNETOM Prisma	Retrospective	44 (51%)
Other research protocols			
C	Verio syngo	Prospective	2 (2%)
D	MAGNETOM Prisma	Retrospective	7 (8%)

All follow-up scans were performed using the same MRI protocol as the baseline scan. The 4D flow MRI data were acquired during free breathing using navigator gating of diaphragmatic motion. Protocols details are as follows:

Main study protocols:

A) RETROSPECTIVE SEQUENCE - Verio syngo MR B17 Siemens, Germany:

flip angle =6°, spatial resolution/voxel size 3.0×3.0×3.0 mm, temporal resolution (TR) = 48.8 ms, reconstructed to 30 time frames, TE = 3.66 ms, imaging acceleration (GRAPPA technique) with an acceleration factor of R=3, total acquisition time = 10-20 min depending on heart rate, velocity encoding sensitivity = 110 cm/s. The FOV was axial and adjusted to encompass the entire left atrium in each subject.

B) RETROSPECTIVE SEQUENCE - MAGNETOM Prisma VE11C, Siemens, Germany:

flip angle =6°, spatial resolution/voxel size 3.0×3.0×3.0 mm, TR = 43.5 ms, reconstructed to 30 time frames, TE = 3.42 ms, imaging acceleration (GRAPPA technique) with an acceleration factor of R=3, total acquisition time = 5-20 min depending on heart rate, velocity encoding sensitivity = 110 cm/s. The FOV was axial and adjusted to encompass the entire left atrium in each subject.

Other research protocols:

C) PROSPECTIVE SEQUENCE - Verio syngo MR B17 Siemens, Germany:

flip angle =6°, spatial resolution/voxel size 3.0×3.0×3.0 mm, temporal resolution (TR) = 48.8 ms, reconstructed to 14-15 time frames, TE = 3.66 ms, imaging

acceleration (GRAPPA technique) with an acceleration factor of R=3, total acquisition time = 5-15 min depending on heart rate, velocity encoding sensitivity = 110 cm/s. The FOV was axial and adjusted to encompass the entire left atrium in each subject.

D) RETROSPECTIVE SEQUENCE - MAGNETOM Prisma VE11C, Siemens, Germany:

flip angle =7°, spatial resolution/voxel size 2.4×2.4×2.5 mm, TR = 39.5 ms, reconstructed to 30 time frames, TE = 2.39 ms, imaging acceleration (GRAPPA technique) with an acceleration factor of R=3, total acquisition time = 10-20 min depending on heart rate, velocity encoding sensitivity = 110 cm/s. The FOV was axial and adjusted to encompass the entire left atrium in each subject.

3.3.3 LA 4D Flow processing

All 4D flow were acquired with Maxwell term correction[161], DICOM tools from the OXSA toolbox were used [162], and data were corrected for velocity aliasing[163], and eddy currents[164] using Matlab-based in-house software designed by ATH and MS (MATLAB R2015 8.6.0.267246; Mathworks, Nattick, USA), available on the Oxford University Research Archive (ORA) platform (https://doi.org/10.5287/bodleian:ey4ovzdbB). A three-dimensional time-averaged phase contrast angiogram was generated to facilitate better orientation in the context of the atrial anatomy and interpretation of the flow data[165]. To isolate

the atrial velocity data, data analysis included 3D segmentation of the minimum LA volume (directly on magnitude images in the 4D Flow dataset) using cvi42 software.

Two sets of parameters were derived from 4D flow dataset: (A) absolute velocities and (B) directionality of flow and LA flow patterns.

The absolute atrial velocities for each voxel inside the segmented LA were determined as described previously[28]. Briefly, for each voxel, the peak & mean velocities (m/s) were determined; stasis was calculated as the ratio of the total number of cardiac time frames (n) with a velocity below the threshold of 0.1 m/s (n stasis) to the total number of frames (NTot) [28, 149]: stasis = $\frac{\text{n stasis}}{\text{NTot}}$. Global LA stasis was defined as the average proportion of stasis across all LA voxels and it is expressed as a proportion from 0 to 1, where 0 is the lowest amount of stasis and 1 is the highest[28, 149].

Regarding flow patterns, a 4D velocity field within the LA was used to generate 3D pathlines and to evaluate atrial flow patterns during both ventricular systole and diastole using the Runge-Kutta method[166, 167] with Ensight software (ANSYS 2019 R1, Canonsburg, PA, USA). Pathlines were emitted at each time-frame from probe planes positioned at each of the pulmonary veins (starting at the beginning of the cardiac cycle), allowing derivation of flow patterns inside the atrium during both ventricular systole and diastole (based on mitral valve opening time derived from the magnitude images). Flow patterns were evaluated after quality control steps were applied, as previously described[168]. Normal flow within the LA is characterized by the presence of a vortex[150, 166, 169] (i.e. pathlines with a

circular/elliptic trajectory). Atypical flow patterns observed were classified visually into *short-ranged* vortex (pathlines failing to reach the mitral valve plane during one averaged cardiac cycle), and into *other patterns*. Further, for all scans, after flow denoising using divergence free wavelets[170], the volumes of the largest vortex rings inside the LA were calculated automatically using the lambda2 (λ2) method[166]. In each case, a specific lambda threshold for vortices was defined as half the mean λ2 value over the cardiac cycle[155]. LA vortex volume (ml) is reported as the mean of LA vortex volumes throughout the cardiac cycle alongside peak LA vortex volumes (ml) within systole and diastole. Finally, we also applied a measure of tendency of the blood flow to rotate using the volume-averaged magnitude of vorticity (units radians/sec)[171, 172], after flow denoising [170]. LA vorticity is reported as the area under the vorticity-time curve over the entire cardiac cycle (in radians or rad).

3.3.4 Blinding

All imaging assessments (including LA and LV function, 4D flow parameters, and flow visualization data) for all the scans (including scan 1a, 1b, and 2) were conducted by investigators blinded to all clinical information including rhythm at the time of the scan. After appropriate training, a single observer (GPA) contoured all cine imaging and LA 4D Flow sequence, according to a dedicated in-house post-processing protocol. A single observer (AS) processed all the qualitative data regarding flow patterns using the Ensight software, according to a separate dedicated in-house post-processing protocol. To evaluate intra-observer variability, the scans were re-contoured by the same observer (GPA) after an interval of at least 2 weeks. Inter-observer variability was conducted independently by a second

independent observer (MS) according to the same post-processing protocol, and the 2 observers were blinded to each other. In order to ensure that the observers of scan 1a were blinded to the results of their own analysis of scan 1a and 1b (for intra-/inter- observer CV and rescan CV), the contours performed by GPA/MS were then imported into our MATLAB software independently by AS who produced the MATLAB output with the results. Finally, to evaluate interval-scan CV, scan 1 and scan 2 were anonymized with a different code in a way that it was impossible to ascertain that scan 1 and 2 belonged to the same research participant.

3.3.5 Statistical analysis

Data were examined for normality by visual inspection of histograms and Q-Q plots, and for homoscedasticity using Levene's test. Data are shown as mean ± SD if normally distributed, or median (Q1-Q3) if non-normally distributed, or number (percentage), unless otherwise specified.

To quantify reproducibility and temporal variability, the following metrics were used: Bland-Altman limits of agreement and the CV[179], which was calculated using the root mean square method and is reported as a proportion (from 0 to 1). Bootstrap resampling (1000 samples) was used to calculate a non-parametric 95% confidence interval (CI) for the CV[179], as well as to estimate 95% CIs and p-values for the difference in CV values between independent groups (i.e. AF vs SR patients; subjects with longitudinal change ≥10 mmHg vs <10 mmHg in blood pressure; and subjects with longitudinal change ≥10 bpm vs <10 bpm in heart rate, where changes are calculated from scan 1a to scan 2). A similar resampling strategy

(10,000 bootstrap samples) was used to test differences between dependent CVs (e.g. scan-rescan vs scan-interval scan). Further, the absolute agreement of the LA flow characteristics values obtained by the two independent observers (i.e. inter-rater variability) was assessed using the intra-class correlation coefficient (ICC) with a two-way mixed model.

Normally-distributed baseline data with equal variances across two independent groups (e.g. AF vs SR) were compared using the unpaired t-test, and Welch's tests for normal data with unequal variances. Non-normally distributed unpaired baseline data were compared using the Mann-Whitney U test. Categorical baseline data were compared by using the Chi square or Fischer's exact tests (if cell size <5). Flow patterns from related measures were compared with McNemar's test. Inter-correlations among flow parameters were calculated using Pearson's coefficient with 1000 bootstraps 95% CI (with sampling stratification for rhythm at the time of the scan).

All tests were 2-tailed, and values of $p<0.05$ were considered significant. All p values from pairwise comparisons were adjusted using the Bonferroni method.

We calculated that recruitment of a minimum of 74 subjects would provide 90% power (with two-tailed 0.05 type I error) to detect a 0.01 point mean difference in LA stasis between scan and rescan and between scan and interval scan, with an expected standard deviation of differences of 0.05 and pre-defined clinical agreement limit of 0.15 (based on pilot data).

Statistical analyses were performed with IBM SPSS Statistics for Windows (version 25.0, IBM Corp, Armonk, NY), R 3.6.3 for computation of CV and bootstrapped 95% CI, GraphPad Prism version 6.01 (GraphPad Software, San Diego, CA) for the figures and graphs, and MedCalc Version 19.1.3 (MedCalc Software, Belgium, BE) for power calculations.

3.4 **Results**

A total of 86 participants were included: 64 in SR at the time of the scan, and 22 in AF at the time of the scan. Baseline characteristics of all subjects are summarised in **Table 3**.

Table 3: Baseline clinical characteristics.

		Rhythm at the time of scan		*SR vs AF*
	Whole cohort	Sinus Rhythm (SR)	Atrial Fibrillation (AF)	P value
N Total	**86**	**64**	**22**	
Age, years old	66 (54 - 71)	66 (48 - 72)	66 (58 - 69)	0.984
Male / BSA, m^2 / BMI, Kg/m^2	54 (63) / 2.0 ± 0.2 / 27.5 ± 5.2	36 (56) / 1.9 ± 0.2 / 27.0 ± 5.4	18 (82) / 2.1 ± 0.2 / 28.8 ± 5.3	**0.041 / <0.001/** 0.190
CHA_2DS_2VASc	2 (0 – 4)	2 (0 – 4)	2 (1 – 3)	0.915
Hypertension /Heart Failure	47 (55) / 8 (9)	34 (53) / 2 (3)	13 (59) / 6 (27)	0.804 / **0.003**
Diabetes / Vascular	11 (13) / 12 (14)	10 (16) / 9 (14)	1 (5) / 3 (14)	0.276 / >0.999
Stroke or TIA	5 (6)	3 (5)	2 (9)	0.599
Paroxysmal / Persistent / Permanent AF	2 (2) / 17 (20) / 5 (6)	2 (3) / 0 (0) / 0 (0)	0 (0) / 17 (77) / 5 (23)	0.615 / **<0.001 / 0.001**
Systolic / Diastolic BP, mmHg	118 (112 - 128) / 69 ± 10	120 (113 - 134)/ 67 ± 10	113 (109 - 119) / 74 ± 10	**0.005 / 0.005**
Heart Rate, bpm	67 (60 - 75)	63 (57 - 69)	77 (70 - 83)	**<0.001**
LV EDV, ml	150 (127 - 180)	146 (125 - 170)	166 (129 - 210)	**0.049**
LV EF, %	60 (50 - 66)	63 (58 – 67)	45 (39 - 51)	**<0.001**
LA volume, ml	91 (73 - 116)	86 (69 - 100)	120 (101 - 171)	**<0.001**
LA EF, %	44 ± 19	54 ± 10	17 ± 7	**<0.001**

Values are expressed as mean ± SD or median (q1-q3) or N (%). Significant P values (<0.05) are shown in bold. BMI, body mass index; BSA, body surface area; HR, heart rate; DBP, diastolic blood pressure; SBP, systolic blood pressure; TIA, transient ischaemic attack; LV, Left Ventricle; EDV, End Diastolic Volume; LA, Left Atrium; EF, Ejection Fraction or Emptying Fraction.

As expected, AF patients had profoundly altered LA flow characteristics compared to subjects in SR, as characterised by greater stasis, lower peak velocity, lower vorticity, and larger vortex size (all p≤0.001; **Figure 11**), as well as changes in other LA flow measurements (**Table 4).**

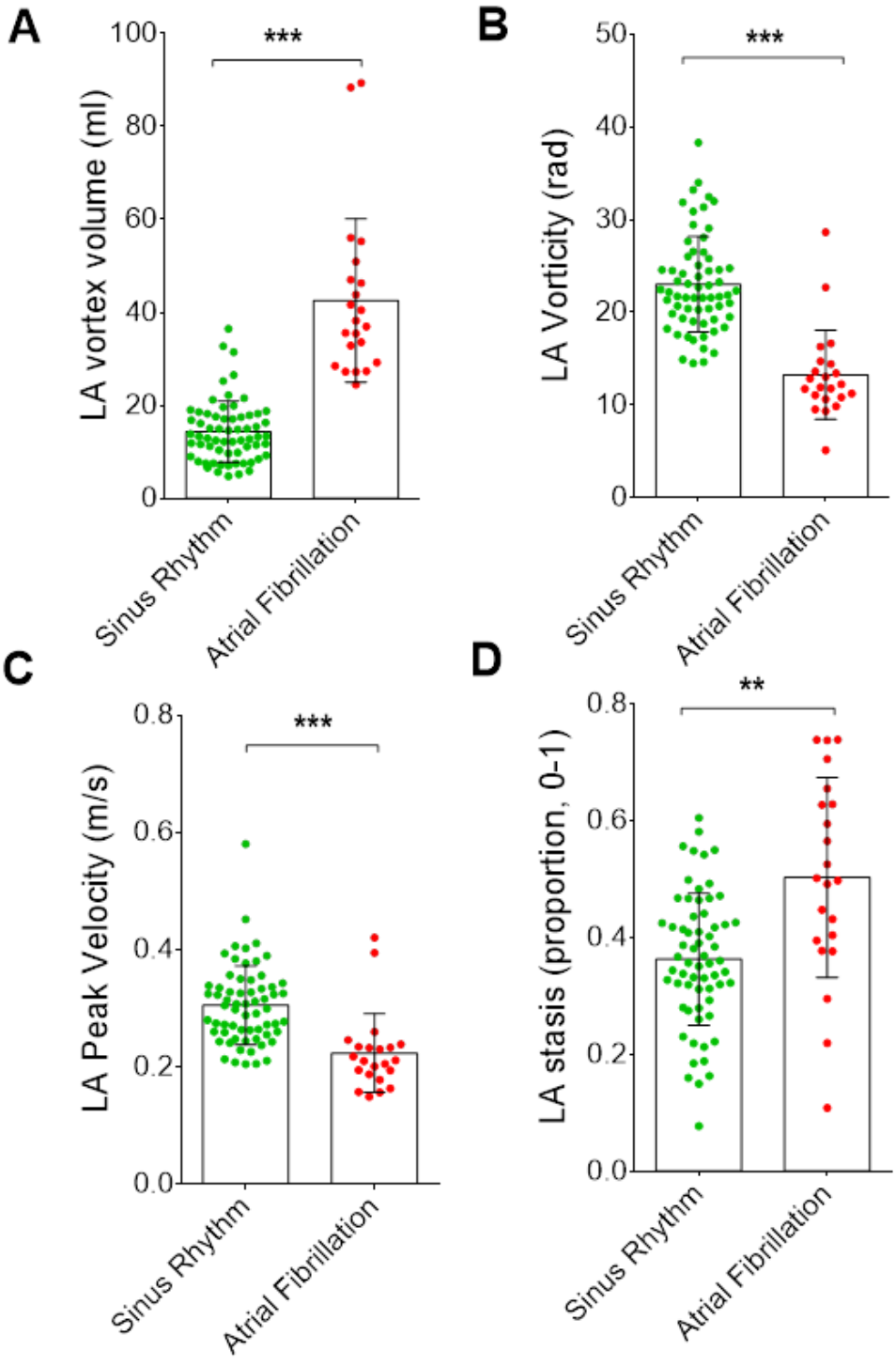


Figure 11: Comparison in LA flow characteristics in SR and AF at baseline. *LA mean vortex volume (A), LA vorticity (B), LA peak velocity (C), and LA stasis (D) in the overall study cohort stratified per rhythm at the time of the scan. Data expressed as mean ± SD. Statistically significant P values are marked (*P<0.05), and smaller P values are stratified by size (**P<0.01, ***P<0.001).*

Table 4: Baseline LA flow characteristics

	Rhythm at the time of scan		
	Sinus Rhythm	Atrial Fibrillation	P value
N Total	**64**	**22**	**-**
Global LA flow			
LA stasis, proportion 0-1	0.36 ± 0.11	0.50 ± 0.17	**0.001**
LA peak velocity, m/s	0.30 ± 0.07	0.22 ± 0.07	**<0.001**
LA mean velocity, m/s	0.14 ± 0.03	0.11 ± 0.03	**0.001**
LA vortex volume (mean), ml	14 ± 6.6	42 ± 17	**<0.001**
LA vorticity, rad	23.0 ± 5.1	13.2 ± 4.8	**<0.001**
Systolic patterns			
LA vortex pattern	56 (87)	2 (9)	**<0.001**
LA peak vortex volume (systole), ml	19 ± 9	48 ± 22	**<0.001**
LA short-range vortex	1 (2)	17 (77)	**<0.001**
Other patterns	7 (11)	3 (14)	0.733
Diastolic patterns			
LA vortex pattern	43 (67)	5 (23)	**<0.001**
LA peak vortex volume (diastole), ml	18 ± 8	48 ± 21	**<0.001**
LA short-range vortex	0 (0)	11 (50)	**<0.001**
Other patterns	21 (33)	6 (27)	0.629

Values are expressed as mean ± SD or median (q1-q3) or N (%). Significant P values (<0.05) are shown in bold.

A total of 84 baseline scans (62 in SR and 22 in AF) were re-contoured and re-analysed by the same blinded investigator, while 75 baseline scans (53 in SR and 22 in AF) were also re-contoured and re-analysed by a second blinded investigator. A total of 85 participants (63 in SR and 22 in AF) underwent the same 4D Flow sequence twice during the same visit with removal from the scanner and re-positioning for assessment of same-day scan-rescan variability. After an interval of 30 (27-35) days, the scan was repeated ('scan 2') in 74 subjects (56 in SR and 18 in AF) for assessment of interval scan-rescan variability. All subjects scanned in SR at scan 1 were in SR at scan 2, and all subjects scanned in AF at scan 1 remained in AF at scan 2.

3.4.1 Reproducibility and temporal variability in the whole cohort

Intra-observer and inter-observer CVs ranged from 1 to 3% and from 4 to 8%, respectively, for LA mean and peak velocity, and stasis (**Table 5** and **Figure 12**), but were larger for vortex volume, which displayed an intra-observer CV of 7.6% and an inter-observer CV of 11.2%.

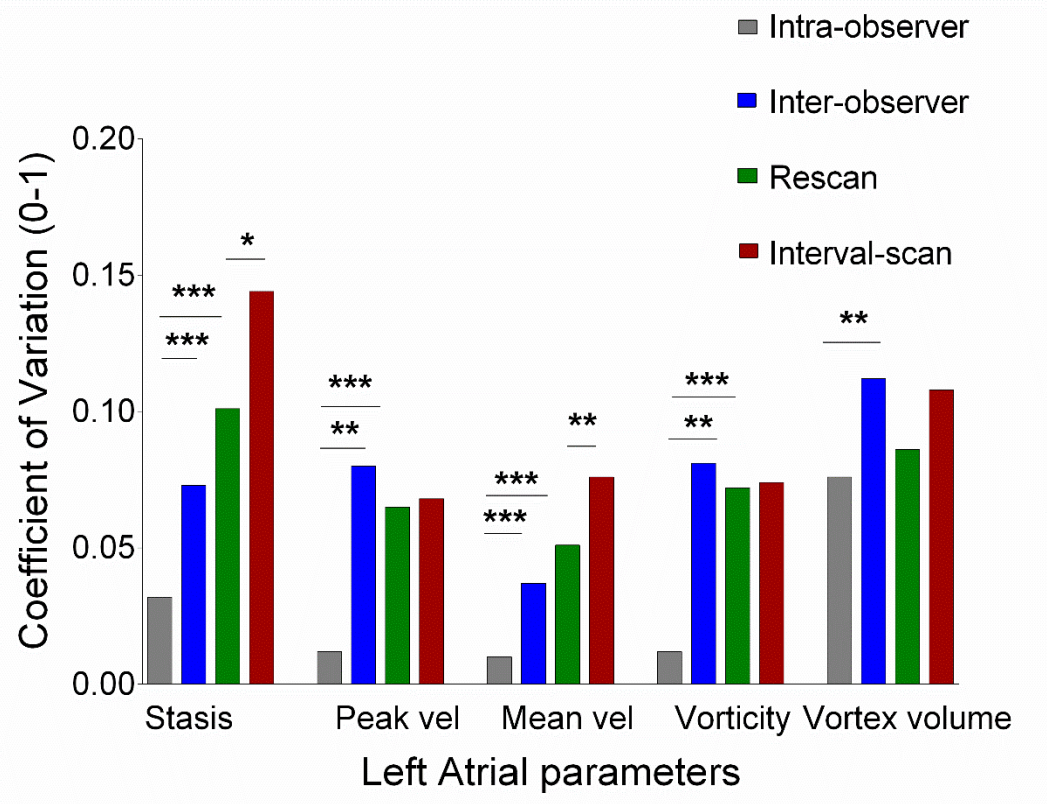


Figure 12: Variability assessment of LA 4D Flow parameters. *Coefficients of variation (CV) for each flow parameter for intra-observer (grey), inter-observer (blue), rescan (green), and interval scan (red).CV are expressed as proportion (0-1). Statistically significant P values are marked *(<0.05), and smaller P values are stratified by size (**P<0.01, ***P<0.001).*

Table 5.

Table 5. Reproducibility in the whole cohort

		1	2	3	4	1 vs 2	1 vs 3	2 vs 3	3 vs 4
		Intra-observer **N = 84**	Inter-observer **N = 75**	Same-day Rescan **N = 85**	Interval Scan **N = 74**	**p value for CV**			
LA stasis, %	CV (95% CI)	0.032 (0.023-0.041)	0.073 (0.052-0.097)	0.101 (0.080-0.124)	0.144 (0.116-0.175)	**<0.001**	**<0.001**	0.076	**0.015**
	Bias (BA limits)	0.01 (-0.02 to 0.02)	0.00 (-0.09 to 0.07)	0.00 (-0.09 to 0.09)	-0.01 (-0.16 to 0.14)	n/a	n/a	n/a	n/a
LA peak velocity, m/s	CV (95% CI)	0.012 (0.009-0.015)	0.080 (0.039-0.131)	0.065 (0.042-0.093)	0.068 (0.058-0.079)	**0.007**	**<0.001**	0.645	0.795
	Bias (BA limits)	0.00 (-0.01 to 0.01)	0.01 (-0.09 to 0.07)	0.00 (-0.05 to 0.06)	0.00 (-0.05 to 0.06)	n/a	n/a	n/a	n/a

LA mean velocity, m/s	CV (95% CI)	0.010 (0.008-0.013)	0.037 (0.025-0.051)	0.051 (0.038-0.064)	0.076 (0.063-0.088)	**<0.001**	**<0.001**	0.134	**0.007**
	Bias (BA limits)	0.00 (0.00 to 0.00)	0.00 (-0.01 to 0.01)	0.00 (-0.02 to 0.02)	0.00 (-0.03 to 0.03)	n/a	n/a	n/a	n/a
LA vorticity, rad	CV (95% CI)	0.012 (0.010-0.014)	0.081 (0.041-0.126)	0.072 (0.052-0.094)	0.074 (0.059-0.090)	**0.002**	**<0.001**	0.816	0.875
	Bias (BA limits)	0.00 (-0.73 to 0.73)	-0.17 (-4.67 to 4.32)	-0.01 (-4.12 to 4.15)	0.41 (-3.90 to 4.73)	n/a	n/a	n/a	n/a
LA vortex volume, ml	CV (95% CI)	0.076 (0.053-0.099)	0.112 (0.083-0.143)	0.086 (0.059-0.115)	0.108 (0.080-0.137)	**0.045**	0.564	0.172	0.254
	Bias (BA limits)	-1.12 (-5.44 to 3.05)	-1.18 (-6.45 to 4.10)	0.42 (-3.22 to 4.06)	-0.51 (-7.32 to 60.30)	n/a	n/a	n/a	n/a

Within-subject Coefficients of Variation (CV, reported as proportion) are presented with bootstrapped 95% CIs (1000 bootstraps). Mean bias and Bland-Altman (BA) 95% limits of agreement are also reported. P values are obtained by bootstrapped differences (10000 bootstraps) between CV values for each parameter. Significant P values (<0.05) are shown in bold.

Inter-observer variability was excellent for all parameters (ICC ≥ 0.91, all p < 0.001, **Table 6**).

Table 6. Inter-rater Correlation Coefficient (ICC).

	Inter-rater ICC (95% CI) **N = 75**	p value
LA stasis, proportion 0-1	0.98 (0.96 – 0.98)	**p < 0.001**
LA peak velocity, m/s	0.91 (0.85 – 0.94)	**p < 0.001**
LA mean velocity, m/s	0.99 (0.98 – 0.99)	**p < 0.001**
LA vorticity, rad	0.97 (0.95 – 0.98)	**p < 0.001**
LA vortex volume, ml	0.99 (0.98 – 0.99)	**p < 0.001**

Inter-Rater Correlation Coefficient (ICC) is reported with (95% CI). Significant P values (<0.05) of the two-way mixed effects models are shown in bold. LA; Left Atrium.

Scan-rescan variability ranged between 5% and 7% for all LA flow parameters, except for vortex volume and stasis (CVs of 9% and 10%, respectively).

Interval-scan variability ranged from 7% (for peak velocity and vorticity) to 14% (for stasis, **Table 5** and **Figure 13**).

Bland-Altman plots are presented in **Figure 13** (for intra- and inter-observer measurements) and in **Figure 14** (for rescan and interval scan measurements), with the corresponding mean bias and 95% limits of agreement (LoA) reported in **Table 5**. Bland-Altman plots revealed no likely proportional bias for any parameter except LA vortex volume which displayed a wider spread at higher values in the interval scan (**Table 5** and **Figure 14**).

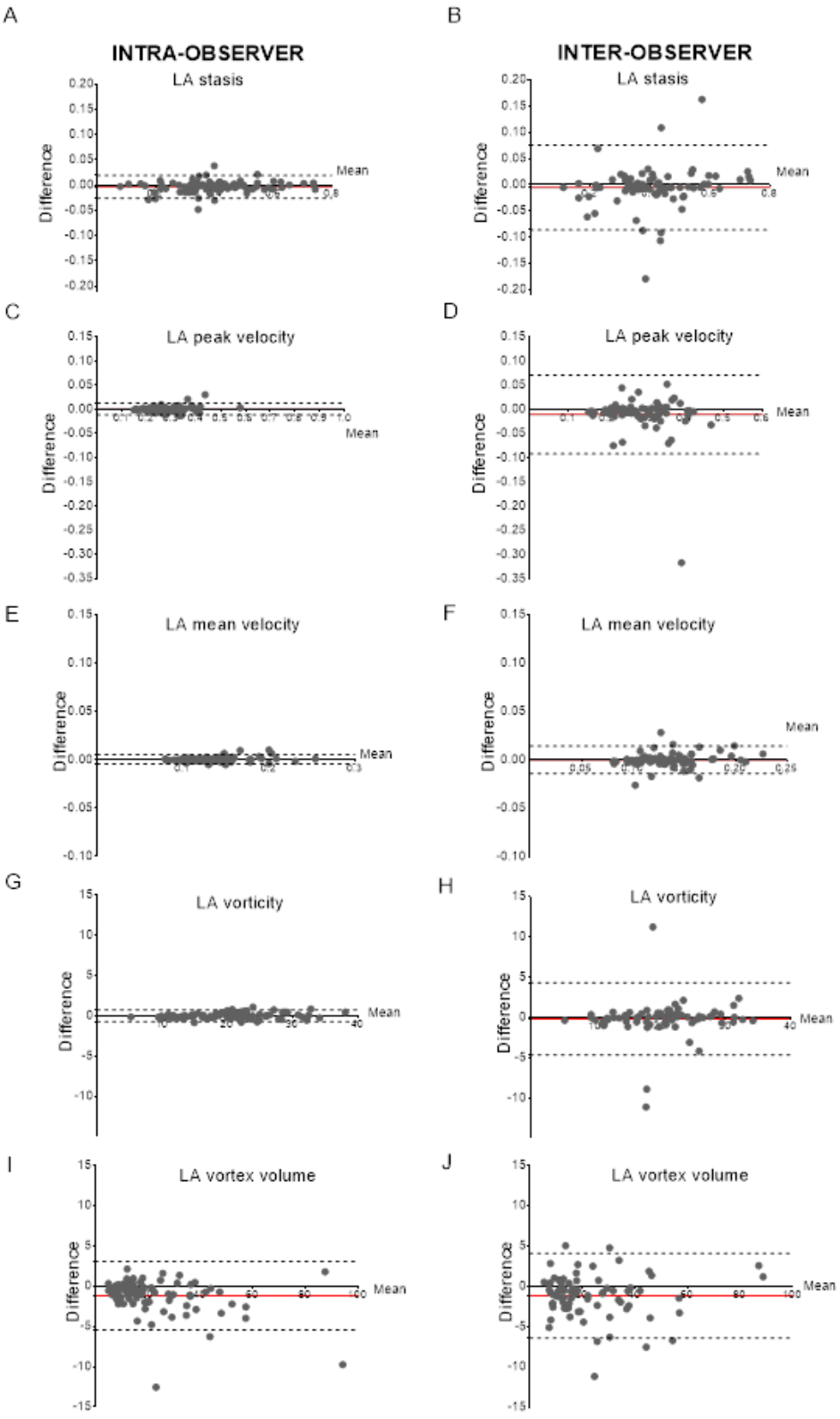


Figure 13: Intra- and Inter-observer Bland-Altman plots. *Bland-Altman plot of intra-observer (A, C, E, G, I) and inter-observer (B, D, F, H, J) variability in LA stasis, LA peak velocity, LA mean velocity, LA vorticity, and LA vortex volume in the whole population.*

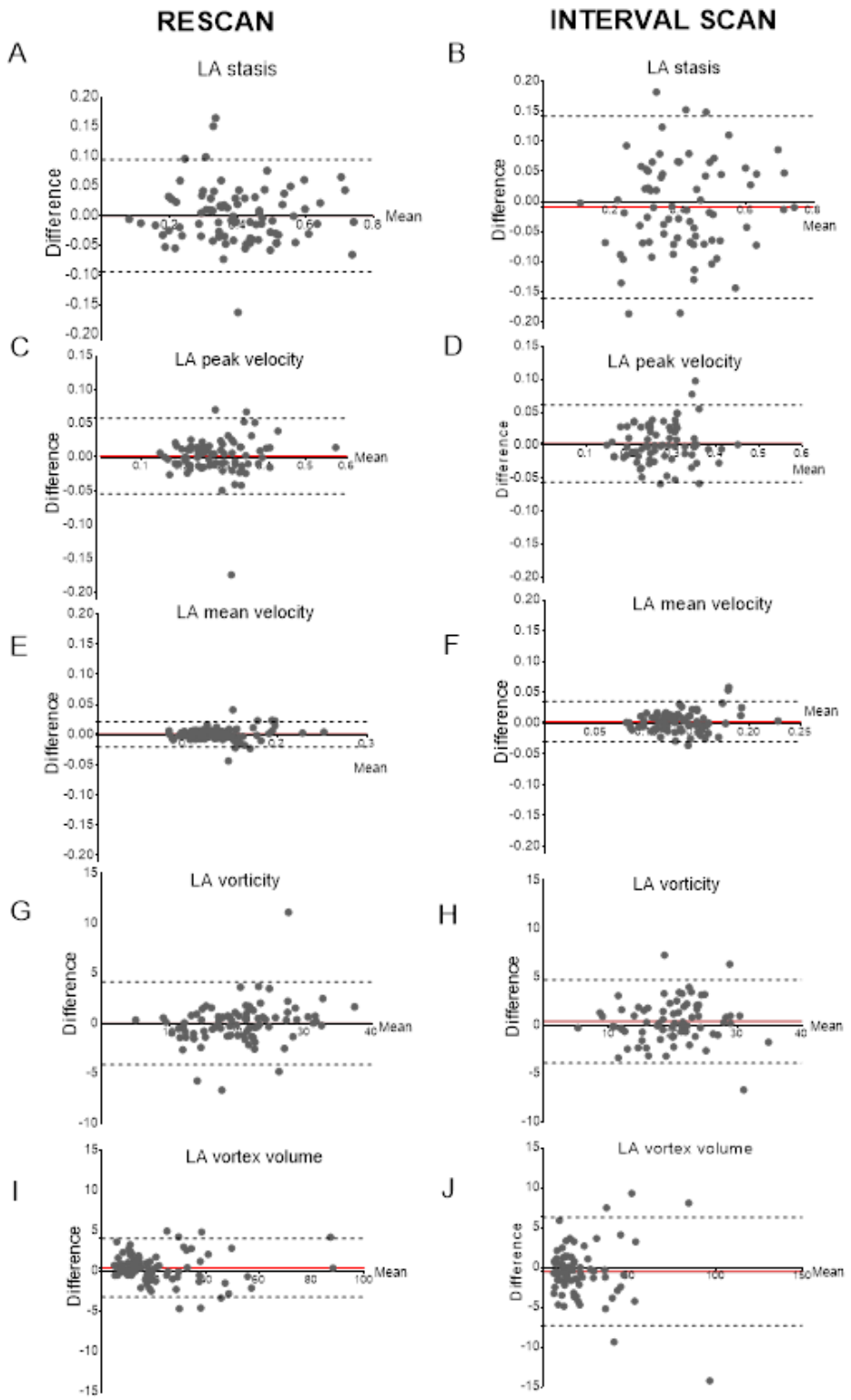


Figure 14: Rescan and Interval-scan Bland-Altman plots. *Bland-Altman plot of rescan variability (A, C, E, G, I) and interval scan variability (B, D, F, H, J) in LA stasis, LA peak velocity, LA mean velocity, LA vorticity, and LA vortex volume in the whole population.*

Analyses of the reproducibility and temporal variability of qualitative flow patterns assessed by means of pathlines are presented in **Table 7**. There were no significant paired changes in flow patterns between scan and rescan and no significant changes over time in the interval scans (all $p>0.05$; **Table 7**).

Table 7. Reproducibility and temporal variability of flow patterns

	Scan (N = 84)	**Same-day Rescan (N = 84)**	P value	**Scan (N = 74)**	**Interval scan (N = 74)**	P value
Systolic patterns						
LA vortex pattern	56 (67)	54 (64)	0.500	50 (68)	51 (69)	>0.999
LA short-range vortex	18 (21)	19 (24)	>0.999	16 (22)	15 (20)	>0.999
Others	10 (12)	11 (13)	>0.999	8 (11)	8 (11)	>0.999
Diastolic patterns						
LA vortex pattern	46 (55)	46 (55)	>0.999	37 (50)	41 (55)	0.454
LA short-range vortex	11 (13)	10 (12)	>0.999	11 (15)	9 (12)	0.625
Others	27 (31)	28 (33)	>0.999	26 (35)	24 (32)	0.815

Data presented as N (%). P values refer to paired comparison of proportions by McNemar's test.

Significant P values (<0.05) are shown in bold.

3.4.2 Assessment of sources of variability in LA flow characteristics

In order to assess the sources of variability, comparison among CVs is reported for all flow parameters in **Table 4** and **Figure 11.**

All flow parameters showed statistically significant differences in variability due to manual segmentation by two independent observers (intra-observer vs inter-observer CV differences from 3% to 7%, all $p<0.05$, **Table 4** and **Figure 11**). By contrast, we found no significant differences in variability related to the rescan (i.e., to repositioning and re-acquisition within the same session) over inter-observer variability for any of the parameters evaluated ($p>0.05$), although all parameters (except for LA vortex volume) showed a significantly higher rescan variability than intra-observer variability ($p<0.001$). Finally, interval-scan variability was significantly higher than the technical rescan variability for LA stasis and LA mean velocity (both $p<0.05$), but not for other flow parameters (all $p>0.05$) (**Table 4** and **Figure 11)**.

Rescan and interval scan CVs, stratified for rhythm at the time of the scan (AF and SR), are shown for each parameter in **Table 8**. We found no significant differences in rescan CVs by rhythm for any of the evaluated LA flow parameters (all $p>0.05$). However, patients in AF displayed lower interval scan CV for stasis, mean velocity, and vortex volume (all $p<0.05$) compared with patients in SR. By contrast, no significant differences in interval scan CVs by rhythm were present for vorticity and peak velocity (all $p>0.05$).

Table 8. Coefficient of Variations for rescan and interval-scan variability by rhythm at the time of the scan.

	SR	**AF**	**AF-SR Difference (95%CI)**	**P value**
CV scan-rescan				
LA stasis	0.104	0.085	-0.019 (-0.07, 0.039)	0.504
LA mean velocity	0.049	0.054	0.006 (-0.025, 0.042)	0.759
LA peak velocity	0.051	0.089	0.038 (-0.014, 0.105)	0.271
LA vortex volume	0.093	0.055	-0.038 (-0.077, -0.002)	0.051
LA vorticity	0.057	0.103	0.046 (-0.003, 0.094)	0.062
CV scan-interval				
LA stasis	0.161	0.075	-0.087 (-0.128, -0.046)	**<0.001**
LA mean velocity	0.082	0.055	-0.027 (-0.048, -0.006)	**0.013**
LA peak velocity	0.07	0.064	-0.006 (-0.026, 0.013)	0.546
LA vortex volume	0.119	0.063	-0.056 (-0.094, -0.018)	**0.004**
LA vorticity	0.069	0.085	0.016 (-0.018, 0.048)	0.353

CV; Coefficient of Variation. CI; Confidence Interval. LA; Left Atrium. Significant P values (<0.05) are shown in bold.

Finally, we conducted analysis to investigate whether changes in heart rate (HR) and blood pressure (BP) from scan 1a to scan 2 were associated with differences in interval scan variability (from scan 1a to scan 2) for any of the evaluated LA flow parameters. Interval-scan CVs stratified by 'ΔHR≥10 bpm vs ΔHR<10 bpm' and 'ΔBP≥10 mmHg vs ΔBP<10 mmHg' longitudinal changes are reported for each parameter in **Table 9-10**. We found no significant differences in interval-scan CVs by BP for any of the evaluated flow parameters (all p>0.05). However, ≥10 bpm longitudinal changes in HR were associated with higher interval-scan variability for stasis (CV = 17% for ≥10 bpm vs 10% for <10 bpm; p=0.024); and were borderline associated with higher interval-scan variability for LA mean velocity (CV = 8.5% for ≥10 bpm vs 6.0% for <10 bpm; p=0.067), see **Table 9**. Notably, we found that longitudinal changes in heart rate correlated with changes in LA mean velocity and stasis (p=0.014 and p=0.021, respectively), with reduction of heart rate linked to lower mean velocity and increased stasis (Spearman's coefficient = -0.29 and -0.27, respectively).

Table 9. Coefficient of Variations for interval-scan variability by heart rate paired changes between baseline and interval-scan.

	HR <10 bpm (N=49)	**HR ≥10 bpm (N=24)**	**Difference (95% CI)**			**P value**
CV Scan-interval						
LA stasis	0.104	0.173	0.069	0.008	0.125	**0.024**
LA mean velocity	0.060	0.085	0.025	-0.002	0.051	0.067
LA peak velocity	0.061	0.068	0.006	-0.016	0.028	0.605
LA vortex volume	0.088	0.119	0.031	-0.029	0.085	0.330
LA vorticity	0.065	0.076	0.010	-0.020	0.038	0.497

CV; Coefficient of Variation. CI; Confidence Interval. Heart Rate; HR. LA; Left Atrium.

Significant P values (<0.05) are shown in bold.

Table 10. Coefficient of Variations for interval-scan variability by blood pressure paired changes between baseline and interval-scan.

	Systolic BP <10 mmHg (N=45)	**Systolic BP ≥10 mmHg (N=28)**	**Difference (95% CI)**			**P value**
CV scan-interval						
LA stasis	0.130	0.140	0.010	-0.048	0.067	0.723
LA mean velocity	0.066	0.077	0.011	-0.014	0.037	0.412
LA peak velocity	0.058	0.071	0.013	-0.008	0.033	0.228
LA vortex vol	0.087	0.118	0.031	-0.024	0.083	0.287
LA vorticity	0.068	0.072	0.004	-0.026	0.034	0.840

	Diastolic BP <10 mmHg (N=59)	**Diastolic BP ≥10 mmHg (N=14)**	**Difference (95% CI)**			**P value**
CV scan-interval						
LA stasis	0.075	0.057	-0.019	-0.055	0.016	0.269
LA mean velocity	0.068	0.053	-0.014	-0.045	0.013	0.290
LA peak velocity	0.106	0.085	-0.021	-0.067	0.024	0.370
LA vortex vol	0.071	0.065	-0.006	-0.049	0.036	0.693
LA vorticity	0.145	0.099	-0.046	-0.116	0.02	0.164

CV; Coefficient of Variation. CI; Confidence Interval. BP; Blood Pressure. LA; Left Atrium. Significant P values (<0.05) are shown in bold.

Inter-correlation among flow parameters is reported in **Table 11**. Peak and mean velocity and stasis all display strong and significant inter-correlation (all r ≥ 0.9, all p<0.001), whilst vorticity and vortex volume display moderate or mild correlation with the other flow parameters (all r ≤ 0.8, all p<0.01).

Table 11. Inter-correlation among LA flow parameters stratified by rhythm

	LA stasis			
LA peak velocity	-0.88** (-0.84 to -0.92)	**LA peak velocity**		
LA mean velocity	-0.94** (-0.96 to -0.93)	0.95** (0.92 to 0.97)	**LA mean velocity**	
LA vorticity	-0.71** (-0.84 to -0.92)	0.81** (0.71 to 0.89)	0.75** (0.64 to 0.83)	**LA vorticity**
LA vortex volume	0.34** (0.02 to 0.71)	-0.38** (-0.70 to -0.13)	-0.26* (-0.66 to 0.07)	-0.47** (-0.71 to -0.24)

Pearson's Correlation Coefficients were calculated with bootstrapped 95%CI (1000 resamples) stratified by rhythm. Significant P values are stratified as follows: * (P<0.05), ** (P<0.01).

3.5 Discussion

This is the first study investigating reproducibility and temporal variability of LA flow characteristic parameters, which is an important first step to determining their potential clinical applicability and use as imaging biomarkers. Using a large and comprehensive dataset, we quantified the degree of variability for several different flow parameters, and assessed potential contributing sources of errors including manual segmentation, subject positioning in the scanner, data acquisition, temporal changes, and rhythm at the time of the scan. Overall, LA peak velocity and vorticity are the most reproducible, temporally stable, and robust to rhythm differences and heart rate changes over time. Furthermore, these markers provide a non-invasive readout of LA haemodynamics that are potentially mechanistically relevant to thrombus formation and embolic stroke[28, 155].

3.5.1 Reproducibility and temporal variability

Of the evaluated LA flow parameters, peak and mean velocity and vorticity demonstrated the highest same-day scan-rescan reproducibility, comparable in magnitude to that for other widely-used cardiac imaging biomarkers such as LV end-diastolic volume and LVEF derived from CMR cine imaging, which are reported to have a scan-rescan CV of 5.7% and 6.1%, respectively[179]. These results are also in agreement with prior data on reproducibility of 4D Flow assessment of LV blood flow components' volume ratio, where scan-rescan CVs ranged between 2.5% and 9.2%[180].

As expected, we found an overall incremental variability from intra-observer to inter-observer and scan-rescan, also in agreement with previous studies[179]. Notably, we found that the variability attributable to human labelling of the LA (intra- and inter-observer CV) was only slightly lower than the scan-rescan variability for LA stasis, and was similar or greater than the scan-rescan variability for all the remaining LA flow parameters. This indicates a high degree of technical reproducibility of LA flow measurement, and is again consistent with CMR assessment of traditional imaging biomarkers such as LVEF[179].

As the ability to detect changes in LA flow parameters over time is of clinical interest, assessment of temporal (scan-interval scan) variability was also a key goal. We found that LA peak velocity and vorticity were the most stable parameters over time, in contrast to stasis and mean velocity, which displayed significantly higher temporal variability compared to their technical variability. Although LA vortex volume was also relatively stable over time, its variability was greater than that of both peak velocity and vorticity.

Importantly, the greater variability recorded with the interval scans over same-day rescan for LA stasis and mean velocity suggests a possible dependence on biological factors. In particular, we found a greater temporal variability in stasis and mean velocity in participants in SR, which was associated with longitudinal changes in heart rate (but not blood pressure). These data are consistent with a previously reported correlation between heart rate and 4D flow parameters in the LV[180], and are biologically plausible, given that changes in heart rate affect the dynamics of ventricular filling (i.e. the diastolic phase of the cardiac cycle), and therefore also

affect atrial flow components when the mitral valve is open[181-183]. Previous experimental[184] and echocardiographic Doppler studies[183] demonstrated that a higher heart rate was associated with an increased atrial contribution to ventricular filling by (a) a predominant effect on the atrial flow integral, rather than peak velocities which remained stable[185], and (b) by affecting the passive filling phase, rather than the atrial booster phase[185]. In agreement with previous evidence[185], our data show that peak velocities are stable over time, but we showed for the first time that a reduction in heart rate is associated with increased LA stasis in SR. If confirmed in larger cohorts, this finding could provide novel insight into the finding that ivabradine (a negatively chronotropic agent) has been associated with an increased risk of incident AF[186] and ischemic stroke in patients with systolic heart failure in SR, in contrast to its beneficial effect on mortality and hospital re-admissions[187]. Nevertheless, heart rate changes are likely to only partially explain the temporal variability observed in LA stasis, given the mild correlation observed, and other factors are likely to also be involved.

3.5.2 Suitability for potential clinical application

Low blood flow velocities (linked with activation of the coagulation cascade[90, 147] and loss of normal coherent vortical flow (linked with platelet aggregation[151, 152]) have been associated with clinical stroke risk in recent validation 4D Flow CMR studies [28, 155]. Further studies assessing the association of LA 4D Flow parameters in patients with paroxysmal or undiagnosed AF and thromboembolic

events are needed. In order to design and plan such studies, the choice of which LA 4D flow biomarkers are most suitable to be tested for clinical application hinges on (a) reproducibility and temporal variability, (b) selection of those parameters that, in combination, provide complementary/additive information to each other, and (c) feasibility in terms of minimum sample size required for detection of a clinically meaningful difference.

Of the LA 4D Flow parameters evaluated in this study, stasis showed the highest technical and temporal variability, whilst peak velocity and vorticity were the most stable over time. Whilst adjustment for rhythm at the time of the scan is important for all 4D flow parameters to account for the dramatic rhythm-related changes in flow, it is particularly important for stasis, vortex volume, and mean velocity, which displayed higher temporal variability in SR than in AF. Furthermore, the apparent sensitivity of stasis and mean velocity to heart rate is also relevant, particularly for longitudinal studies, whereas peak velocity and vorticity appear to be heart-rate independent.

Calculations of sample size for future clinical studies are not yet possible due to the lack of large longitudinal studies showing a meaningful significant difference based on prediction of embolic risk or AF. Further research is now needed to identify normal values for these 4D Flow parameters in the general population, as well as to determine thresholds that may identify patients at higher risk of incident AF and/or embolic risk.

It is important to emphasise that, in principle, each parameter assesses different aspects of LA flow, and are all therefore potentially relevant markers of the overall propensity for thrombogenesis. Nevertheless, results from our study show that peak and mean velocity and stasis display a statistically significant strong correlation with each other, implying they are likely to convey similar information. On the other hand, vorticity and vortex volume display only moderate or mild inter-correlation with the other parameters, making it more likely that they convey unique and complementary information.

Taken together, our study shows that LA peak velocity and vorticity seem the most promising biomarkers to be tested for potential clinical application, since they are the most reproducible and stable over time, are robust to differences in heart rate and rhythm, and are likely to provide unique complementary information. Both parameters are also mechanistically relevant, since low LA blood flow velocities are linked to activation of the coagulation cascade and increased red blood cell and plasma protein aggregation[90, 147], whilst loss of the normal coherent vortical LA flow pattern[150] is associated with platelet adhesion and aggregation[151, 152].

3.5.3 Limitations

Firstly, this study was undertaken at a single centre in a mixed cohort and reproducibility assessment would need to be confirmed across multiple centres.

Secondly, we chose to focus on assessment of global LA flow characteristics in this initial validation work. Whilst assessment of local flow within the LAA or in

other regions of the atrium is possible in principle [28], the post-processing tools for this are not widely available, and the reproducibility and temporal variability of LAA flow assessment are unknown.

Thirdly, although the majority of patients underwent a follow-up scan, analysis of the differences in rescan vs interval scans variability may be limited by the fact that the subjects who underwent scan 2 are a subset (86%) of those who underwent scan 1. However, the 14% of patients who did not undergo an interval follow-up scan did not display significantly different rescan variability for any parameter compared to those who completed the follow-up visit (all $p>0.05$).

In the presented work, we have not compared LA 4D Flow parameters against transoesophageal echocardiography as a reference method. Another potential limitation is the use of 4 different 4D Flow protocols (A,B,C,D). We used two similar retrospective protocols ('A' and 'B', one on each MRI system, both with spatial resolution 3.0×3.0×3.0 mm and retrospective gating) for 90% of the study population. In the remaining 10% of the population, we used 2 different research sequences which were part of our technical development at the beginning of the study: a prospective protocol ('C' with the same parameters as protocol 'A' but prospectively gated) in 2 participants, and a separate retrospective protocol 'D' (with higher spatial resolution: 2.4×2.4×2.5 mm) in 7 participants (8%). All follow-up scans were performed using the same MRI protocol as the respective baseline scan. We have now also reported exploratory analysis of scan-rescan CV for each 4D Flow CMR protocol (available as **Table 12**). Overall, the 2 main retrospective protocols (A and B) displayed better scan-rescan CV than protocols C and D. .

Table 12. Scan-rescan coefficient of variation for left atrial 4D Flow parameters according to each CMR protocol

		Main protocols		**Others**	
(% of study population)	**Overall**	Protocol A (**38%**)	Protocol B (**51%**)	Protocol C (**2%**)	Protocol D (**8%**)
Stasis	0.101	0.098	0.082	0.241	0.149
Peak velocity	0.065	0.054	0.048	0.273	0.063
Mean velocity	0.051	0.047	0.036	0.153	0.084
Vorticity	0.072	0.073	0.051	0.203	0.110
Vortex vol	0.086	0.068	0.072	0.041	0.194

Finally, 7 subjects (8% of those who underwent an interval scan, 4 in SR and 3 in AF) had changes to prescribed cardiovascular medications at the time of the interval scan compared to baseline. Whilst this could in principle confound the observed changes in LA stasis and mean velocity, there was no evidence of a statistical interaction between changes in these parameters and alterations to medication at follow-up (p=0.833).

3.6 Conclusion

LA peak velocity and vorticity were the most reproducible and temporally stable novel LA 4D Flow biomarkers, and are robust to changes in heart rate, blood pressure, and differences in heart rhythm.

Chapter 4

Impact of Atrial Fibrillation and Stroke Risk Factors on Left Atrial Blood Flow Characteristics

4.1 Abstract

4.1.1 Background

In AF, altered LA blood flow characteristics increase risk of LA thrombus formation and cardioembolic stroke. We hypothesised that similar LA blood flow abnormalities may also be present in at-risk patients in SR.

4.1.2 Methods

We recruited 95 individuals: patients with persistent AF, studied before and after cardioversion [Group 1; N=37, median CHA2DS2-VASc = 2.0 (1.5-3.5); median age 69 (65 - 75) years]; individuals in SR with similar age and stroke risk [Group 2; N=35, median CHA_2DS_2-VASc = 3.0 (2.0-4.0); median age 69 (65 - 73) years]; and younger low-risk individuals in SR [Group 3; N=23, median CHA2DS2-VASc = 0.0 (0.0-0.0); median age 33 (30 – 57) years]. Cardiac function and LA flow were assessed using magnetic resonance imaging.

4.1.3 Results

Before cardioversion, patients in Group 1 displayed significantly impaired LV and LA function, reduced LA flow velocities, and significant alterations in LA flow vorticity and vortex-to-LA volume ratio (all P<0.001 vs Group 2 and 3). In patients in SR at ≥4 weeks post-cardioversion (n=24, 65%), LV systolic function normalized, and all LA flow parameters significantly improved (including peak velocity from 0.21±0.04 to 0.27±0.05 m/s and vorticity from 12.9±3.6 to 21.3±4.5 radians; all P<0.001 vs pre-cardioversion), and were no longer significantly different from those in Group 2 (all P=ns). However, in both Group 1 and Group 2 in SR, LA function and LV early diastolic strain rate were impaired compared to Group 3, and these changes were associated with adverse LA flow characteristics, e.g. lower peak velocity and impaired vorticity (all P<0.01 vs Group 3).

4.1.4 Conclusions

Compared with individuals with no risk factors for stroke, patients at moderate-to-high stroke risk in SR display altered LA flow characteristics in association with an LA myopathic phenotype and LV diastolic dysfunction, regardless of a history of AF. A cardioembolic aetiology may be contribute to a greater proportion of ischaemic strokes in SR than currently recognised.

4.2 Introduction

AF is associated with profound alterations in LA blood flow characteristics which, in turn, increase the risk of LA thrombus formation and, consequently, of cardioembolic stroke [90]. In keeping with this paradigm, anticoagulation is highly effective in preventing ischaemic stroke in patients with AF and stroke risk factors[2]. More recently, it has been suggested that a cardioembolic aetiology may also underlie a proportion of ischaemic strokes that occur in the absence of AF, on the grounds that imaging biomarkers of LA remodelling and dysfunction are associated with greater stroke risk in patients in SR[20].

To date, the potential mechanisms behind the association between LA myopathy and increased stroke risk remain unclear. For instance, LA remodelling could be a marker of extra-cardiac stroke risk factors, such as large-artery atherosclerosis [22] or small vessel disease [23], as suggested by the association between LA dysfunction and lacunar brain infarcts [23]. Altered LA features may also be a consequence of subclinical episodes of paroxysmal AF, with only the latter responsible for the increased stroke risk [24]. Alternatively, a cardiomyopathic process, brought about by ageing and exposure to cardiovascular risk factors, may lead to both cardiac dysfunction and adverse LA flow characteristics in the absence of AF [25], as suggested by the findings that anticoagulation reduces ischaemic stroke in high-risk patients in SR [26, 27] and that LA emptying fraction (LAEF) is a strong predictor of incident ischemic stroke, independent of AF, in a large prospective cohort [20].

Here, we used advanced CMR imaging to test the hypothesis that stroke risk factors are associated with abnormal LA blood flow characteristics in SR both in patients with a history of persistent AF after cardioversion and in individuals with no history of AF.

4.3 Methods

This study was undertaken at the Radcliffe Department of Medicine of the University of Oxford, UK. The study protocol was approved by Leeds East Ethics Committee (18/YH/0096), and all patients gave written informed consent.

4.3.1 Study design

We recruited three groups of participants: N=37 patients with persistent AF scheduled for cardioversion (Group 1); N=35 individuals in SR with no history of AF but with similar stroke risk to Group 1, as evaluated by the CHA_2DS_2-VASc score (Group 2); and N=23 low-risk controls with no history of hypertension, diabetes, heart failure, vascular disease, or stroke (Group 3). A history of AF was an exclusion criterion for all SR participants; individuals in Group 2 were offered an optional 7-day ECG monitor to exclude clinically silent AF.

To assess the effect of rhythm on LA flow profile, patients with persistent AF (Group 1) underwent the same CMR protocol before and at a minimum of 4 weeks after cardioversion. To assess the effect of stroke risk factors on LA flow

parameters in individuals without AF, patients in Group 2 were compared to low-risk controls without stroke risk factors (i.e. Group 3).

4.3.2 Recruitment of the study population

Patients with persistent AF were recruited from the list of patients referred for direct current cardioversion (DCCV) at Oxford University Hospitals NHS Foundation Trust. Participants in SR were recruited from outpatient clinics, clinical CMR referrals, a pool of control participants who had participated in other research studies at our institution, or through word of mouth. Fourteen (61%) of the low-risk controls were in-house volunteers who provided verbal consent under an ethically-approved technical development protocol.

4.3.3 Cardiovascular magnetic resonance

Full details of the study protocol are contained in Chapter 2. Briefly, LA flow characteristics were assessed using ECG-gated time-resolved 3D phase-contrast CMR with 3-directional velocity encoding imaging ('4D flow'). All data were acquired using retrospective gating except for one case where a prospectively gated sequence was used. Data analysis included 3D segmentation of LA volume, and determination of two sets of parameters (details in **Chapters 2-3**). Firstly, LA peak and mean velocities were assessed, since low atrial velocities are thought to be linked to activation of the coagulation cascade with increased red blood cell and plasma protein aggregation[90]. Secondly, 'rotational' flow parameters were

measured, since the normal flow pattern within the LA is characterized by the presence of systolic and diastolic vortices[150], and disruption of vortical flow is associated with altered shear stress and platelet adhesion and aggregation in computational and silicone replica models of intra-cardiac blood flow[151, 152]. Rotational parameters included flow patterns by pathlines, mean vortex to LA volume ratio by the lambda2 method, and LA vorticity defined as the tendency of flow to rotate using the area under the vorticity-time curve over the averaged cardiac cycle using volume-weighted vorticity measures, in radians. The CMR protocol also included ECG-gated balanced steady-state free precession (SSFP) cine imaging in four-chamber and two-chamber orientations for evaluation of LV and LA structure and function. All imaging assessments were conducted by investigators blinded to all clinical information, including rhythm at the time of the scan.

4.3.4 Power Calculation and Statistical Analysis

A difference of 0.05 m/s in LA peak velocity was chosen based on published data indicating that LA peak velocity in AF patients with $CHA_2DS_2VASc \geq 3$ is 0.05 m/s lower than that in AF patients with CHA_2DS_2VASc 0-1 [188]. Assuming that LA peak velocity in patients in AF is 0.29 ± 0.05 m/s [28], recruitment of 13 participants with persistent AF would give >90% power (2-tailed-alpha=0.05) to detect a 0.05 m/s change in peak velocity after successful DCCV. Assuming that AF patients who recovered SR have an LA peak velocity of 0.33±0.05 m/s whereas peak velocity in healthy controls is 0.40±0.04 m/s [28], recruitment of 23 subjects per group (i.e., SR

after successful DCCV, SR participants without AF, and low-risk controls) would provide >90% power (2-tailed-alpha=0.05 after Bonferroni correction) to detect a 0.05 m/s between-groups difference in peak velocity. Considering 35% of patients may be in AF at 4 weeks after DCCV, we aimed to recruit at least 36 patients with persistent AF.

Details of statistical tests and software used are reported in **Chapters 2-3**. Briefly, normally distributed continuous variables were compared with unpaired t-test, one-way ANOVA, or Welch's test whereas non-normally distributed data were compared using the Mann-Whitney U test or Kruskal-Wallis test. Categorical data were compared using the $\chi 2$ test or exact method. Paired data were compared with paired t test, Wilcoxon signed-rank test or McNemar test, depending on the data distribution.

All tests were 2-tailed, and values of $P<0.05$ were considered statistically significant. All reported P values for comparisons between groups were adjusted for pairwise comparisons using the Bonferroni or Games-Howell methods.

4.4 Results

We recruited a total of 95 participants. There were no significant differences between Group 1 and Group 2, with the exception of a lower heart rate (HR, $P<0.01$) and diastolic blood pressure (DBP, $P<0.05$) in the latter (**Table 13)**.

Table 13: Baseline characteristics of the study groups.

	Group 1 **AF**	**Group 2** **SR**	**Group 3** **Low-risk controls**
N	37	35	23
Age, years	69 (65 – 75)	69 (65 – 73)	33 (30 - 57)
Male, n (%)	21 (57)	22 (63)	14 (61)
BMI, kg/m^2	27 (25 - 31)	28 (25 - 30)	24 (22 - 27)
Hypertension, n (%)	24 (65)	26 (74)	0 (0)
Heart Failure, n (%)	5 (13)	2 (6)	0 (0)
Stroke / TIA, n (%)	0 (0)	0 (0)	0 (0)
Type 2 diabetes, n (%)	7 (19)	10 (29)	0 (0)
Vascular disease, n (%)	2 (5)	7 (20)	0 (0)
CHA_2DS_2-VASc Score	2.0 (1.5 – 3.5)	3.0 (2.0 – 4.0)	0.0 (0.0 – 0.0)
HR, bpm	79 (74 – 91)	60 (55 – 68)	67 (60 – 75)
SBP, mmHg	123 (109 - 136)	121 (115 - 134)	114 (111 – 122)
DBP, mmHg	77 (67 - 88)	65 (58 - 72)	67 (64 - 72)

Values are expressed as mean ± SD or median (Q1-Q3) for continuous variables and as n (%) for categorical variables. BMI, body mass index; BSA, body surface area; HR, heart rate; DBP, diastolic blood pressure; SBP, systolic blood pressure; TIA, transient ischaemic attack; DCCV, direct current cardioversion.

Individuals in Group 3 were significantly younger and had a lower BMI than Groups 1 and 2, and also had significantly lower HR and DBP than Group 1 (all $P<0.05$). Medication use was also similar, except that anticoagulants and amiodarone were more frequently prescribed to Group 1, and anti-platelets to Group 2 (**Table 14**). Twenty-seven patients in Group 2 (77%) agreed to undergo 7-day ECG monitoring and the remaining 8 (23%) had a resting 12-lead ECG confirming SR. Cardiac rhythm was monitored during CMR scans in all participants. No evidence of AF was found in any participant in Groups 2 or 3.

Table 14 – Medications at the time of baseline scan.

Baseline scan	**Group 1**	**Group 2**	**Group 3**	***P value**
N	37	35	23	-
Antiplatelets	0 (0)	12 (34)	0 (0)	**<0.001**
ACE inhibitor	17 (46)	10 (29)	0 (0)	0.128
Angiotensin II receptor blocker	5 (13)	8 (23)	0 (0)	0.303
β-blocker	23 (62)	18 (51)	0 (0)	0.358
Aldosterone antagonist	4 (11)	2 (6)	0 (0)	0.675
Statins	17 (46)	19 (54)	0 (0)	0.479
Warfarin	2 (5)	0 (0)	0 (0)	0.493
Non-vitamin K oral anticoagulants	34 (92)	1 (3)	0 (0)	**<0.001**
Diuretics	5 (13)	9 (26)	0 (0)	0.191
Calcium channel blockers	8 (22)	12 (34)	0 (0)	0.230
Amiodarone	10 (27)	0 (0)	0 (0)	**0.001**

*Values are expressed as N (%). *Comparisons between patients with persistent AF (Group 1) and SR controls (Group 2).*

4.4.1 CMR findings at the baseline scan

Patients in Group 1 who were in AF at the time of the baseline scan, had significantly impaired LV systolic function (as evidenced by lower LVEF and less negative LV longitudinal strain), and adverse LA functional and structural remodelling (as evidenced by higher LA volume, lower LAEF, and impaired LA reservoir and conduit strain), compared to Groups 2 and 3 (all P<0.001; **Table 15**).

Table 15 – Baseline CMR characteristics

	Group 1 **AF** (N=37)	**Group 2** **SR controls** (N=35)	**Group 3** **Low-risk controls** (N=23)	**P value** **1 vs 2**	**P value** **1 vs 3**	**P value** **2 vs 3**
LV EDV, ml/m^2	71 ± 21	72 ± 19	89 ± 19	>0.999	**0.003**	**0.005**
LV EF, %	46 ± 14	63 ± 9	60 ± 8	**<0.001**	**<0.001**	0. 248
LV longitudinal strain, %	-10.5 ± 3.7	-17.0 ± 3.2	-18.2 ± 2.8	**<0.001**	**<0.001**	0.631
LA volume, ml/m^2	64 (51 - 72)	45 (37 - 56)	39 (32 - 49)	**<0.001**	**<0.001**	0.510
LA EF, %	16 ± 7	50 ± 9	61 ± 8	**<0.001**	**<0.001**	**<0.001**
LA reservoir strain, %	6.6 ± 3.2	29.3 ± 10.6	40.8 ± 13.7	**<0.001**	**<0.001**	**0.005**
LA conduit strain, %	6.5 ± 3.2	15.2 ± 9.1	26.4 ± 11.4	**<0.001**	**<0.001**	**0.001**
LA peak velocity, m/s	0.20 ± 0.04	0.29 ± 0.07	0.34 ± 0.05	**<0.001**	**<0.001**	**0.001**
LA mean velocity, m/s	0.10 ± 0.02	0.14 ± 0.03	0.16 ± 0.03	**<0.001**	**<0.001**	**0.016**
LA vorticity, rad	12.9 ± 3.2	22.0 ± 4.4	25.8 ± 5.0	**<0.001**	**<0.001**	**0.002**
LA vortex/LA volume ratio	0.30 ± 0.06	0.18 ± 0.04	0.14 ± 0.04	**<0.001**	**<0.001**	**0.022**
LA flow patterns, N (%)						
Systolic Vortex	0 (0)	27 (77)	23 (100)	**<0.001**	**<0.001**	0.051
Systolic Short-range	32 (87)	1 (3)	0 (0)	**<0.001**	**<0.001**	>0.999
Systolic - Other patterns	5 (14)	7 (20)	0 (0)	>0.999	0.438	0.105
Diastolic Vortex	5 (14)	21 (60)	22 (96)	**<0.001**	**<0.001**	**0.006**
Diastolic Short-range	17 (46)	0 (0)	0 (0)	**<0.001**	**<0.001**	-
Diastolic – Other patterns	15 (41)	14 (40)	1 (4)	>0.999	**0.006**	**0.006**

Values are expressed as mean ± SD or median (q1-q3) for continuous variables; categorical values are reported as N (%). Significant P values are shown in bold, <0.05 adjusted for 3 pairwise comparisons using Bonferroni (for one-way ANOVA or Kruskal-Wallis or Chi-square or Exact method) or Games-Howell (for Welch's one-way ANOVA) methods. LV EDV, Left Ventricular End-Diastolic Volume; LV EF, LV Ejection Fraction; LA, Left Atrium; LAEF, LA Emptying Fraction.

LA flow velocities were significantly reduced in the presence of AF compared to both groups in SR (all P<0.001; **Figure 15A** and **15B,** and **Table 15**). In SR, blood flow emitted from the pulmonary veins typically forms an anticlockwise vortex before reaching the mitral valve plane; this phenomenon has been reported to prevent platelet adhesion and aggregation in preliminary studies [151, 152]. In patients with AF, the typical vortex pattern was significantly less prevalent compared to both groups in SR, and was largely replaced by short-ranged flow patterns. Further, patients with AF had significantly reduced vorticity (i.e., a reduced tendency of LA blood flow to rotate) and a greater vortex-to-LA volume ratio (all P<0.001; **Figure 15C** and **15D**, and **Table 15**).

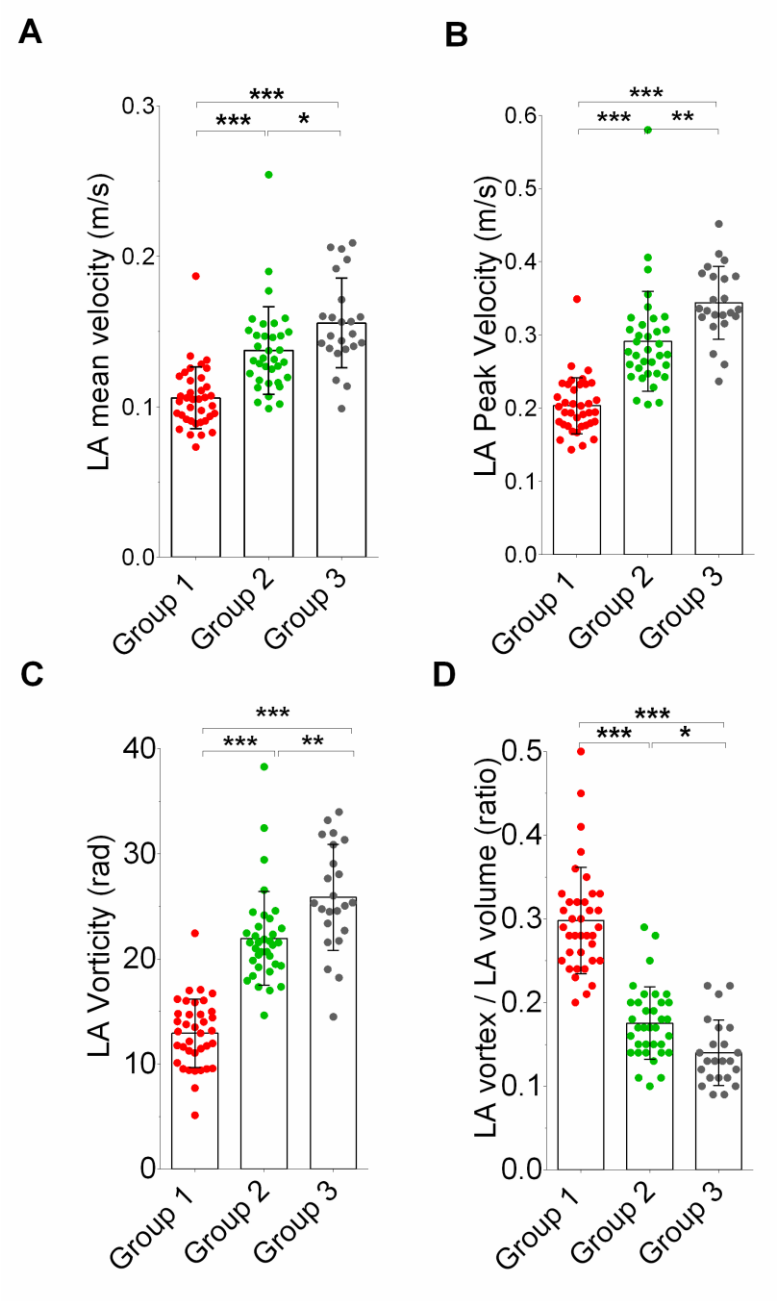


Figure 15: LA flow characteristics at baseline. *LA mean velocity (A), LA peak velocity (B), LA vorticity (C), and LA vortex volume ratio (D) in Group 1 patients before cardioversion (in AF, in red), Group 2 patients (in SR, in green) and Group 3 low-risk controls (in SR, in grey). Data are shown as mean±SD. *P<0.05; **P<0.01; ***P<0.001.*

4.4.2 Effects of cardioversion in individuals with persistent AF

A follow-up CMR was undertaken in all patients in Group 1 at a median of 56 days (IQR 40-87 days) after the first CMR. In the intervening period, 33 patients (89%) underwent DCCV (including on two occasions in 4), 2 (6%) cardioverted pharmacologically, and 2 (6%) cardioverted spontaneously. Twenty-four patients (65%) were in SR ('AF-SR' subgroup) at a median of 32 days (IQR 29-41 days) after successful DCCV (n=20), pharmacological cardioversion (n=2, including 1 who had a previous unsuccessful DCCV), or spontaneous return to SR (n=2). The remaining 13 (35%) were still in AF at the follow-up scan ('AF-AF' subgroup), due to primary failure of DCCV (n=3), early recurrence of AF after an initially successful DCCV (n=9), or early recurrence of AF after pharmacological cardioversion (n=1).

There were no significant differences in patients' characteristics between the AF-SR subgroup (from Group 1) and Group 2 (all P>0.05, **Table 16**).

Table 16 – Clinical risk in AF patients (Group 1) who recovered SR (AF-SR) or remained in AF (AF-AF) at follow-up and in SR controls (Group 2).

	AF-AF (from Group 1)	**AF-SR (from Group 1)**	**SR controls (Group 2)**	**P value (AF-SR vs SR)**	**P value (AF-AF vs AF-SR)**
N	13	24	35		
Age, years old	68 (63 - 76)	69 (65 - 74)	69 (65 – 73)	>0.999	>0.999
Male	4 (31)	17 (71)	22 (63)	>0.999	**0.038**
BMI, Kg/m^2	28 (24 - 30)	27 (25 - 32)	28 (25 - 30)	>0.999	>0.999
Hypertension	9 (69)	15 (62)	26 (74)	0.668	>0.999
Heart Failure	2 (15)	3 (12)	2 (6)	>0.999	>0.999
Stroke / TIA	0 (0)	0 (0)	0 (0)	-	-
Diabetes	1 (8)	6 (25)	10 (29)	>0.999	0.766
Vascular disease	1 (8)	1 (4)	7 (20)	0.25	>0.999
CHA_2DS_2-VASc Score	3 (2 – 4)	2 (1 – 3)	3 (2 – 4)	>0.999	0.582
Previous ablation	3 (23)	5 (21)	0 (0)	-	>0.999

Values are expressed as mean ± SD or median (q1-q3) or N (%). P values are adjusted for 2 pairwise comparisons using Bonferroni method.

Changes in medication between the baseline and follow-up scans were similar between the AF-AF and AF-SR groups (all P>0.05, **Table 17**).

Table 17 – CMR characteristics and medications in Group 1 patients who were successfully cardioverted at follow-up (AF-SR) versus those who remained in AF (AF-AF)

	AF-AF	**AF-SR**	**P value**
	N = 13	N = 24	
HR, bpm	79 (75 – 93)	80 (74 - 89)	0.962
SBP, mmHg	119 (111 - 135)	124 (109 - 138)	>0.999
DBP, mmHg	70 (64 - 80)	81 (69 - 92)	0.077
CMR scan (baseline)			
LV EDV, ml/m^2	56 ± 10	79 ± 21	**0.001**
LV EF, %	52 ± 7	42 ± 15	**0.009**
LA Volume, ml	106 (98 - 135)	139 (108 - 151)	0.109
LA EF, %	15 ± 7	16 ± 6	0.907
LA reservoir strain, %	7.0 ± 3.6	6.3 ± 3.1	0.584
LA conduit strain, %	6.9 ± 3.5	6.3 ± 3.1	0.623
LA mean velocity, m/s	0.10 ± 0.01	0.11 ± 0.02	0.157
LA peak velocity, m/s	0.19 ± 0.02	0.21 ± 0.04	0.102
LA vorticity, rad	12.9 ± 2.6	12.9 ± 3.6	0.960
LA vortex/LA vol, ratio	0.30 ± 0.06	0.30 ± 0.07	0.943

Patients with changes in medications at follow-up scan	**AF-AF**	**AF-SR**	**P value**
N (%)	4 (31)	8 (33)	>0.999
Added Amiodarone	0 (0)	2 (8)	0.532
Added Flecainide	2 (15)	0 (0)	0.117
Added β-blocker	1 (8)	0 (0)	0.351
Added statin	0 (0)	1 (4)	>0.999
Added Verapamil	1 (8)	0 (0)	0.351
Withheld angiotensin-converting enzyme inhibitor	0 (0)	1 (4)	>0.999
Withheld β-blocker	0 (0)	2 (8)	0.532
Withheld statin	0 (0)	1 (4)	>0.999
Withheld amiodarone	0 (0)	1 (4)	>0.999
Values are expressed as mean ± SD or median (q1-q3) or N (%). Significant P values (< 0.05) in bold.			

Restoration of SR was associated with significant improvement in LV and LA function (all P<0.001), and borderline-significant reduction in LA volume (P=0.067; **Figure 16** and **Table 18**). LA flow characteristics also improved, with significant increases in peak velocity, mean velocity, and vorticity, and a reduction in vortex volume ratio (all P<0.001; **Figure 16** and **Table 18**), and a greater proportion of typical vortical flow patterns (P<0.01; **Figure 17**). There was no significant

correlation between any LA parameter at the follow-up CMR and the time interval from restoration of SR to follow-up (all P>0.05). No significant changes from baseline were observed for any parameter in patients still in AF at the follow-up CMR (**Figure 16**, all P>0.05).

Table 18 – Characteristics and CMR data in Group 1 patients who reverted to SR (AF-SR) and those who were still in AF (AF-AF) at follow-up

	AF-SR (baseline)	**AF-SR (follow-up)**	**P value**	**AF-AF (baseline)**	**AF-AF (follow-up)**	**P value**
N	24	24	-	13	13	-
Weight, Kg	87 ± 15	87 ± 15	0.665	83 ± 12	83 ± 11	0.255
HR, bpm	80 (74 - 89)	54 (50 - 64)	**<0.001**	79 (75 - 93)	78 (71 - 87)	0.600
SBP, mmHg	124 (109 - 138)	133 (113 - 153)	**0.028**	119 (111 - 135)	111 (107 - 126)	0.221
DBP, mmHg	81 (69 - 92)	73 (60 - 76)	**0.001**	70 (64 - 80)	72 (65 - 81)	0.844
LV EF, %	42 ± 15	59 ± 10	**<0.001**	51 ± 5	48 ± 12	0.294
LV long strain, %	-10.1 ± 4.0	-16.5 ± 2.6	**<0.001**	-11.2 ± 3.2	-13.1 ± 2.9	0.094
LA Volume, ml	139 (108 - 151)	118 (104 - 143)	0.067	106 (98 - 135)	121 (93 - 145)	0.422
LA EF, %	16 ± 6	36 ± 11	**<0.001**	15 ± 7	20 ± 14	0.281
LA reservoir strain, %	6.3 ± 3.1	18.9 ± 6.6	**<0.001**	7.0 ± 3.6	6.2 ± 3.5	0.154
LA conduit strain, %	6.3 ± 3.1	10.1 ± 4.3	**<0.001**	6.9 ± 3.5	6.2 ± 3.5	0.212
LA mean velocity, m/s	0.11 ± 0.02	0.13 ± 0.02	**<0.001**	0.10 ± 0.01	0.10 ± 0.01	0.733
LA peak velocity, m/s	0.21 ± 0.04	0.27 ± 0.05	**<0.001**	0.19 ± 0.02	0.19 ± 0.03	0.971
LA vorticity, rad	12.9 ± 3.6	21.3 ± 4.5	**<0.001**	12.9 ± 2.6	13.3 ± 2.9	0.429
LA vortex/LA vol	0.30 ± 0.07	0.20 ± 0.04	**<0.001**	0.30 ± 0.06	0.29 ± 0.06	0.693

Values are expressed as mean (SD) or median (q1-q3). Significant P values (<0.05) for paired comparisons in bold. LV EDV, Left Ventricular End-Diastolic Volume; LV EF, LV Ejection Fraction; LV early diastolic Strain Rate, GLSR-E; LA Emptying Fraction, LAEF.

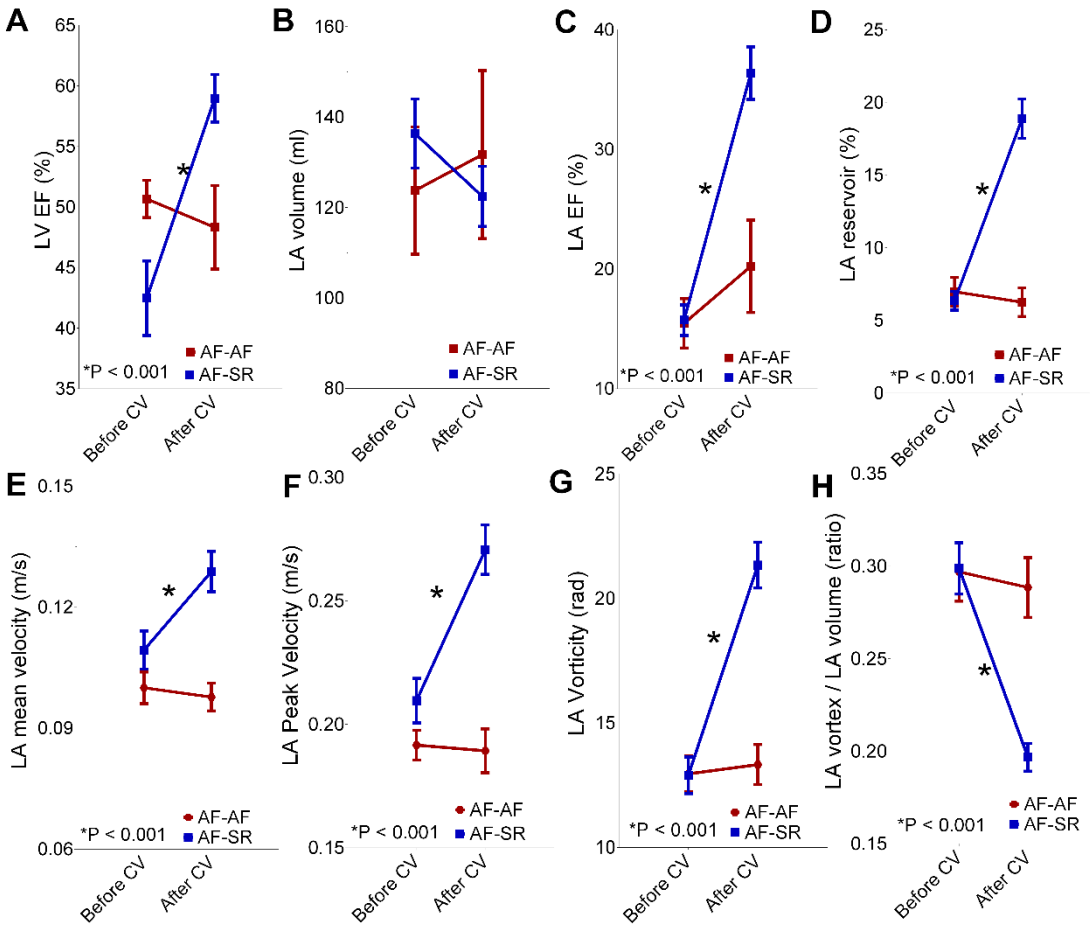


Figure 16: LV and LA CMR parameters in patients with persistent AF before and after cardioversion. *Changes in LVEF (A), LA volume (B), LAEF (C), LA reservoir strain (D), LA mean velocity (E), LA peak velocity (F), LA vorticity (G), and LA vortex volume ratio (H) are reported in AF patients after successful restoration of SR (AF-SR subgroup, in blue) and in those with early AF relapse or failed cardioversion (AF-AF subgroup, in red). Data are presented as mean±SE. Significant P values from paired t tests are marked with *. CV, cardioversion.*

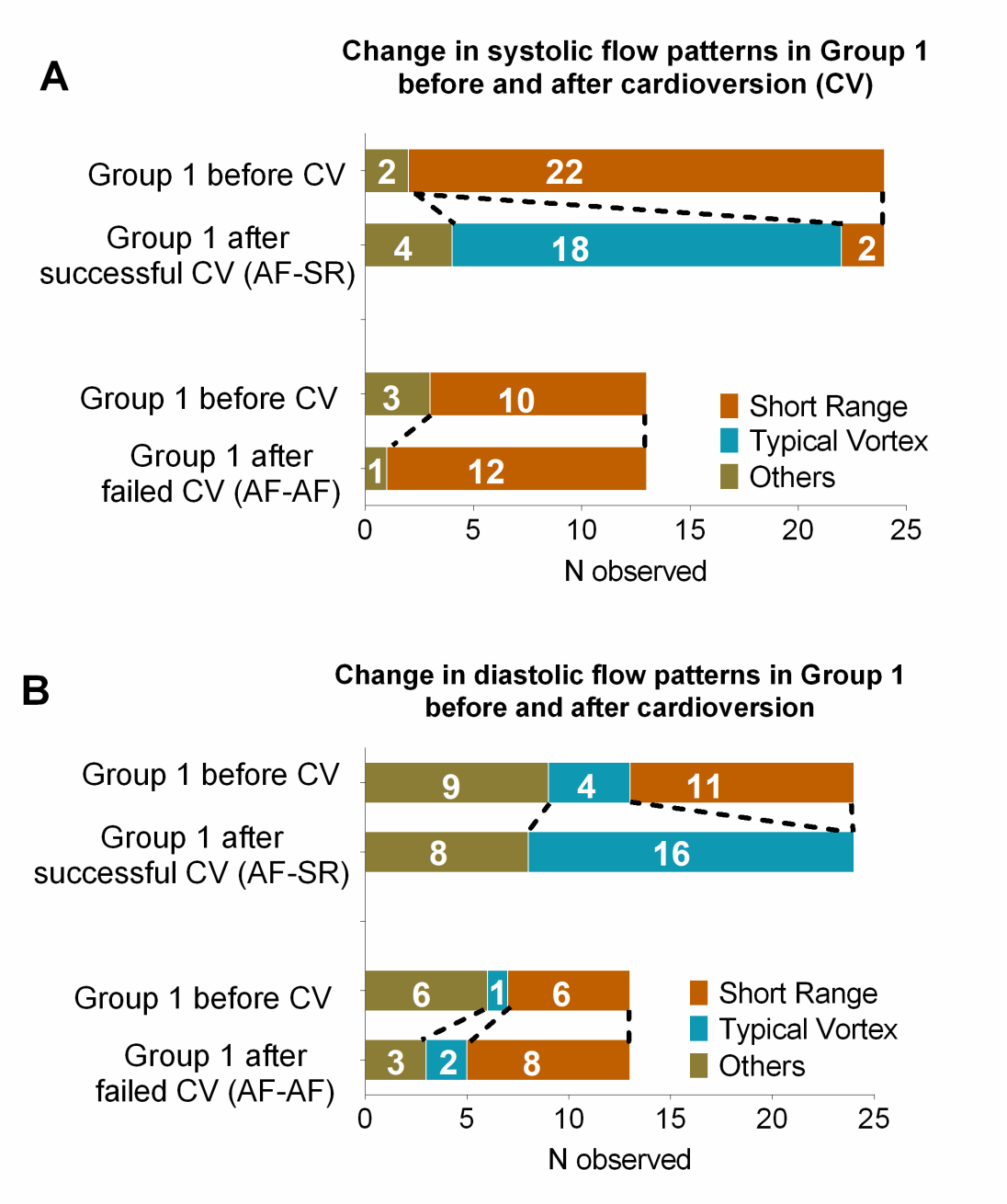


Figure 17: LA flow patterns assessed with pathlines. *Bar charts illustrate paired changes in systolic (A) and diastolic (B) LA flow patterns observed within each group (expressed as N of observations). There is a conspicuous reduction in short-ranged patterns from baseline at the follow-up scan in the AF-SR group (McNemar's test; P<0.001) with a parallel increase in vortex prevalence (McNemar's test; P<0.01). No significant changes in flow patterns were observed from baseline to follow-up for AF-AF patients (all McNemar's test P=ns). CV, cardioversion. Definition of typical vortex, short-range vortex, and other patterns can be found in the methods and supplementary methods.*

4.4.3 Comparison between groups in SR

Recovery of SR in Group 1 patients (i.e., in the AF-SR subgroup) abolished the difference in LV systolic function between groups (all P>0.05; **Figure 18** and **Table 19**). However, both SR groups at higher clinical stroke risk (i.e. the AF-SR subgroup and Group 2) had significantly impaired LV diastolic function (as evidenced by reduced LV early diastolic strain rate) compared with the low-risk controls in Group 3 (all P<0.001; **Figure 18** and **Table 19**). Furthermore, the AF-SR subgroup continued to display LA dilatation and dysfunction compared to both groups in SR (all P<0.05; **Figure 18** and **Table 19**). By contrast, the LA flow profile of AF-SR patients was now similar to that seen in SR participants in Group 2 (all P>0.05), with both groups showing clear evidence of impaired LA function and flow characteristics (e.g., lower peak and mean velocity, reduced vorticity, and a higher vortex-to-LA volume ratio) compared to low risk controls in Group 3 (all P<0.01; **Figure 18** and **Table 19**).

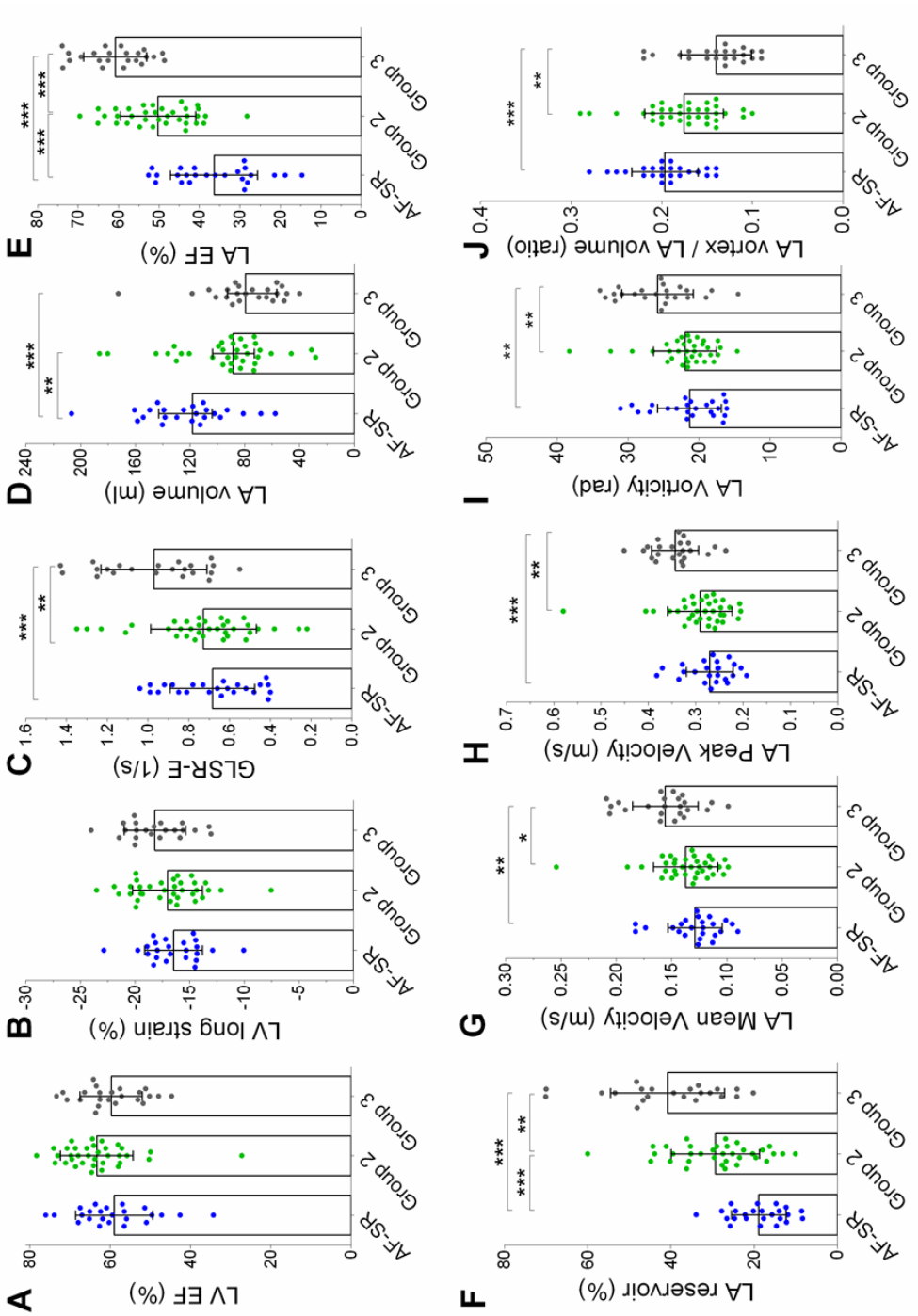


Figure 18: LV and LA parameters in the 3 groups in SR. *LVEF (A), LV longitudinal strain (B), LV early diastolic strain rate (GLSR-E, C), LA volume (D), LAEF (E), LA reservoir strain (F), LA mean velocity (G), LA peak velocity (H), LA vorticity (I), and LA vortex volume ratio (J) in Group 1 patients after successful restoration of SR (AF-SR subgroup, in blue), Group 2 patients (in green) and Group 3 low-risk controls (in grey). Data are shown as mean±SD, with the exception of LA volume which is shown as median (IQR). *P<0.05; **P<0.01; ***P<0.001.*

Table 19 – Haemodynamics and CMR parameters for all Groups in SR

	Group 1	**Group 2**	**Group 3**	**P value**	**P value**	**P value**
	AF-SR subgroup	**SR**	**Low-risk controls**	**1 vs 2**	**1 vs 3**	**2 vs 3**
N	24	35	23			
HR, bpm	55 (50 – 64)	60 (55 – 68)	67 (60 - 75)	0.166	**0.005**	0.392
SBP, mmHg	133 (113 - 153)	121 (115 - 134)	114 (111 - 122)	0.710	**0.013**	0.157
DBP, mmHg	73 (60 - 76)	65 (58 - 72)	67 (64 - 72)	0.507	0.810	>0.999
LV EDV, ml	182 ± 35	142 ± 39	170 ± 49	**0.001**	0.977	**0.041**
LV EF, %	59 ± 10	63 ± 9	60 ± 8	0.205	>0.999	0.404
LV long strain, %	-16.5 ± 2.6	-17.0 ± 3.2	-18.2 ± 2.8	>0.999	0.153	0.468
GLSR-E, 1/s	0.68 ± 0.21	0.72 ± 0.26	0.97 ± 0.26	>0.999	**<0.001**	**0.001**
LA Volume, ml	118 (104 - 143)	88 (73 - 102)	79 (57 - 93)	**0.004**	**<0.001**	0.292
LA EF, %	36 ± 11	50 ± 9	61 ± 8	**<0.001**	**<0.001**	**<0.001**
LA reservoir strain, %	18.9 ± 6.6	29.3 ± 10.6	40.8 ± 13.7	**<0.001**	**<0.001**	**0.005**
LA conduit strain, %	10.1 ± 4.3	15.3 ± 9.1	26.4 ± 11.4	**0. 015**	**<0.001**	**0.001**
LA booster strain, %	8.7 ± 3.6	14.4 ± 5.7	14.4 ± 4.9	**<0.001**	**<0.001**	0.999
LA mean velocity, m/s	0.13 ± 0.02	0.14 ± 0.03	0.16 ± 0.03	0.538	**0.002**	**0.041**
LA peak velocity, m/s	0.27 ± 0.05	0.29 ± 0.07	0.34 ± 0.05	0.579	**<0.001**	**0.003**
LA vorticity, rad	21.3 ± 4.5	22.0 ± 4.4	25.8 ± 5.0	>0.999	**0.004**	**0.007**
LA vortex/LA vol	0.20 ± 0.04	0.18 ± 0.04	0.14 ± 0.04	0.215	**<0.001**	**0.002**

Values are expressed as mean ± SD or median (Q1-Q3). Significant P values (<0.05 adjusted for 3 pairwise comparisons) are in bold. HR, Heart Rate; SBP, Systolic Blood Pressure; DBP, Diastolic Blood Pressure; LV EDV, Left Ventricular End-Diastolic Volume; LV EF, LV Ejection Fraction; LA Emptying Fraction, LAEF; GLSR-E, Global Longitudinal Strain Rate – Early Diastolic.

When considered individually, LA and LV structural and functional parameters were weakly or non-significantly correlated with measures of LA flow (**Table 20**).

Table 20 – Correlation coefficients between LA flow and structural/functional parameters in the whole population in SR at the time of the scan.

N=82	LVEF									
LV long strain	**-0.634****	LV long strain								
LV early diastolic strain rate	0.233*	**-0.546****	LV early diastolic strain rate							
LA volume	-0.092	0.099	-0.104	LA volume						
LAEF	0.248*	-0.426**	0.333**	**-0.577****	LAEF					
LA reservoir strain	0.305**	**-0.514****	0.441**	**-0.512****	**0.813****	LA reservoir strain				
LA conduit strain	0.217	-0.457**	**0.584****	-0.429**	**0.695****	**0.913****	LA conduit strain			
LA mean velocity	0.227*	-0.194	0.329**	-0.317**	0.336**	0.382**	0.366**	LA mean velocity		
LA peak velocity	0.181	-0.208	0.328**	-0.334**	0.358**	0.391**	0.375**	**0.938****	LA peak velocity	
LA vorticity	0.121	-0.168	0.302**	-0.092	0.260*	0.261*	0.296**	**0.611****	**0.689****	LA vorticity
LA vortex volume ratio	-0.084	0.373**	-0.456**	0.205	**-0.599****	-0.506**	-0.453**	-0.383**	-0.371**	-0.338**

*Pearson's coefficient and Spearman's rho are reported as appropriate in the study population in sinus rhythm at the time of the scan (namely, successfully cardioverted AF patients in Group 1, matched SR controls in Group 2, and healthy controls in Group 3). Table entries with * indicate statistically significant relationships (2-tailed P < 0.05) and smaller P values stratified by size (**P < 0.01). Moderate correlation (coefficient > 0.5) is marked in bold. Strong correlation (coefficient equal or greater than 0.7) is marked in bold with light grey background*

However, in the sample of participants in SR (i.e. the AF-SR subgroup, Group 2, and Group 3), there was a significant interaction between LAEF and LV early diastolic function in their effects on LA peak and mean velocities (both $P < 0.05$; **Figure 19**).

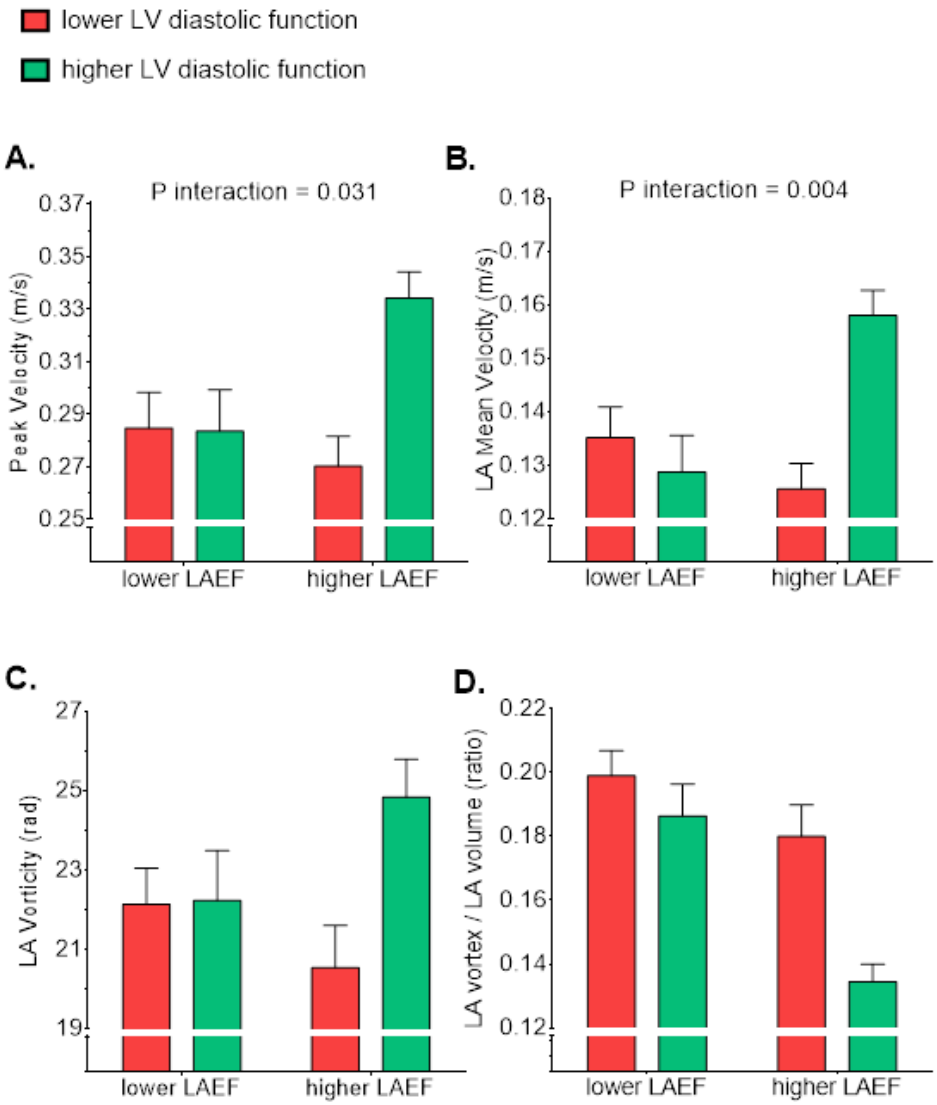


Figure 19: Relationships between LA emptying fraction, LV diastolic function, and LA flow. *Bar charts illustrate mean (SE) values of LA peak velocity (A), mean velocity (B), vorticity (C), and vortex/LA volume ratio (D), stratified by higher and lower levels of LA emptying fraction (LAEF) and LV early diastolic strain rate (GLSR-E), defined by the top 50% / bottom 50% of the distribution in SR. Significant P values are by two-way ANOVA.*

Specifically, whereas the most favourable LA flow profile was observed when both LAEF and LV early diastolic function were least impaired, LA flow velocities were compromised even in the presence of preserved LAEF if LV diastolic function was impaired. After adjusting for history of AF, $CHADS_2$-VA_2Sc score, and LVEF,

these interactions maintained statistical significance (all P < 0.05, **Table 21**). Additional adjustment for age resulted in a non-significant trend to interaction for LA peak velocity (P = 0.085), whilst a significant interaction remained for LA mean velocity (P = 0.011).

Table 21 – Relationships between LA emptying fraction, LV diastolic function, and LA flow after adjustment for covariates in SR groups

Independent variables	Dependent variable	Adjustment Covariates	P value
GLSR-E low/high levels	LA peak velocity	-	**0.005**
LAEF low/high levels	LA peak velocity	-	**0.029**
GLSR-E * LAEF low/high levels	LA peak velocity	-	**0.031**
GLSR-E * LAEF low/high levels	LA peak velocity	LVEF	**0.025**
GLSR-E * LAEF low/high levels	LA peak velocity	CHA_2DS_2VASc	**0.034**
GLSR-E * LAEF low/high levels	LA peak velocity	History of AF	**0.047**
GLSR-E * LAEF low/high levels	LA peak velocity	Age	0.085
GLSR-E * LAEF low/high levels	LA peak velocity	CHA_2DS_2VASc, History of AF, Age	0.118
GLSR-E low/high levels	LA mean velocity	-	**0.006**
LAEF low/high levels	LA mean velocity	-	**0.018**
GLSR-E * LAEF low/high levels	LA mean velocity	-	**0.004**
GLSR-E * LAEF low/high levels	LA mean velocity	LVEF	**0.002**
GLSR-E * LAEF low/high levels	LA mean velocity	CHA_2DS_2VASc	**0.004**
GLSR-E * LAEF low/high levels	LA mean velocity	History of AF	**0.006**
GLSR-E * LAEF low/high levels	LA mean velocity	Age	**0.011**
GLSR-E * LAEF low/high levels	LA mean velocity	CHA_2DS_2VASc, History of AF, Age	**0.018**

*General linear regression models in the study population in sinus rhythm at the time of the scan (namely, successfully cardioverted AF patients in Group 1, matched SR controls in Group 2, and healthy controls in Group 3). Statistically significant P values (<0.05) are marked in bold. LAEF, LA emptying fraction. LVEF, LV ejection fraction. GLSR-E, LV early diastolic strain rate. * expresses interaction terms*

4.5 Discussion

This is the first study to evaluate the effect of clinical stroke risk factors and cardiac function on LA blood flow characteristics in individuals in SR and in patients with persistent AF before and after cardioversion. The findings suggest that, in the presence of SR, both LAEF and LV diastolic function may have a significant impact on LA flow velocities, such that both need to be preserved to prevent the development of potentially adverse reductions in LA flow velocities. Although reduced LA flow velocities and increased vortex volume were all observed in high-risk patients in SR regardless of a history of AF, the degree of perturbation was relatively subtle when compared to the profoundly disruptive effects of AF on these flow characteristics.

Taken together, my results indicate that ageing and exposure to risk factors are associated with a subclinical cardiomyopathy (affecting both LA and LV function) that results in potentially adverse LA flow characteristics, which are dramatically exacerbated in the presence of AF (see proposed schematic representation in **Figure 20** which also shows representative cases and related **videos 1-4**). These findings are in keeping with prior evidence suggesting that AF burden is positively correlated with stroke risk [24], as time in AF would increase the exposure to disrupted LA flow conditions, which are largely (but incompletely) normalized by restoration of SR after cardioversion. More broadly, our results suggest that most of the excess risk of ischaemic stroke reported in patients in SR with LA/LV dysfunction [20] may result from the combination of incident AF [136],

particularly when including subclinical episodes [9], as well as the impact of the underlying cardiomyopathic process on LA flow characteristics. This paradigm would explain the lack of a plausible temporal relationship between the majority of episodes of subclinical AF and stroke events [17], the relationship between AF episodes' duration and incident thromboembolic events [189], and the results of the COMPASS trial, which showed that therapy with low-dose rivaroxaban and aspirin or rivaroxaban alone was more effective than aspirin in reducing ischaemic stroke in patients with a high CHA_2DS_2-VASc score but no history of AF [26].

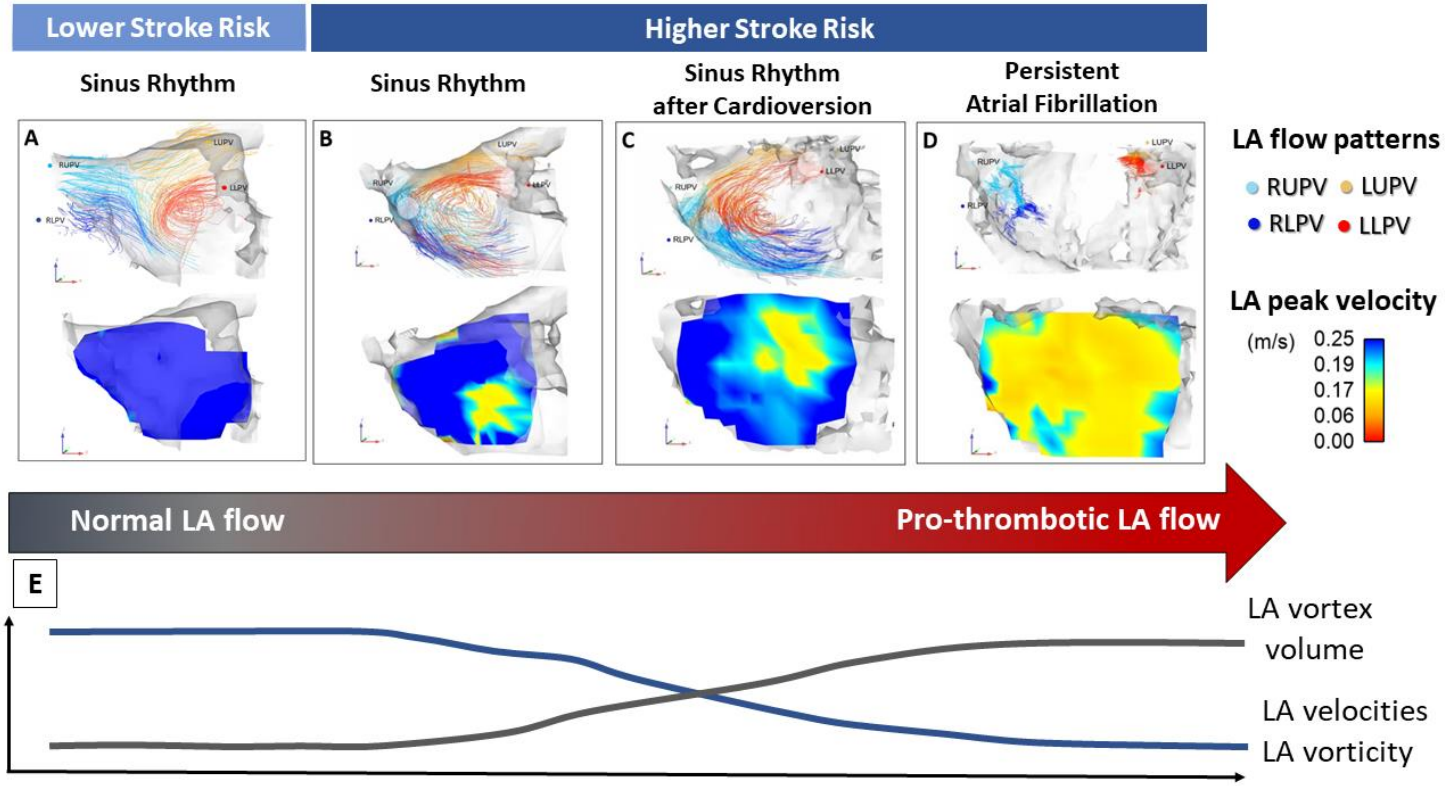


Figure 20: LA 4D flow characteristics in SR and AF. *Flow pathlines emitted from each pulmonary vein (PV) and LA peak velocities are colour-coded, as indicated in the legend. A. In a low-risk control in SR (CHADS2-VA2Sc score = 0), LA peak flow velocity is uniformly high across the LA (0.33 ± 0.08 m/s), and flow from the pulmonary veins forms a typical vortex with a small vortex-to-LA volume ratio (0.14) and high vorticity (24.7 rad; see also* ***Video 1****). B. In the presence of SR and moderate stroke risk (CHADS2-VA2Sc score = 4), average LA peak flow velocity is lower and more variable (0.29 ± 0.11 m/s) than in panel A. Flow from the pulmonary veins forms a vortex with a larger vortex-to-LA volume ratio (0.18) and lower vorticity (21.0 rad; see also* ***Video 2****). C. In the presence of SR at forty days after successful cardioversion of AF in a patient at moderate stroke risk (CHADS2-VA2Sc score = 4), LA flow characteristics are similar to those observed in panel B (peak velocity = 0.24 ± 0.11 m/s, vortex-to-LA volume ratio = 0.22, vorticity = 20.9 rad; see also* ***Video 3****). D. In the presence of persistent AF (prior to cardioversion in the same subject as in panel C), LA peak velocity is uniformly much lower (0.16 ± 0.04 m/s), and the typical flow architecture is disrupted (vortex-to-LA volume ratio = 0.28, vorticity = 11.6 rad; see also* ***Video 4****). E. Schematic representation of LA flow characteristics across the clinical categories shown in panels A to D. Lower; LU, Left Upper; LL, Left Lower.*

4.5.1 LA flow characteristics and predisposition to thrombus formation

Recent studies in patients with AF (persistent and paroxysmal) have reported an abnormal LA flow profile that is related to clinical stroke risk [28, 155]. The present study extends these observations to patients in SR with or without a history of AF, and demonstrates that multiple flow domains are affected by both AF and stroke risk factors, including reduced vorticity and loss of normal vortical flow patterns, as well as reduced blood flow velocities. Intriguingly, our results indicate that LA flow velocity only has a weak direct relationship with LA function in SR, and instead may be related to the combination of LA mechanical function and LV diastolic function, in keeping with previous epidemiological evidence of an association between LV diastolic dysfunction and ischaemic stroke in patients in SR [123]. Development and persistence of AF is associated with mild LV systolic dysfunction, further worsening LA function, and significant adverse changes in LA flow.

Overall, our results are consistent with growing evidence that ageing and long-term exposure to cardiovascular risk factors leads to an occult cardiomyopathy, which affects both the LA and the LV [190], and which is associated with altered LA flow characteristics, potentially leading to an increased risk of cardioembolic stroke even before the development of AF.

4.5.2 Limitations

Patients with AF underwent follow-up CMR at 4 weeks after cardioversion. This interval was chosen as a compromise between maximizing the proportion of patients remaining in SR whilst also minimising the potential confounding effects of atrial stunning. A previous study showed that stunning improves progressively after DCCV, with complete (or near-complete) resolution at 4 weeks [191], and current clinical guidelines recommend anticoagulation therapy for 4 weeks after DCCV in patients without a long-term indication for anticoagulation. No correlations were present between time from restoration of SR and any LA parameter at follow-up CMR, suggesting that post-cardioversion stunning was not a significant confounder.

Our 4D flow post-processing tools do not include assessment of flow within the LAA, which is the preferential site for LA thrombus formation. However, a previous study showed that in the presence of SR flow parameters in the LA and LAA are very well correlated [28].

4.6 Conclusion

Compared with individuals with no risk factors for stroke, patients at moderate-to-high stroke risk in SR display altered LA flow characteristics in association with an LA myopathic phenotype and LV diastolic dysfunction, regardless of a history of AF. A cardioembolic aetiology may contribute to a greater proportion of ischaemic strokes in SR than currently recognised.

Chapter 5

Reduced left atrial rotational blood flow is independently associated with embolic brain infarct: a potential novel mechanism of cardioembolic risk in sinus rhythm

5.1 Abstract

5.1.1 Background

Up to 25% of embolic strokes occur in individuals without AF or any other identifiable mechanism. We hypothesised that abnormal LA blood flow characteristics may be associated with embolic brain infarct, independently of AF and stroke risk factors.

5.1.2 Methods

We recruited 134 patients at risk of brain infarct: 44 with a clinical history of ischaemic stroke and 90 with no history of stroke but at least one risk factor (i.e. CHA2DS2VASc score ≥1). All patients underwent CMR, to evaluate cardiac function and LA 4D Flow, and brain MR to detect infarct. Infarcts were classified either as

large (≥ 15 mm) non-cortical infarcts or cortical infarcts (LNCCIs), likely to be embolic, or as non-embolic lacunar infarcts.

5.1.3 Results

Patients (41% female; age 70±9 years) had moderate stroke risk with CHA2DS2VASc 3 [Q1-Q3, 2-4]. Sixty-eight (51%) had diagnosed AF and 58 (43%) were in AF during MR. Thirty-nine (29%) had ≥1 LNCCI, 20 (15%) had ≥1 lacunar infarct, and 75 (56%) had none. Baseline characteristics were similar between patients with and without LNCCIs. In patients in SR, average LA and left ventricular (LV) structure and function were within the normal range. LA vorticity, a parameter that measures the typical rotational tendency of LA flow and is linked to biomechanical platelet activation, was significantly and independently associated with LNCCIs (P=0.02). After adjusting for age, rhythm during CMR, AF diagnosis, and CHA2DS2VASc, lower LA vorticity was associated with a 2-fold higher risk of LNCCIs (OR per SD 2.10, 95% CI 1.12-3.92). This association remained robust after adjusting for LV/LA structural and functional parameters (all P<0.05). By contrast, LA peak velocity was not associated with large brain infarcts (P=0.21). Neither LA vorticity nor LA peak velocity was associated with lacunar brain infarct (both P>0.05).

5.1.4 Conclusions

Reduced rotational LA blood flow is associated with embolic (but not lacunar) brain infarct, independently of age, heart rhythm, stroke risk factors, and cardiac structure or function. Prospective studies are needed to assess whether LA flow

vorticity can identify high-risk individuals in SR who would benefit from antithrombotic therapy.

5.2 Introduction

AF is a major risk factor for ischaemic stroke[59]. Low blood flow velocities within the fibrillating left atrium (LA) predisposes to activation of the coagulation cascade[90, 147] and local thrombus formation[90, 192], with consequent higher risk of embolic stroke[28, 59, 147]. Nevertheless, up to 20-25% of embolic strokes occur in the absence of AF or any other identifiable cause[47, 63] thus implying that there are mechanisms of embolic strokes which are currently unrecognised[47, 63]. Although preliminary data suggested that covert AF and LA dilation/dysfunction[15] may be a common underlying mechanism of embolic stroke in patients without clinical AF, recent data[27] show that this is likely to be a less important aetiologic mechanism than was initially conceived[7]. In fact, the vast majority (>90%) of patients with a recent history of embolic stroke of undetermined source (ESUS) display normal LA size and normal LVEF, is in keeping with the fact that ESUS patients do not benefit from rivaroxaban therapy[27]. Currently, the mechanisms of embolic stroke in patients with normal LA size and LVEF are unknown.

Recent development of 4D Flow CMR technique have allowed comprehensive assessment of in vivo blood flow within the LA. In humans, a fast vortical LA blood flow pattern [150] has been associated with more efficient cardiac work and a disruption of vortical patterns is associated with biomechanical platelet

activation[151, 152] via alteration of shear stress forces. Abnormal cardiac flow patterns have also been linked to thrombus formation in other regions of the cardiovascular system, such as the LV of patients after acute myocardial infarct[153] as well as in abdominal aortic aneurysms[154]. To date, it is still unclear whether abnormal LA blood flow rotation (i.e. LA vorticity) is an unrecognised pathophysiological mechanism leading to increased cardioembolic risk in patients with normal LA and LV mechanical parameters regardless of AF.

In this study, we tested whether LA flow parameters are associated with embolic brain infarct, independently of AF, LA/LV size and function, and clinical stroke risk (as defined by the CHA_2DS_2-VASc score). LA blood flow velocities and vorticity were chosen as primary 4D Flow measurements (based on reproducibility data) and assessed in vivo using 4D flow CMR[176].

5.3 Methods

This study was undertaken in a single tertiary hospital (Oxford University Hospital NHS Foundation Trust, University of Oxford, Radcliffe Department of Medicine, John Radcliffe Hospital, Oxford, UK). The protocol was approved by a Research Ethics Committee, and all patients gave written informed consent.

5.3.1 Design

We undertook CMR and concomitant brain Magnetic Resonance Imaging (MRI) (i) in patients with previous/recent history of ischaemic stroke and (ii) in patients with no history of stroke but with at least one clinical stroke risk factor (i.e.

CHA_2DS_2VASc score ≥1). All brain scans were reported by a board-certified neuroradiologist (VY), blinded to other research data. Binary logistic regression analyses were then performed to assess independent associations between LA flow parameters and LNCCIs (silent and overt).

Data on AF history and CHA_2DS_2VASc score[156] were extracted from a research questionnaire that was administered to all participants. Individuals without a history of AF had their rhythm closely monitored during the CMR scan and were also offered an optional 7-day ECG monitor to exclude clinically silent AF.

5.3.2 Patient Population

Patients with a recent diagnosis of ischaemic stroke were prospectively recruited from the Stroke Unit at the John Radcliffe Hospital. Patients with clinical stroke risk factors and/or a history of ischaemic stroke were recruited from outpatient cardiology services at the same hospital. Exclusion criteria for the whole study population were related to conditions that would not allow a safe MRI scan including claustrophobia, inability to lie flat and still, implantable devices or other ferromagnetic implants, internal defibrillator, cranial aneurysm clips, metallic ocular foreign bodies, pregnancy, shrapnel injury, severe claustrophobia, and female participants who are pregnant, lactating or planning pregnancy during the course of the study.

Further, patients admitted to hospital with a clinical diagnosis of ischaemic stroke were not invited to participate to this study if the clinical team judged the stroke as being caused by rarer conditions such as peri-procedural stroke, dissection, arteritis, vasospasm, intravenous drug use, left ventricular thrombus, active endocarditis.

5.3.3 CMR protocol

CMR scans were performed on one of two 3T MRI systems (Verio syngo MR B17 or MAGNETOM Prisma VE 11C, Siemens, Germany). For assessment of LA flow characteristics, all patients underwent ECG-gated time-resolved 3D phase-contrast CMR with 3-directional velocity encoding imaging ('4D flow'), using validated methods as previously described[155, 188]. The LA 4D Flow parameters investigated as potential predictors of brain infarcts were LA peak velocity (m/s), since reduced velocities are linked to activation of the coagulation cascade[90, 147], and LA vorticity in radians (rad), as the loss of typical vortical flow[150] with reduced vorticity is linked to platelet aggregation[151, 152] (**Figure 21**). Full details of 4D flow protocols are available in **Chapter 2-3**.

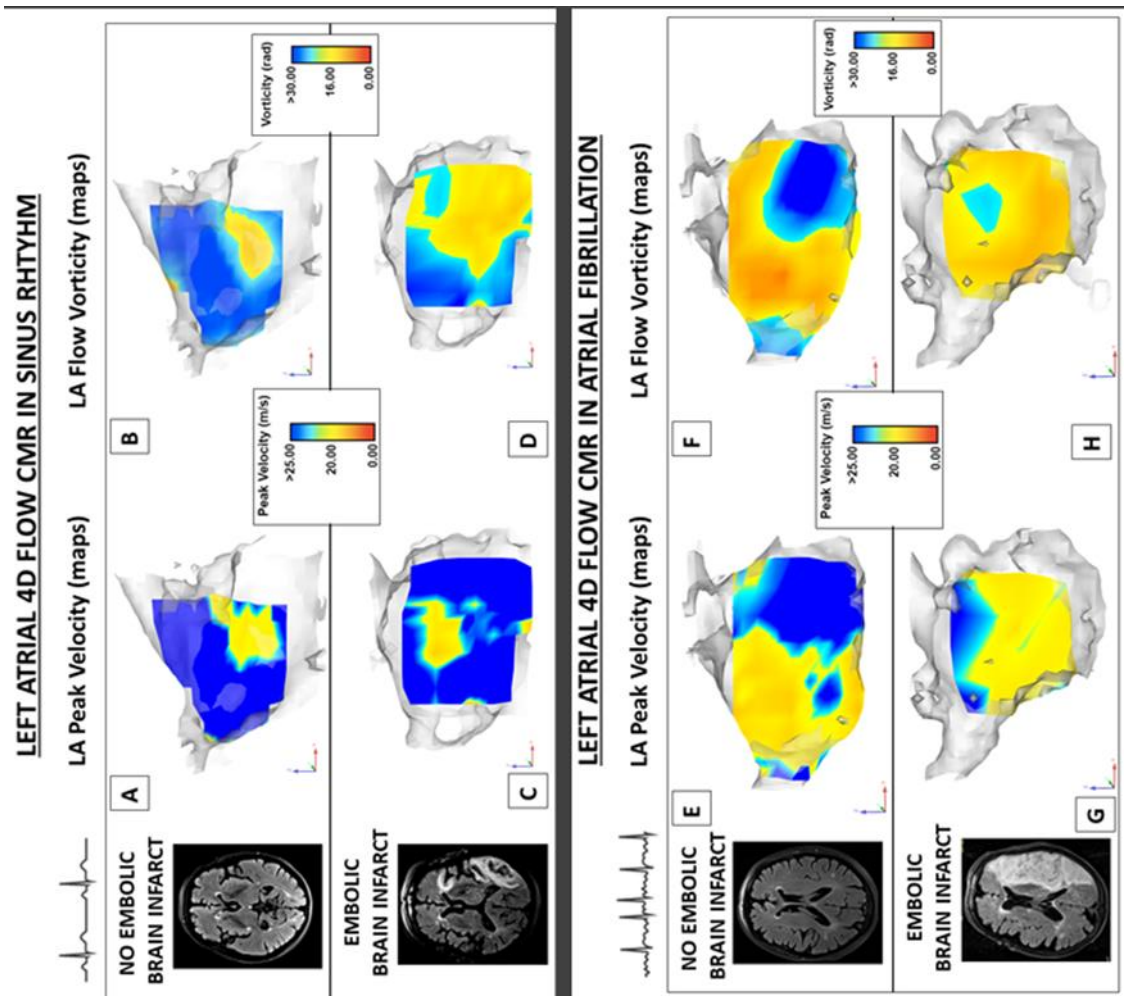


Figure 21: Left atrial 4D Flow CMR and embolic brain infarcts. *A legend for colour-coded levels of LA peak velocity and LA vorticity is shown with blue and red representing the highest and lowest (i.e. more abnormal) values, respectively. The upper left panel (A-D) shows representative cases in sinus rhythm: patient (A-B, 81 yo, female, CHA2DS2VASc = 4, no history of AF or evidence of AF on 7-day ECG monitor) with no history of stroke and no MRI evidence of brain infarct (FLAIR sequence shown), in whom we found preserved LA vorticity (20.7 rad) and LA peak velocity (0.29 m/s). Representative patient (C-D, 79 yo, female, CHA2DS2VASc = 5, no history of AF or evidence of AF on 7-day ECG monitor) with an acute ischaemic stroke involving the middle cerebral artery on brain MRI (FLAIR sequence shown), in whom we found comparatively reduced LA vorticity (13.9 rad) but similar LA peak velocity (0.24 m/s). The lower right panel (E-H) shows representative cases in atrial fibrillation: patient (E-F, 74 yo, male, CHA2DS2VASc = 2, in persistent AF) with no history of stroke and no MRI evidence of embolic brain infarct (FLAIR sequence shown), in whom we found deranged LA vorticity (16.7 rad) and LA peak velocity (0.24 m/s). Representative patient (G-H, 89 yo, female, CHA2DS2VASc = 4, in persistent AF) with an acute ischaemic stroke involving the middle cerebral artery on brain MRI (FLAIR sequence shown), in whom we found comparatively lower LA vorticity (9.8 rad) but similar LA peak velocity (0.23 m/s).). LA, Left Atrium; Rad, Radians.*

The CMR protocol also included ECG-gated balanced steady-state free precession (SSFP) cine imaging in four-chamber and two-chamber axis orientations of the left ventricle (LV), for the evaluation of LVEF, end-diastolic and end-systolic volume (LVEDV and LVESV, respectively), and LAEF. The SSFP cine imaging also allowed the derivation of LV and LA longitudinal strain and strain rate parameters by feature tracking as described previously[157-159] (see **Chapter 2**).

A trained single observer (GPA), who was blinded to all clinical information including brain MRI reports and rhythm at the time of the scan, contoured all the datasets derived from cine imaging and from the 4D Flow sequence, according to a standardized post-processing protocol.

5.3.4 Brain MRI protocol

Brain MRI scans were performed on 1.5T-3T MRI systems. The protocol included an axial fluid-attenuated inversion recovery (FLAIR) and axial diffusion-weighted imaging (DWI) sequences, for detection of chronic1, 22 and acute23 brain infarct, respectively. The standardized research 3T protocol included a 2-dimensional axial FLAIR (spatial resolution 1.8 × 1.8 × 3.0 mm^3), and 2-dimensional axial diffusion-weighted imaging (DWI, spatial resolution 1.8 × 1.8 × 5.0 mm3, b=0 and 1000mm/s with apparent diffusion coefficient calculation) sequence with whole brain coverage and without interpolation. The vast majority (93%) of scans were undertaken on a 3T MRI research system (Verio syngo MR B17, Siemens, Germany) and N=9 (7%) on 1.5 MRI clinical systems (Achieva 1.5T, Philips, Netherlands; Signa HDxt 1.5T,

General Electric, USA). The 1.5T protocol included a 2-dimensional axial FLAIR (spatial resolution 0.9-1.0 mm × 1.1 mm x 2-5 mm), and 2-dimensional axial diffusion-weighted imaging (DWI, spatial resolution 2.0 mm × 2.0-2.5 mm x 5 mm).

All brain scans were reported by a board-certified neuroradiologist (VY), blinded to other research data in terms of (a) presence of brain infarcts and (b) location of the brain infarcts. Location of brain infarcts was coded according to standard vascular territory distribution[193] into Anterior Cerebral Artery (ACA), Middle Cerebral Artery (MCA), Posterior Cerebral Artery (PCA), Cerebellar Arteries, Deep Penetrating Arteries. A trained blinded observer (AS) measured in a standardized fashion the maximum diameter of all brain infarcts described by the neuroradiologists.

A trained blinded observer (AS) measured the maximum diameter of all reported brain infarcts in a standardized fashion to allow for their dichotomous classification either as LNCCIs or as Small Non-Cortical Infarcts (SNCIs), following consolidated neuroimaging criteria[41, 59, 60, 62]. Briefly, LNCCIs (recognized to be embolic in origin[41, 47]) were defined as either (a) large non-cortical infarcts (on FLAIR or DWI) with a diameter >15 mm on FLAIR (or >20 mm on DWI) on axial sections[47, 62], and/or (b) cortical infarcts, defined as hyperintense lesions (on FLAIR or DWI) involving the cortex, regardless of their size or non-cortical involvement[62]. Patients were classified as not having embolic brain infarcts if they had (a) no evidence of brain infarct at brain MRI or (b) if they had SNCIs (i.e. lacunar likely non-

embolic in origin) which were defined as infarcts with maximum diameter ≤15 mm on FLAIR (or ≤20 mm on DWI) on axial sections and not involving the cortex.

Brain infarcts detected on brain MRI were classified as 'clinically overt' if they were detected in patients with a recent clinical acute stroke or with a clinical history of previous stroke, whilst all other lesions were considered clinically silent. In a single subject with recent lacunar stroke who was not able to complete the brain MRI protocol, clinical computed tomography brain imaging was used for the analysis.

5.3.5 Sample Size Determination

The primary analysis used binary logistic regression to assess whether rhythm-adjusted LA peak velocity and LA vorticity were associated with silent or overt embolic brain infarcts (i.e. LNCCIs), independently of AF diagnosis, age, and CHA_2DS_2-VASc score. Based on prior literature[59] and pilot data, we planned for 25% prevalence of LNCCIs in our cohort. A priori power calculations showed that complete data from 134 subjects would yield >80% power (2-tailed alpha = 0.05) to detect a minimum odds ratio of 1.8 per SD change in each parameter, given a 25% probability of LNCCI when LA peak velocity and LA vorticity are at the sample mean (null hypothesis).

5.3.6 Statistical Analysis

Binary logistic regression models assessed the association between CMR parameters and MRI-identified LNCCIs. Key control variables were age, rhythm at the time of the scan (AF vs SR), diagnosis of AF, and CHA_2DS_2-VASc score. Other control variables of interest included gender, BMI, heart rate, systolic and diastolic blood pressure, use of anticoagulation and antiplatelet therapy, recent AF (onset within 12 months before the CMR scan), LA volume and function, LV mass and function. Since the events-to-variable ratio for a multivariable model including all predictors would be small, separate models were fitted using different subsets of covariates (e.g. AF, age, CHADSVASC, gender, and BMI) to assess the robustness of the effects of primary predictors to different covariate specifications.

A Mantel-Haenszel test was used to test the trend in the proportions of LNCCI cases across LA vorticity tertiles. Baseline characteristics were compared between brain-MRI groups using Student's t-test or one-way ANOVA (normally distributed data with homogenous variances) with the Welch's correction for unequal variance when present. Non-normally distributed unpaired data were compared by using the Mann-Whitney U test or the Kruskal-Wallis test. Categorical data were compared by using the $\chi 2$ test, or the exact method if cell size <5.

Correlations between the time from stroke admission to CMR and between CMR parameters were calculated using Spearman's rho.

All tests were 2-tailed, and values of $P<0.05$ were considered statistically significant. All P values from post-hoc comparisons from one-way ANOVA and

Kruskal-Wallis tests were adjusted for multiple pairwise comparisons using the Bonferroni method.

Statistical analyses were performed with GraphPad Prism version 6.01 (GraphPad Software, San Diego, CA) for graphs design, G*Power version 3.1.9.2 for power calculations, and IBM SPSS Statistics (for Windows, version 25.0, IBM Corp, Armonk, NY) for the remaining statistical analyses.

5.4 Results

5.4.1 Clinical characteristics

A total of 137 participants were recruited, but 3 did not complete the CMR protocol, hence data from 134 individuals were included in the final analysis. Brain and cardiac scans were undertaken on the same day in 121 participants (90%), whilst 13 subjects (10%) underwent the brain and cardiac scan on two separate occasions with a median (Q1-Q3) of 1 (1-7) days of interval.

Of the 134 participants, 44 (33%) had a previous history of ischaemic stroke. A total of 67 (50%) had a diagnosis of AF and 58 (43%) were in AF at the time of the scan. Among the 67 (50%) participants in SR without a past history of AF, 58 agreed to undergo an optional 7-day ECG monitor, resulting in a new diagnosis of silent AF in 1 patient.

5.4.2 Brain and cardiac magnetic resonance

On brain MRI, 39 participants (29%) displayed at least one LNCCI, 20 (15%) had evidence of lacunar brain infarct (i.e. SNCI), and 75 (56%) had no evidence of brain infarct (**Table 22-23-24**). Patients with LNCCI had a higher prevalence of clinical stroke and more frequent involvement of the Middle Cerebral Artery (MCA) compared to the group without embolic brain infarct (**Table 25**).

There were no significant differences between patients with and without LNCCI with respect to baseline clinical characteristics (**Tables 22**), except for a higher prevalence of prior history of stroke and transient ischaemic attack in the LNCCI group ($P<0.05$). Anti-platelet agents were more frequently prescribed in the LNCCIs group; instead, beta blockers were more frequently used in those with no evidence of LNCCI (**Table 23**). All other medication use, including anticoagulants, was not significantly different between groups (**Table 23**).

Table 22. Clinical and CMR characteristics by brain MRI outcome

Clinical characteristics	**Embolic brain infarct (N = 39)**	**Without embolic brain infarct (N = 95)**	**P value**
Age, years old	71 ± 9	69 ± 8	0.291
Male	24 (61)	55 (58)	0.697
BMI, Kg/m^2	26.9 ± 5.4	28.4 ± 5.5	0.131
Hypertension / Heart Failure	29 (74) / 6 (15)	73 (77) / 12 (13)	0.759 / 0.671
Previous Stroke/TIA*	8 (21)	5 (5)	**0.007**
Type 2 diabetes	12 (31)	19 (20)	0.179
Vascular disease	6 (15)	14 (15)	0.924
CHA_2DS_2-VASc Score*	3 (2 – 4)	3 (2 – 4)	0.190
Rhythm	**Embolic brain infarct**	**No embolic brain infarct**	**P value**
Sinus Rhythm (without AF diagnosis)	20 (51)	46 (48)	0.763
AF (persistent/permanent)	15 (39)	43 (45)	0.470
AF (paroxysmal)	3 (8)	6 (6)	0.772
AF (silent)	1 (3)	0 (0)	0.291
Recent AF onset (≤ 12 months before research visit)	8 (21)	17 (18)	0.724
Brain outcome	**Embolic brain infarct**	**Without embolic brain infarct**	**P value**
Brain infarct (all types)	39 (100)	20 (21)	**<0.001**
Clinically overt brain infarct	31 (79)	5 (25)	**<0.001**
Silent brain infarct	8 (21)	15 (75)	**<0.001**

*Values are expressed as mean ± SD or median (q1-q3) for continuous variables and as N (%) for categorical variables. Statistically significant P values (<0.05) are marked in bold.AF history is defined as previous history of AF or evidence of AF from ECG monitor. BMI, body mass index; BSA, body surface area; DBP, diastolic blood pressure; SBP, systolic blood pressure; TIA, transient ischaemic attack; Left Atrium, LA; Left Ventricle, LV. *calculated without considering presenting stroke event*

Table 23. Medication use at the time of the scan stratified by brain outcome

Medications	**Without embolic brain infarct**	**Embolic brain infarct**	**P value**
N	95	39	-
Antiplatelets	23 (24)	26 (67)	**<0.001**
ACE inhibitor	35 (37)	16 (41)	0.650
Angiotensin II receptor blocker	21 (22)	6 (15)	0.378
β-blocker	55 (58)	13 (33)	**0.010**
Aldosterone antagonist	5 (5)	2 (5)	0.975
Statins	53 (56)	25 (64)	0.375
Oral Anticoagulants	46 (48)	13 (33)	0.110
Diuretics	17 (18)	11 (28)	0.182
Calcium channel blockers	26 (27)	13 (33)	0.490
Amiodarone	10 (11)	2 (5)	0.320

Table 24: Brain imaging characteristics by brain outcomes

	Without embolic brain infarct	**Embolic brain infarct**	**P value**
N	95	39	-
Overt Brain Infarct, n (%)	5 (5)	31 (79)	**<0.001**
Silent Brain Infarct, n (%)	15 (16)	8 (21)	0.510
Previous history of ischaemic stroke, n (%)	5 (5)	8 (21)	**0.007**
Admitted to hospital for acute ischaemic stroke, n (%)	8 (8)	30 (77)	**<0.001**
Clinically confirmed acute ischaemic stroke, n (%)	4 (4)	30 (77)	**<0.001**
Cortical Infarct, n (%)	0 (0)	27 (69)	**<0.001**
Cortical Infarct Diameter, mm	-	52 (13 – 74)	-
Non-cortical Infarct, n (%)	20 (21)	29 (74)	**<0.001**
Non-cortical Infarct Diameter, mm	9 (7 - 11)	26 (17 – 36)	**<0.001**
Brain infarcts in multiple territories, n (%)	7 (7)	21 (54)	**<0.001**
Brain Infarct (DWI positive), n (%)	4 (4)	29 (74)	**<0.001**
Brain Infarct (FLAIR positive), n (%)	20 (21)	38 (97)	**<0.001**

Values are expressed as median (q1-q3) for continuous variables, and N (%). Significant P values <0.05 are marked in bold for the comparison between LNCCIs and SNCIs.

Table 25: Brain imaging vascular territory distribution

	Non-embolic brain infarct group	**Embolic brain infarct group**	**P value**
Vascular territory in any DWI positive lesions			
Anterior Cerebral Artery, Left/Right/Bilateral, n (%)	0/0/0 (0/0/0)	2/2/0 (5/5/0)	0.392
Middle Cerebral Artery, Left/Right/Bilateral, n (%)	0/0/0 (0/0/0)	10/9/1 (26/23/0)	**0.001**
Posterior Cerebral Artery, Left/Right/Bilateral, n (%)	0/0/0 (0/0/0)	3/2/1 (8/5/3)	0.371
Cerebellar Arteries, Left/Right/Bilateral, n (%)	0/0/0 (0/0/0)	3/0/2 (8/0/5)	0.258
Penetrating Arteries, Left/Right/Bilateral, n (%)	1/2/1 (5/10/5)	6/6/0 (15/15/0)	0.342
Vascular territory in any FLAIR positive lesions			
Anterior Cerebral Artery, Left/Right/Bilateral, n (%)	0/0/0 (0/0/0)	2/2/1 (5/5/3)	0.531
Middle Cerebral Artery, Left/Right/Bilateral, n (%)	3/1/0 (15/5/0)	11/9/3 (29/24/8)	**0.019**
Posterior Cerebral Artery, Left/Right/Bilateral, n (%)	3/1/1 (15/5/5)	3/4/1 (8/11/3)	0.761
Cerebellar Arteries, Left/Right/Bilateral, n (%)	0/3/2 (0/15/10)	4/2/4 (11/5/11)	0.337
Penetrating Arteries, Left/Right/Bilateral, n (%)	3/3/3 (15/15/15)	7/7/0 (18/18/0)	0.115

Values are expressed as median (q1-q3) for continuous variables, or as N Left/Right/Bilateral (% Left/Right/Bilateral) for each vascular territory location. Significant P values <0.05 are marked in bold for the comparison between LNCCIs and SNCIs.

The cardiac MRI data stratified by rhythm at the time of the scan are shown in **Table 26**. LA and left ventricular (LV) structure and function in patients in SR were, on average, within the normal range (compared to reference values previously reported for in a similar population[194]) whereas, as expected, LA/LV dysfunction was present in patients with AF (**Table 26**).

Table 26. CMR characteristics by brain MRI outcome

Rhythm during CMR scan	**SR**		**AF**		**P values**	
	A **Embolic**	**B** **Non embolic**	**C** **Embolic**	**D** **Non embolic**	**(A vs B)** **SR**	**(C vs D)** **AF**
Rhythm during scan, N (history/evidence of AF)	SR = 24 (4)	SR = 52 (6)	AF = 15 (15)	AF = 43 (43)	**SR (tot) = 76**	**AF (tot) = 58**
LA volume / indexed, ml/m^2	77 ± 24 / 41 ± 14	84 ± 30 / 44 ± 16	123 ± 30 / 66 ± 16	138 ± 52 / 68 ± 27	0.91/>0.99	0.375/>0.999
LA Emptying Fraction, %	51 ± 13	51 ± 10	15 ± 6	15 ± 8	>0.999	>0.999
LV mass, g/m^2	74 ± 29	65 ± 19	71 ± 20	71 ± 17	0.160	>0.999
LV End Diastolic Volume, ml/m^2	68 ± 15	70 ± 16	79 ± 29	76 ± 26	>0.999	>0.999
LV Ejection Fraction, %	63 ± 9	63 ± 9	45 ± 20	46 ± 14	>0.999	>0.999
LV early diastolic strain, 1/s	0.73 ± 0.23	0.71 ± 0.23	-	-	0.793	-
LV longitudinal strain, %	-16 ± 3	-17 ± 3	- 10 ± 4	-10 ± 4	0.489	>0.999
LA reservoir strain, %	28 ± 14	29 ± 10	7 ± 4	6 ± 4	>0.999	>0.999
LA conduit strain, %	15 ± 8	15 ± 8	7 ± 4	6 ± 4	>0.999	>0.999
LA booster strain, %	14 ± 7	14 ± 5	-	-	0.990	-
LA stasis, proportion 0-1	0.35 ± 0.10	0.38 ± 0.11	0.55 ± 0.14	0.52 ± 0.15	0.673	0.858
LA mean velocity, m/s	0.15 ± 0.03	0.14 ± 0.03	0.11 ± 0.02	0.11 ± 0.03	0.304	>0.999
LA vortex volume, ml	15 ± 7	15 ± 7	38 ± 7	40 ± 15	>0.999	0.768
LA peak velocity, m/s	0.31 ± 0.07	0.29 ± 0.06	0.21 ± 0.05	0.21 ± 0.05	0.328	>0.999
LA vorticity, radians	18.8 ± 4.4	21.4 ± 4.6	11.8 ± 3.8	13.5 ± 4.1	**0.032**	0.385

Statistically significant P values (<0.05) are marked in bold and are calculated from 2-way ANOVA with Bonferroni correction for pairwise comparisons. Sinus Rhythm, SR; Atrial Fibrillation, AF; Cardiovascular Magnetic Resonance, CMR; Left Atrium, LA; Left Ventricle, LV.

5.4.3 Predictors of embolic brain infarcts

In order to evaluate the predictors of embolic brain infarct, we investigated relationships between cardiac parameters and LNCCI (**Table 27**). We found that lower LA vorticity was associated with a ~2-fold higher risk of prevalent LNCCI [rhythm-adjusted OR (95% CI) = 2.19 (1.20-4.01) per SD, P = 0.011, **Table 27**]. Conversely, the CHA_2DS_2VASc score was not significantly associated with LNCCIs (P=0.107), nor was the rhythm-adjusted LA peak velocity (P = 0.402) or any other LA/LV functional/structural parameters (**Table 27**).

Table 27. Predictors of LNCCIs in the whole population

Parameters	Odds Ratio	95% CI	P value
CHA_2DS_2VASc score, points	1.26	0.95 – 1.69	0.107
4D Flow parameters per SD increase (Primary predictors)			
LA peak velocity, m/s	1.19	0.79 – 1.81	0.402
LA vorticity, rad	2.19	1.20 – 4.01	**0.011**
CMR parameters per SD increase (Left Atrium)			
LA volume	0.69	0.40 – 1.16	0.159
LAEF	0.92	0.42 – 2.03	0.834
LA reservoir strain	0.99	0.54 – 1.80	0.965
LA conduit strain	1.09	0.70 – 1.69	0.715
LA stasis	0.97	0.62 – 1.50	0.890
LA mean velocity	1.16	0.77 – 1.75	0.463
LA vortex volume	0.86	0.46 – 1.59	0.623
CMR parameters per SD increase (Left Ventricle)			
LVEDV	0.85	0.57 – 2.7	0.414
LV mass	1.13	0.78 – 1.62	0.519
LVEF	0.90	0.56 – 1.44	0.662
LV longitudinal Strain	1.40	0.81 – 2.40	0.232
LV early diastolic Strain Rate*	1.07	0.66 – 1.73	0.790

Logistic regression models for each cardiac magnetic resonance parameters are adjusted for rhythm at the time of the scan. Statistically significant P values (<0.05) are marked in bold. Model for LV early diastolic Strain Rate included patients with SR at the time of the scan only*.

After further adjusting for age and CHA_2DS_2VASc score (**Figure 22**), LA vorticity remained significantly associated with LNCCIs [OR (95% CI) = 2.10 (1.12-3.92) per SD, P=0.021]. **Figure 22** shows the results of further regression analyses to test the associations between LA vorticity and LNCCI under different covariate specifications. The observed age- CHA_2DS_2VASc- rhythm-adjusted association between LA vorticity and LNCCIs remained robust after further adjusting for LA volume and LAEF (OR = 2.06, P=0.033, **Figure 22**) or LVEF and LV mass (OR = 2.02, P = 0.037; **Figure 22**). The relationship between LA vorticity and LNCCIs remained significant also in models adjusted for gender and BMI (OR = 1.94, P=0.032; **Figure 22**), heart rate (OR = 1.95, P=0.040; **Figure 22**), blood pressure (OR = 1.97, P=0.030; **Figure 22**), use of beta-blocker (OR = 1.91, P = 0.040), or use of thrombotic therapies and AF onset within 12 months of onset (OR = 2.01, P=0.040; **Figure 22**).

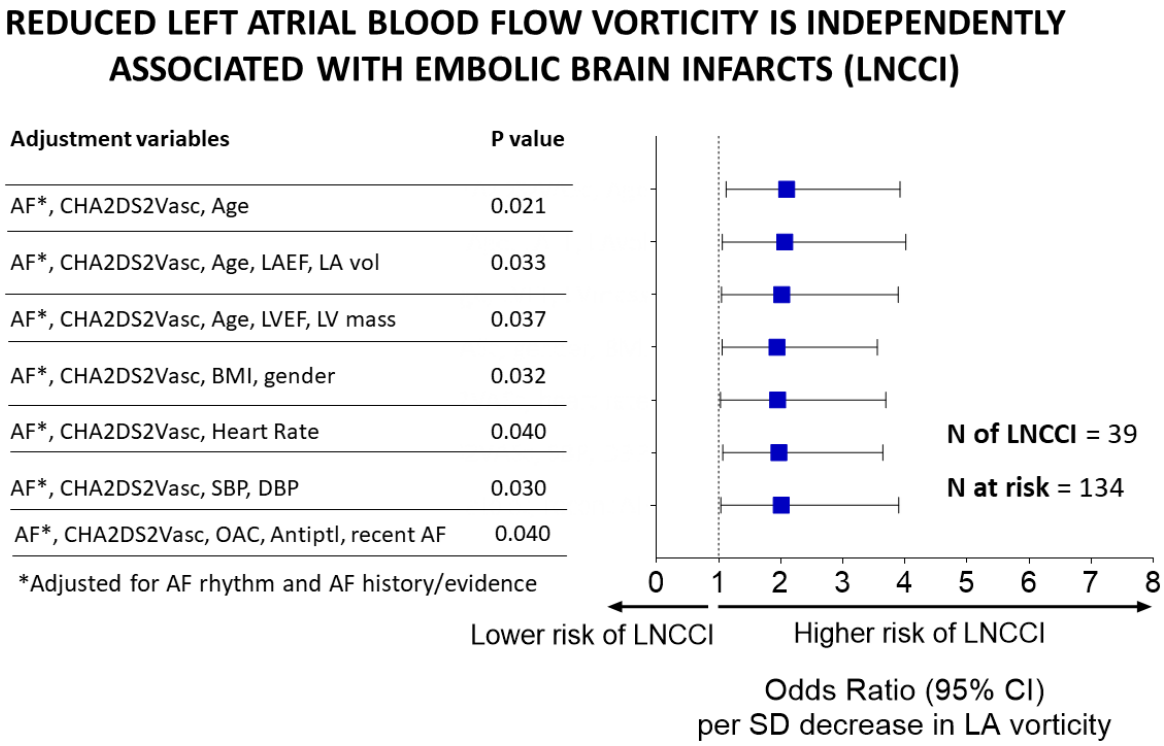


Figure 22: Relationship between Left Atrial (LA) vorticity and embolic brain infarcts.

Reduced LA blood flow vorticity is independently associated with prevalent embolic brain infarcts defined as Large Non-Cortical and Cortical Infarcts (LNCCIs). Such association is robust to baseline differences in clinical, haemodynamic, and CMR structural and functional parameters. Adjustment for AF included both adjustment for rhythm at the time of the scan, and for history/ evidence of AF (including silent AF). Recent AF was defined as AF onset >12 months before study visit. Atrial Fibrillation; LA, Left Atrial; LV, Left Ventricular; EF, Ejection Fraction; BMI, Body Mass Index; S/D BP, Systolic/Diastolic Blood Pressure; OAC, Oral Anticoagulation; Antiptl, Antiplatelet therapy.

Further, exploratory subgroup analysis showed that the association between LA vorticity and LNCCI observed in the whole study population, remained statistically significant in the subgroup of patients in SR [OR for LNCCI = 2.24 per SD decrease, P=0.035; **Figure 23**]. In this subgroup, we found a significant decreasing trend in LNCCI across increasing LA vorticity levels (P trend = 0.045; **Figure 24**).

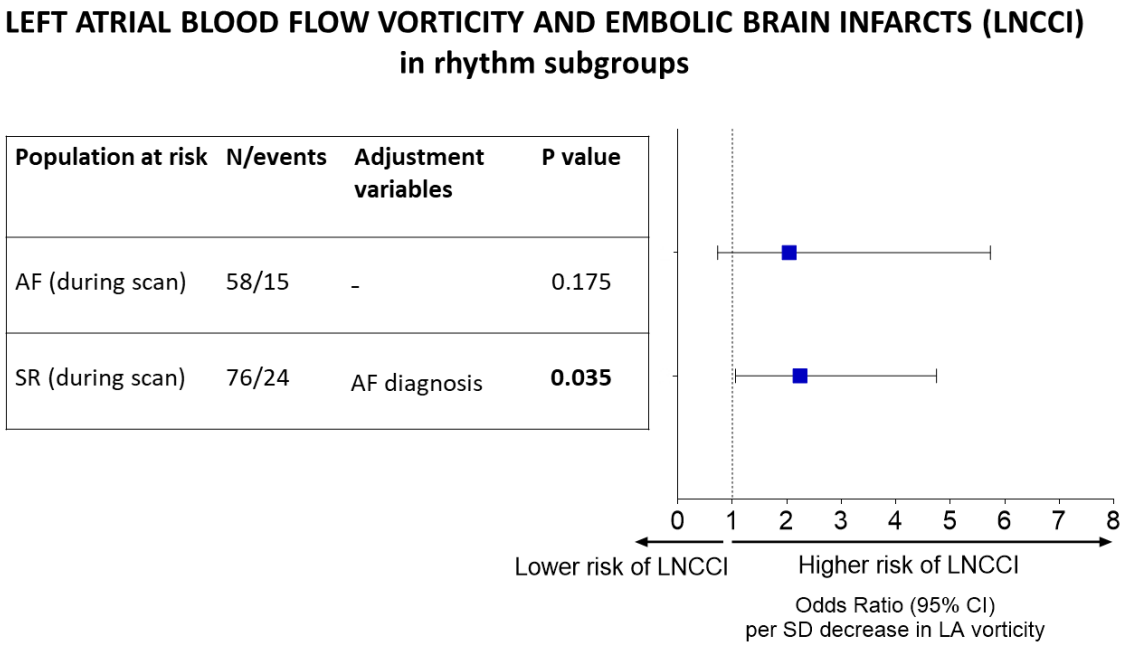


Figure 23: Relationship between Left Atrial (LA) vorticity and embolic brain infarcts in subgroups.

Reduced LA blood flow vorticity is associated with prevalent embolic brain infarcts defined as Large Non-Cortical and Cortical Infarcts (LNCCIs) even in the subgroup of patients in SR after adjusting for history of AF. AF, Atrial Fibrillation; SR, Sinus Rhythm.

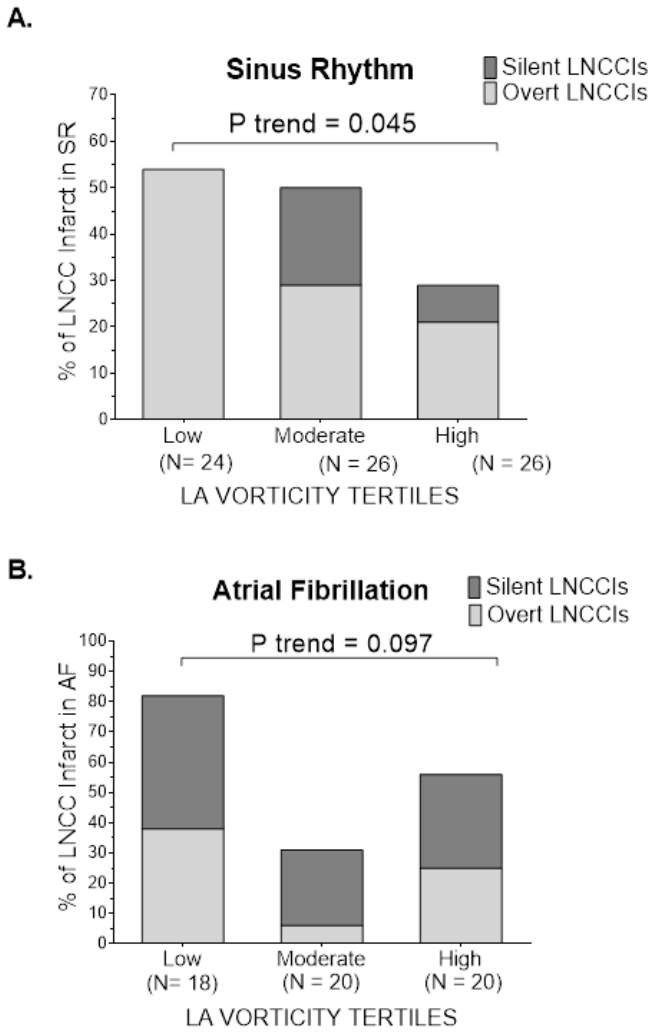


Figure 24: Percentage of embolic brain infarcts for LA vorticity tertiles. *Percentage of patients with MRI-detected embolic brain infarcts (i.e. Large Non-Cortical and Cortical Infarcts, LNCCIs) stratified by Left Atrium (LA) vorticity tertiles and by rhythm at the time of the scan. Further stratification into silent (dark grey) and overt (light grey) brain infarcts is reported. Significant P trend values by Mantel-Haenszel test are reported.*

By contrast, non-embolic SNCI-type brain infarcts were not associated with LA vorticity, LA peak velocity, or any other CMR parameter evaluated (all P>0.05; **Table 28**). Finally, among those patients recently admitted for acute stroke, LA vorticity did not correlate with the time interval from hospital admission to the CMR scan (Spearman's Rho = -0.079, P = 0.690 in SR; -0.426, P = 0.220 in AF).

Table 28. Relationship between CMR parameters and Small Non-Cortical Infarcts

Parameters	Covariates	Subjects at risk	P value
CHA_2DS_2Vasc score	-	Whole cohort (N=134)	0.480
Left atrium			
LA volume	AF	Whole cohort (N=134)	0.923
LAEF	AF	Whole cohort (N=134)	0.695
LA reservoir strain	AF	Whole cohort (N=134)	0.963
LA conduit strain	AF	Whole cohort (N=134)	0.274
LA peak velocity	AF	Whole cohort (N=134)	0.681
LA vorticity	AF	Whole cohort (N=134)	0.768
Left Ventricle			
LVEF	AF	Whole cohort (N=134)	0.278
LV mass	AF	Whole cohort (N=134)	0.765
LV early diastolic Strain Rate	AF	Whole cohort (N=134)	0.779

5.5 Discussion

Using novel magnetic resonance imaging measurements, we show that impaired LA blood flow vorticity is specifically associated with large non-cortical or cortical brain infarcts (i.e. LNCCI) independently of AF, age, clinical stroke risk, and cardiac function and size.

Larger or cortical brain infarcts are associated with worse neurological symptoms[58] and cognitive decline[59] and they are more likely to be embolic in origin[41, 58]; whilst smaller non-cortical lesions are more likely to be vascular in origin[60]. LNCCI is a neuroimaging construct[41, 59, 60, 62] which is caused by a number of heterogenous mechanisms such as cardiac embolism (e.g. AF, left ventricular disease, patent foramen ovalis) or atherosclerotic plaques[63]. The fact that, after a full diagnostic evaluation, up to 20-25% of LNCCI remain of undetermined cause, suggests that some pathophysiologic mechanisms of embolic stroke are currently unknown. Importantly, these unknown mechanisms may overlap with currently recognized mechanisms where a potential embolic source should not be automatically presumed as exclusive[44, 63]. Our study shows that lower tendency of LA flow to rotate may be a mechanism of LNCCI which is currently unrecognized. Importantly, our study shows that the relationship between LA vorticity and embolic brain infarcts seems significant in patients in SR with structurally normal hearts (on average), regardless of AF diagnosis. Reduced vorticity has been associated with biomechanical (rather than inflammatory) platelet activation due to spoiled shear stress[151, 152], and could promote intra-cardiac thrombus

formation[153]. Although further studies are needed to assess more comprehensively the relationship between platelet activation and LA vorticity, a reduction in LA vorticity may have important pathophysiological implications, either as a risk factor for de novo embolic brain infarcts, or as a contributor to the 27-36% rate of recurrent ischaemic stroke[55].

Together, our results suggest that LA vorticity may also be an important tool for thromboembolic risk stratification in patients in SR[63].

5.5.1 Pro-thrombotic LA flow pattern and pathophysiologic rationale for novel therapeutic targets

Vortical rings within the heart are a trait that is broadly conserved by natural selection across species of the vertebrate line and is an important epigenetic driver of cardiogenesis by providing endocardial shear forces[150, 195]. This is in keeping with the idea that recirculating flows and vortices play a crucial role in transfer of blood flow momentum, minimising energy dissipation, and optimising the overall efficiency of blood flow[152]. In addition to providing a hemodynamic framework for ventricular adaptation [29], vortex-induced shear along its outer boundary seems important to regulate platelet activation and aggregation[151, 152, 154]. In terms of pathophysiology, biomechanical platelet activation appears to be insensitive to aspirin, since biomechanical activation does not involve the cyclooxygenase pathway for activation of glycoprotein IIb/IIIa with fibrinogen as the ligand (i.e. an

aspirin-sensitive pathway); rather, biomechanical activation acts on a different domain on glycoprotein IIb/IIIa with von Willebrand's factor as the ligand (i.e. an aspirin-insensitive pathway)[196]. Recent rodent studies have demonstrated that Adenosine Diphosphate (ADP) plays an important role in shear-induced platelet activation, and suggest that clopidogrel could be a more potent antithrombotic agent than ticlopidine or aspirin in this context[197]. In keeping with this evidence, patients with multi-territory infarcts (as a marker of potential cardioembolic aetiology) experienced the greatest clinical benefit from dual antiplatelet therapy (DAPT) using clopidogrel plus aspirin[198]. Furthermore, building on the same rationale, colchicine, which also reduces ADP-related platelet adhesiveness[199], significantly reduced incident stroke risk among patients with a recent myocardial infarct[200].

Abnormal LA vorticity may also be a relevant pathophysiological mechanism of ESUS. Intriguingly, recent randomized controlled trials have shown that oral anticoagulants (acting directly on the coagulation cascade) do not reduce recurrent stroke risk compared to aspirin in patients in SR with ESUS [81, 82]. The fact that the vast majority (>90%) of patients with a recent history of ESUS display normal LA size and LVEF may explain why ESUS patients do not benefit from rivaroxaban therapy[27]. Our results suggest that disruption of LA flow vorticity may occur even in structurally/functionally normal heart, thus making this an interesting target to explore in in the ESUS population.

Alternatively, or additionally, deranged LA vorticity could be a downstream effect of embolic brain infarcts on the cardiovascular system. This would be in keeping with a number of previously described mechanisms of stroke-induced cardiac damage[201]. Cardiac dysfunction usually manifests in the acute phase following brain injury before resolving over several weeks[201]; this is similar to the timescale during which acute brain lesions change from DWI-positive to DWI-negative[202]. As our cohort includes patients with acute embolic infarcts on imaging (i.e. DWI positive), 75% of whom were scanned within 7 days from admission for acute stroke, the possibility of brain-heart post-stroke interaction cannot be excluded. However, a note of caution is due as we did not observe any significant differences in any LV or LA CMR parameter between subjects with LNCCIs and those without embolic brain infarct, arguing against a significant role of LV/LA structural/functional parameters on LA vorticity. Similarly, LA vorticity was not correlated with the time from stroke onset, and remained significantly associated with LNCCIs after adjusting for LA and LV parameters which are typically sensitive to brain damage.

5.5.2 CMR imaging parameters as biomarkers of stroke risk in SR

Currently, clinical risk of stroke in AF is estimated using CHA_2DS_2-VASc score[31] with some limitations in terms of modest predictive capacity[203]. Although CHA_2DS_2-VASc score also predicts events in SR, its predictive power is even lower in this population[32]. Therefore, there is significant interest in biomarkers of stroke

risk that could be incorporated into risk scoring algorithms, in particular for the identification of high-risk patients in SR who currently do not have an indication for anti-thrombotic preventive treatment.

So far, multiple imaging parameters have been associated with ischaemic stroke in patients without AF, including increased LA size/volume[204-206], reduced LAEF[20], and LA late gadolinium enhancement (as a potential marker of LA fibrosis)[21]. Whilst these parameters may result in a higher likelihood of LA thrombus formation, they may also be linked to extra-cardiac sources of ischaemic stroke, such as hypertension-related small vessel disease (as in the case of LA dysfunction which is associated with non-embolic lacunar brain infarcts[23]) and thus offer limited information as to the appropriateness of initiating anticoagulation. Our study is the first to test associations between CMR biomarkers (such as LA flow parameters, LA volume, LAEF, LA reservoir function, LV mass, LVEF, LV diastolic dysfunction) and specifically non-lacunar brain infarcts, likely to be embolic in origin. Surprisingly, we did not observe significant association between embolic brain infarcts and LA/LV structural/functional/velocity parameters despite previous reports of a link with general ischaemic stroke risk[20, 147, 204, 205]. Such results may be interpreted to suggest that cardiac structural/functional parameters are markers of general stroke risk rather than specifically of larger and cortical brain infarcts (deemed to be embolic in nature). On the other hand, LA vorticity, which in our study is specifically associated with larger and cortical brain infarcts, seems unrelated to conventional LA/LV parameters.

In summary, our data suggest that LA vorticity may be a unique independent predictor of LNCCI, and thus, it may aid risk stratification beyond clinical stroke risk tools and conventional cardiac structural/functional imaging parameters.

5.5.3 Limitations

This single-centre proof-of-principle study has inherent limitations related to its exploratory design. Due to the cross-sectional nature of this study, the chronological sequence of the events cannot be inferred; a reduction in LA flow vorticity may either precede the onset of incident embolic brain infarcts, or, less likely, be a secondary effect of brain ischaemia on LA flow characteristics[201]. Longitudinal studies are now required to confirm the temporality of these initial findings in order to tease out whether impaired LA vorticity is an independent predictor of incident brain infarct, or whether the occurrence of brain infarcts affects LA vorticity. Irrespective of these considerations, a reduction in LA vorticity may have important pathophysiological implications, either as a risk factor for de novo embolic brain infarcts, or as a contributor to the 27-36% rate of recurrent ischaemic stroke[55]. Further, the pre-planned recruitment strategy targeting a patient population with previous/recent ischaemic stroke admission implies non-probability-sampling, with further inherent limitations in generalizing estimates of the association between flow parameters and brain infarcts at an epidemiological level.

Our post-processing tools for 4D flow imaging data do not include assessment of local flow characteristics within the LAA, which is the preferential site for thrombus formation within the LA[207]. Furthermore, our study protocol was contrast-free and hence it did not include assessment of atrial late gadolinium enhancement.

Finally, brain scans were performed on different systems (N = 9, 7% on 1.5 T system vs N= 124, 93% on 3 T vs N = 1, <1% on CT scan). Although, in principle, this could create differences in diagnostic accuracy for analysis of brain infarcts, the main association between LA vorticity and LNCCI was robust after further adjustment for scanner type (OR 2.20, P = 0.12).

5.6 **Conclusions**

Reduced rotational LA blood flow is associated with embolic (but not lacunar) brain infarct, independently of age, heart rhythm, stroke risk factors, and cardiac structure or function. Prospective studies are needed to assess whether LA flow vorticity can identify high-risk individuals in SR who would benefit from antithrombotic therapy.

Chapter 6

General conclusions

In conclusion, this Thesis has provided novel insights into LA flow both in AF and in SR, its relationship with cardiac mechanical function, clinical stroke risk factors, and the relationship with embolic brain infarct. The main findings of this Thesis are:

1. LA 4D Flow parameters show overall good reproducibility and low temporal variability. Among all LA 4D Flow parameters, LA peak velocity and vorticity are the most reproducible and temporally stable LA 4D Flow biomarkers, and are robust to changes in heart rate, blood pressure, and differences in heart rhythm.
2. Patients at moderate clinical stroke risk in SR display adverse LA flow characteristics in association with an LA myopathic phenotype and LV diastolic dysfunction, regardless of a history of AF.
3. LV diastolic dysfunction and impaired LA emptying fraction are associated with adverse LA flow characteristics in patients in SR with stroke risk factors. Such adverse LA flow profile is dramatically exacerbated during AF. These findings suggest that AF burden may directly affect stroke risk, by varying the exposure of the LA to pro-thrombotic flow patterns. They also imply that older individuals in SR with depressed LA emptying fraction and LV diastolic dysfunction are more likely to present with pro-thrombotic LA flow

characteristics and thus, they may benefit from anti-thrombotic therapy, whether or not they have a history of AF.

4. Reduced vorticity of the LA blood flow is associated with embolic (but not lacunar) brain infarct, independently of age, heart rhythm, stroke risk factors, and cardiac structure or function. Reduced tendency to rotate of LA blood flow may be a novel pathophysiological mechanism of embolic stroke which is currently unrecognized.

This Thesis has also established post-processing software and procedures for the application of 4D Flow to the LA.

There are numerous research directions for future studies based on this work. The following concepts may be of greatest interest, in view of the clinical relevance and therapeutic potential:

1. Investigation of the relationship between LA vorticity and platelets activation both in AF and in SR.
2. Investigation of LA vorticity as an imaging biomarker of incident embolic risk in longitudinal studies.
3. Investigation of determinants of LA vorticity and detection of interventions to improve LA vorticity levels.

Bibliography

1. Kirchhof P, Benussi S, Kotecha D, Ahlsson A, Atar D, Casadei B, Castella M, Diener HC, Heidbuchel H, Hendriks J, Hindricks G, Manolis AS, Oldgren J, Popescu BA, Schotten U, Van Putte B, Vardas P, Agewall S, Camm J, Baron Esquivias G, Budts W, Carerj S, Casselman F, Coca A, De Caterina R, Deftereos S, Dobrev D, Ferro JM, Filippatos G, Fitzsimons D, Gorenek B, Guenoun M, Hohnloser SH, Kolh P, Lip GY, Manolis A, McMurray J, Ponikowski P, Rosenhek R, Ruschitzka F, Savelieva I, Sharma S, Suwalski P, Tamargo JL, Taylor CJ, Van Gelder IC, Voors AA, Windecker S, Zamorano JL and Zeppenfeld K. 2016 ESC Guidelines for the management of atrial fibrillation developed in collaboration with EACTS. *European heart journal*. 2016;37:2893-2962.
2. Chugh SS, Havmoeller R, Narayanan K, Singh D, Rienstra M, Benjamin EJ, Gillum RF, Kim YH, McAnulty JH, Jr., Zheng ZJ, Forouzanfar MH, Naghavi M, Mensah GA, Ezzati M and Murray CJ. Worldwide epidemiology of atrial fibrillation: a Global Burden of Disease 2010 Study. *Circulation*. 2014;129:837-47.
3. Lin HJ, Wolf PA, Kelly-Hayes M, Beiser AS, Kase CS, Benjamin EJ and D'Agostino RB. Stroke severity in atrial fibrillation. The Framingham Study. *Stroke; a journal of cerebral circulation*. 1996;27:1760-4.
4. Wolf PA, Abbott RD and Kannel WB. Atrial fibrillation as an independent risk factor for stroke: the Framingham Study. *Stroke*. 1991;22:983-8.
5. Benjamin EJ, Wolf PA, D'Agostino RB, Silbershatz H, Kannel WB and Levy D. Impact of atrial fibrillation on the risk of death: the Framingham Heart Study. *Circulation*. 1998;98:946-52.
6. Luengo-Fernandez R, Gray AM, Bull L, Welch S, Cuthbertson F, Rothwell PM and Oxford Vascular S. Quality of life after TIA and stroke: ten-year results of the Oxford Vascular Study. *Neurology*. 2013;81:1588-95.
7. Petersen P and Godtfredsen J. Embolic complications in paroxysmal atrial fibrillation. *Stroke*. 1986;17:622-6.
8. Wolf PA, Dawber TR, Thomas HE, Jr. and Kannel WB. Epidemiologic assessment of chronic atrial fibrillation and risk of stroke: the Framingham study. *Neurology*. 1978;28:973-7.
9. Gladstone DJ, Spring M, Dorian P, Panzov V, Thorpe KE, Hall J, Vaid H, O'Donnell M, Laupacis A, Cote R, Sharma M, Blakely JA, Shuaib A, Hachinski V, Coutts SB, Sahlas DJ, Teal P, Yip S, Spence JD, Buck B, Verreault S, Casaubon LK, Penn A, Selchen D, Jin A, Howse D, Mehdiratta M, Boyle K, Aviv R, Kapral MK, Mamdani M, Investigators E and Coordinators. Atrial fibrillation in patients with cryptogenic stroke. *The New England journal of medicine*. 2014;370:2467-77.
10. Delgado V, Di Biase L, Leung M, Romero J, Tops LF, Casadei B, Marrouche N and Bax JJ. Structure and Function of the Left Atrium and Left Atrial Appendage: AF and Stroke Implications. *J Am Coll Cardiol*. 2017;70:3157-3172.
11. Boston Area Anticoagulation Trial for Atrial Fibrillation I, Singer DE, Hughes RA, Gress DR, Sheehan MA, Oertel LB, Maraventano SW, Blewett DR,

Rosner B and Kistler JP. The effect of low-dose warfarin on the risk of stroke in patients with nonrheumatic atrial fibrillation. *N Engl J Med*. 1990;323:1505-11.
12. Granger CB, Alexander JH, McMurray JJ, Lopes RD, Hylek EM, Hanna M, Al-Khalidi HR, Ansell J, Atar D, Avezum A, Bahit MC, Diaz R, Easton JD, Ezekowitz JA, Flaker G, Garcia D, Geraldes M, Gersh BJ, Golitsyn S, Goto S, Hermosillo AG, Hohnloser SH, Horowitz J, Mohan P, Jansky P, Lewis BS, Lopez-Sendon JL, Pais P, Parkhomenko A, Verheugt FW, Zhu J, Wallentin L, Committees A and Investigators. Apixaban versus warfarin in patients with atrial fibrillation. *N Engl J Med*. 2011;365:981-92.
13. Patel MR, Mahaffey KW, Garg J, Pan G, Singer DE, Hacke W, Breithardt G, Halperin JL, Hankey GJ, Piccini JP, Becker RC, Nessel CC, Paolini JF, Berkowitz SD, Fox KA, Califf RM and Investigators RA. Rivaroxaban versus warfarin in nonvalvular atrial fibrillation. *N Engl J Med*. 2011;365:883-91.
14. Connolly SJ, Ezekowitz MD, Yusuf S, Eikelboom J, Oldgren J, Parekh A, Pogue J, Reilly PA, Themeles E, Varrone J, Wang S, Alings M, Xavier D, Zhu J, Diaz R, Lewis BS, Darius H, Diener HC, Joyner CD, Wallentin L, Committee R-LS and Investigators. Dabigatran versus warfarin in patients with atrial fibrillation. *N Engl J Med*. 2009;361:1139-51.
15. Kamel H, Okin PM, Elkind MS and Iadecola C. Atrial Fibrillation and Mechanisms of Stroke: Time for a New Model. *Stroke*. 2016;47:895-900.
16. Van Gelder IC, Healey JS, Crijns HJ, Wang J, Hohnloser SH, Gold MR, Capucci A, Lau CP, Morillo CA, Hobbelt AH, Rienstra M and Connolly SJ. Duration of device-detected subclinical atrial fibrillation and occurrence of stroke in ASSERT. *Eur Heart J*. 2017.
17. Brambatti M, Connolly SJ, Gold MR, Morillo CA, Capucci A, Muto C, Lau CP, Van Gelder IC, Hohnloser SH, Carlson M, Fain E, Nakamya J, Mairesse GH, Halytska M, Deng WQ, Israel CW, Healey JS and Investigators A. Temporal relationship between subclinical atrial fibrillation and embolic events. *Circulation*. 2014;129:2094-9.
18. Wyse DG, Waldo AL, DiMarco JP, Domanski MJ, Rosenberg Y, Schron EB, Kellen JC, Greene HL, Mickel MC, Dalquist JE, Corley SD and Atrial Fibrillation Follow-up Investigation of Rhythm Management I. A comparison of rate control and rhythm control in patients with atrial fibrillation. *The New England journal of medicine*. 2002;347:1825-33.
19. Roy D, Talajic M, Nattel S, Wyse DG, Dorian P, Lee KL, Bourassa MG, Arnold JM, Buxton AE, Camm AJ, Connolly SJ, Dubuc M, Ducharme A, Guerra PG, Hohnloser SH, Lambert J, Le Heuzey JY, O'Hara G, Pedersen OD, Rouleau JL, Singh BN, Stevenson LW, Stevenson WG, Thibault B, Waldo AL, Atrial F and Congestive Heart Failure I. Rhythm control versus rate control for atrial fibrillation and heart failure. *N Engl J Med*. 2008;358:2667-77.
20. Habibi M, Zareian M, Ambale Venkatesh B, Samiei S, Imai M, Wu C, Launer LJ, Shea S, Gottesman RF, Heckbert SR, Bluemke DA and Lima JAC. Left Atrial Mechanical Function and Incident Ischemic Cerebrovascular Events Independent of AF: Insights From the MESA Study. *JACC Cardiovasc Imaging*. 2019;12:2417-2427.
21. Fonseca AC, Alves P, Inacio N, Marto JP, Viana-Baptista M, Pinho EMT, Ferro JM and Almeida AG. Patients With Undetermined Stroke Have Increased Atrial Fibrosis: A Cardiac Magnetic Resonance Imaging Study. *Stroke*. 2018;49:734-737.

22. Ntaios G, Perlepe K, Lambrou D, Sirimarco G, Strambo D, Eskandari A, Karagkiozi E, Vemmou A, Koroboki E, Manios E, Makaritsis K, Vemmos K and Michel P. Prevalence and Overlap of Potential Embolic Sources in Patients With Embolic Stroke of Undetermined Source. *J Am Heart Assoc*. 2019;8:e012858.
23. Russo C, Jin Z, Liu R, Iwata S, Tugcu A, Yoshita M, Homma S, Elkind MS, Rundek T, Decarli C, Wright CB, Sacco RL and Di Tullio MR. LA volumes and reservoir function are associated with subclinical cerebrovascular disease: the CABL (Cardiovascular Abnormalities and Brain Lesions) study. *JACC Cardiovasc Imaging*. 2013;6:313-23.
24. Kaplan RM, Koehler J, Ziegler PD, Sarkar S, Zweibel S and Passman RS. Stroke Risk as a Function of Atrial Fibrillation Duration and CHA2DS2-VASc Score. *Circulation*. 2019;140:1639-1646.
25. Bisbal F, Baranchuk A, Braunwald E, Bayes de Luna A and Bayes-Genis A. Atrial Failure as a Clinical Entity: JACC Review Topic of the Week. *J Am Coll Cardiol*. 2020;75:222-232.
26. Eikelboom JW, Connolly SJ, Bosch J, Dagenais GR, Hart RG, Shestakovska O, Diaz R, Alings M, Lonn EM, Anand SS, Widimsky P, Hori M, Avezum A, Piegas LS, Branch KRH, Probstfield J, Bhatt DL, Zhu J, Liang Y, Maggioni AP, Lopez-Jaramillo P, O'Donnell M, Kakkar AK, Fox KAA, Parkhomenko AN, Ertl G, Stork S, Keltai M, Ryden L, Pogosova N, Dans AL, Lanas F, Commerford PJ, Torp-Pedersen C, Guzik TJ, Verhamme PB, Vinereanu D, Kim JH, Tonkin AM, Lewis BS, Felix C, Yusoff K, Steg PG, Metsarinne KP, Cook Bruns N, Misselwitz F, Chen E, Leong D, Yusuf S and Investigators C. Rivaroxaban with or without Aspirin in Stable Cardiovascular Disease. *N Engl J Med*. 2017;377:1319-1330.
27. Healey JS, Gladstone DJ, Swaminathan B, Eckstein J, Mundl H, Epstein AE, Haeusler KG, Mikulik R, Kasner SE, Toni D, Arauz A, Ntaios G, Hankey GJ, Perera K, Pagola J, Shuaib A, Lutsep H, Yang X, Uchiyama S, Endres M, Coutts SB, Karlinski M, Czlonkowska A, Molina CA, Santo G, Berkowitz SD, Hart RG and Connolly SJ. Recurrent Stroke With Rivaroxaban Compared With Aspirin According to Predictors of Atrial Fibrillation: Secondary Analysis of the NAVIGATE ESUS Randomized Clinical Trial. *JAMA Neurol*. 2019;76:764-773.
28. Markl M, Lee DC, Furiasse N, Carr M, Foucar C, Ng J, Carr J and Goldberger JJ. Left Atrial and Left Atrial Appendage 4D Blood Flow Dynamics in Atrial Fibrillation. *Circulation Cardiovascular imaging*. 2016;9:e004984.
29. Friberg L, Rosenqvist M and Lip GY. Evaluation of risk stratification schemes for ischaemic stroke and bleeding in 182 678 patients with atrial fibrillation: the Swedish Atrial Fibrillation cohort study. *Eur Heart J*. 2012;33:1500-10.
30. Ntaios G, Lip GY, Makaritsis K, Papavasileiou V, Vemmou A, Koroboki E, Savvari P, Manios E, Milionis H and Vemmos K. CHADS(2), CHA(2)S(2)DS(2)-VASc, and long-term stroke outcome in patients without atrial fibrillation. *Neurology*. 2013;80:1009-17.
31. Lip GY, Nieuwlaat R, Pisters R, Lane DA and Crijns HJ. Refining clinical risk stratification for predicting stroke and thromboembolism in atrial fibrillation using a novel risk factor-based approach: the euro heart survey on atrial fibrillation. *Chest*. 2010;137:263-72.
32. Melgaard L, Gorst-Rasmussen A, Lane DA, Rasmussen LH, Larsen TB and Lip GY. Assessment of the CHA2DS2-VASc Score in Predicting Ischemic Stroke,

Thromboembolism, and Death in Patients With Heart Failure With and Without Atrial Fibrillation. *JAMA*. 2015;314:1030-8.
33. Mitchell LB, Southern DA, Galbraith D, Ghali WA, Knudtson M and Wilton SB. Prediction of stroke or TIA in patients without atrial fibrillation using CHADS2 and CHA2DS2-VASc scores. *Heart*. 2014;100:1524-30.
34. Renda G, Ricci F, Patti G, Aung N, Petersen SE, Gallina S, Hamrefors V, Melander O, Sutton R, Engstrom G, Caterina R and Fedorowski A. CHA(2)DS(2)VASc score and adverse outcomes in middle-aged individuals without atrial fibrillation. *Eur J Prev Cardiol*. 2019;26:1987-1997.
35. Meah MN, Dweck MR and Newby DE. Cardiovascular imaging to guide primary prevention. *Heart*. 2020;106:1267-1275.
36. Royal College of Physicians Sentinel Stroke National Audit Programme (SSNAP). National clinical audit annual results portfolio March 2016-April 2017. Available: http://bit.ly/1NHYlqH Last accessed 24 October 2017.
37. National Institute for Health and Clinical Excellence. Clopidogrel and modified-release dipyridamole for the prevention of occlusive vascular events. December 2010. www.nice.org.uk/ta210 (accessed 3 May 2011).
38. Adamson J, Beswick A and Ebrahim S. Is stroke the most common cause of disability? *J Stroke Cerebrovasc Dis*. 2004;13:171-7.
39. National Institute for Health and Clinical Excellence. Diagnosis and initial management of acute stroke and transient ischaemic attack. July 2008. www.nice.org.uk/cg68 (accessed 3 May 2011).
40. Amarenco P, Bogousslavsky J, Caplan LR, Donnan GA and Hennerici MG. Classification of Stroke Subtypes. *Cerebrovascular Diseases*. 2009;27:493-501.
41. Hart RG, Diener HC, Coutts SB, Easton JD, Granger CB, O'Donnell MJ, Sacco RL, Connolly SJ and Cryptogenic Stroke EIWG. Embolic strokes of undetermined source: the case for a new clinical construct. *Lancet Neurol*. 2014;13:429-38.
42. Li L, Yiin GS, Geraghty OC, Schulz UG, Kuker W, Mehta Z and Rothwell PM. Incidence, outcome, risk factors, and long-term prognosis of cryptogenic transient ischaemic attack and ischaemic stroke: a population-based study. *Lancet Neurol*. 2015;14:903-913.
43. Campbell BCV, De Silva DA, Macleod MR, Coutts SB, Schwamm LH, Davis SM and Donnan GA. Ischaemic stroke. *Nature Reviews Disease Primers*. 2019;5:70.
44. Ntaios G and Hart RG. Embolic Stroke. *Circulation*. 2017;136:2403-2405.
45. Murphy BP, Harford FJ and Cramer FS. Cerebral air embolism resulting from invasive medical procedures. Treatment with hyperbaric oxygen. *Ann Surg*. 1985;201:242-5.
46. Mijalski C, Lovett A, Mahajan R, Sundararajan S, Silverman S and Feske S. Cerebral Fat Embolism: A Case of Rapid-Onset Coma. *Stroke*. 2015;46:e251-3.
47. Hart RG, Catanese L, Perera KS, Ntaios G and Connolly SJ. Embolic Stroke of Undetermined Source: A Systematic Review and Clinical Update. *Stroke*. 2017;48:867-872.
48. Gorelick PB, Wong KS, Bae HJ and Pandey DK. Large artery intracranial occlusive disease: a large worldwide burden but a relatively neglected frontier. *Stroke*. 2008;39:2396-9.
49. Banerjee C and Chimowitz MI. Stroke Caused by Atherosclerosis of the Major Intracranial Arteries. *Circulation Research*. 2017;120:502-513.

50. Radu RA, Terecoasa EO, Bajenaru OA and Tiu C. Etiologic classification of ischemic stroke: Where do we stand? *Clin Neurol Neurosurg*. 2017;159:93-106.
51. Stroke and TIA CKS.NICE, Scenario: Secondary prevention following stroke and TIA. Last revised in March 2017. https://cks.nice.org.uk/stroke-and-tia#!scenario:2

52. Chung JW, Park SH, Kim N, Kim WJ, Park JH, Ko Y, Yang MH, Jang MS, Han MK, Jung C, Kim JH, Oh CW and Bae HJ. Trial of ORG 10172 in Acute Stroke Treatment (TOAST) classification and vascular territory of ischemic stroke lesions diagnosed by diffusion-weighted imaging. *J Am Heart Assoc*. 2014;3.
53. Adams HP, Jr., Bendixen BH, Kappelle LJ, Biller J, Love BB, Gordon DL and Marsh EE, 3rd. Classification of subtype of acute ischemic stroke. Definitions for use in a multicenter clinical trial. TOAST. Trial of Org 10172 in Acute Stroke Treatment. *Stroke*. 1993;24:35-41.
54. Marnane M, Duggan CA, Sheehan OC, Merwick A, Hannon N, Curtin D, Harris D, Williams EB, Horgan G, Kyne L, McCormack PM, Duggan J, Moore A, Crispino-O'Connell G and Kelly PJ. Stroke subtype classification to mechanism-specific and undetermined categories by TOAST, A-S-C-O, and causative classification system: direct comparison in the North Dublin population stroke study. *Stroke*. 2010;41:1579-86.
55. Li L, Yiin GS, Geraghty OC, Schulz UG, Kuker W, Mehta Z, Rothwell PM and Oxford Vascular S. Incidence, outcome, risk factors, and long-term prognosis of cryptogenic transient ischaemic attack and ischaemic stroke: a population-based study. *Lancet Neurol*. 2015;14:903-13.
56. Wolf PA, Abbott RD and Kannel WB. Atrial fibrillation: a major contributor to stroke in the elderly. The Framingham Study. *Arch Intern Med*. 1987;147:1561-4.
57. Arsava EM, Helenius J, Avery R, Sorgun MH, Kim GM, Pontes-Neto OM, Park KY, Rosand J, Vangel M and Ay H. Assessment of the Predictive Validity of Etiologic Stroke Classification. *JAMA Neurol*. 2017;74:419-426.
58. Yamaguchi T, Minematsu K, Choki J and Ikeda M. Clinical and neuroradiological analysis of thrombotic and embolic cerebral infarction. *Jpn Circ J*. 1984;48:50-8.
59. Conen D, Rodondi N, Muller A, Beer JH, Ammann P, Moschovitis G, Auricchio A, Hayoz D, Kobza R, Shah D, Novak J, Schlapfer J, Di Valentino M, Aeschbacher S, Blum S, Meyre P, Sticherling C, Bonati LH, Ehret G, Moutzouri E, Fischer U, Monsch AU, Stippich C, Wuerfel J, Sinnecker T, Coslovsky M, Schwenkglenks M, Kuhne M, Osswald S and Swiss AFSI. Relationships of Overt and Silent Brain Lesions With Cognitive Function in Patients With Atrial Fibrillation. *J Am Coll Cardiol*. 2019;73:989-999.
60. Wardlaw JM, Smith EE, Biessels GJ, Cordonnier C, Fazekas F, Frayne R, Lindley RI, O'Brien JT, Barkhof F, Benavente OR, Black SE, Brayne C, Breteler M, Chabriat H, Decarli C, de Leeuw FE, Doubal F, Duering M, Fox NC, Greenberg S, Hachinski V, Kilimann I, Mok V, Oostenbrugge R, Pantoni L, Speck O, Stephan BC, Teipel S, Viswanathan A, Werring D, Chen C, Smith C, van Buchem M, Norrving B, Gorelick PB, Dichgans M and nEuroimaging STfRVco. Neuroimaging standards for

research into small vessel disease and its contribution to ageing and neurodegeneration. *Lancet Neurol*. 2013;12:822-38.
61. Pantoni L. Cerebral small vessel disease: from pathogenesis and clinical characteristics to therapeutic challenges. *Lancet Neurol*. 2010;9:689-701.
62. Anand SS, Tu JV, Desai D, Awadalla P, Robson P, Jacquemont S, Dummer T, Le N, Parker L, Poirier P, Teo K, Lear SA, Yusuf S, Tardif JC, Marcotte F, Busseuil D, Despres JP, Black SE, Kirpalani A, Parraga G, Noseworthy MD, Dick A, Leipsic J, Kelton D, Vena J, Thomas M, Schulze KM, Larose E, Moody AR, Smith EE, Friedrich MG, Canadian Alliance for Healthy H and Minds C. Cardiovascular risk scoring and magnetic resonance imaging detected subclinical cerebrovascular disease. *Eur Heart J Cardiovasc Imaging*. 2019.
63. Ntaios G. Embolic Stroke of Undetermined Source: JACC Review Topic of the Week. *J Am Coll Cardiol*. 2020;75:333-340.
64. Hindricks G, Potpara T, Dagres N, Arbelo E, Bax JJ, Blomstrom-Lundqvist C, Boriani G, Castella M, Dan GA, Dilaveris PE, Fauchier L, Filippatos G, Kalman JM, La Meir M, Lane DA, Lebeau JP, Lettino M, Lip GYH, Pinto FJ, Thomas GN, Valgimigli M, Van Gelder IC, Van Putte BP, Watkins CL and Group ESCSD. 2020 ESC Guidelines for the diagnosis and management of atrial fibrillation developed in collaboration with the European Association of Cardio-Thoracic Surgery (EACTS). *Eur Heart J*. 2020.
65. Hart RG, Pearce LA and Aguilar MI. Meta-analysis: antithrombotic therapy to prevent stroke in patients who have nonvalvular atrial fibrillation. *Ann Intern Med*. 2007;146:857-67.
66. Lamberts M, Staerk L, Olesen JB, Fosbol EL, Hansen ML, Harboe L, Lefevre C, Evans D and Gislason GH. Major Bleeding Complications and Persistence With Oral Anticoagulation in Non-Valvular Atrial Fibrillation: Contemporary Findings in Real-Life Danish Patients. *J Am Heart Assoc*. 2017;6.
67. Shrestha NK, Moreno FL, Narciso FV, Torres L and Calleja HB. Two-dimensional echocardiographic diagnosis of left-atrial thrombus in rheumatic heart disease. A clinicopathologic study. *Circulation*. 1983;67:341-7.
68. Blackshear JL and Odell JA. Appendage obliteration to reduce stroke in cardiac surgical patients with atrial fibrillation. *Ann Thorac Surg*. 1996;61:755-9.
69. Reddy VY, Doshi SK, Kar S, Gibson DN, Price MJ, Huber K, Horton RP, Buchbinder M, Neuzil P, Gordon NT, Holmes DR, Jr., Prevail and Investigators PA. 5-Year Outcomes After Left Atrial Appendage Closure: From the PREVAIL and PROTECT AF Trials. *J Am Coll Cardiol*. 2017;70:2964-2975.
70. Holmes DR, Reddy VY, Turi ZG, Doshi SK, Sievert H, Buchbinder M, Mullin CM, Sick P and Investigators PA. Percutaneous closure of the left atrial appendage versus warfarin therapy for prevention of stroke in patients with atrial fibrillation: a randomised non-inferiority trial. *Lancet*. 2009;374:534-42.
71. Saver JL, Carroll JD, Thaler DE, Smalling RW, MacDonald LA, Marks DS, Tirschwell DL and Investigators R. Long-Term Outcomes of Patent Foramen Ovale Closure or Medical Therapy after Stroke. *N Engl J Med*. 2017;377:1022-1032.
72. Sondergaard L, Kasner SE, Rhodes JF, Andersen G, Iversen HK, Nielsen-Kudsk JE, Settergren M, Sjostrand C, Roine RO, Hildick-Smith D, Spence JD, Thomassen L and Gore RCSI. Patent Foramen Ovale Closure or Antiplatelet Therapy for Cryptogenic Stroke. *N Engl J Med*. 2017;377:1033-1042.

73. Mas JL, Derumeaux G, Guillon B, Massardier E, Hosseini H, Mechtouff L, Arquizan C, Bejot Y, Vuillier F, Detante O, Guidoux C, Canaple S, Vaduva C, Dequatre-Ponchelle N, Sibon I, Garnier P, Ferrier A, Timsit S, Robinet-Borgomano E, Sablot D, Lacour JC, Zuber M, Favrole P, Pinel JF, Apoil M, Reiner P, Lefebvre C, Guerin P, Piot C, Rossi R, Dubois-Rande JL, Eicher JC, Meneveau N, Lusson JR, Bertrand B, Schleich JM, Godart F, Thambo JB, Leborgne L, Michel P, Pierard L, Turc G, Barthelet M, Charles-Nelson A, Weimar C, Moulin T, Juliard JM, Chatellier G and Investigators C. Patent Foramen Ovale Closure or Anticoagulation vs. Antiplatelets after Stroke. *N Engl J Med*. 2017;377:1011-1021.
74. Carroll JD, Saver JL, Thaler DE, Smalling RW, Berry S, MacDonald LA, Marks DS, Tirschwell DL and Investigators R. Closure of patent foramen ovale versus medical therapy after cryptogenic stroke. *N Engl J Med*. 2013;368:1092-100.
75. Furlan AJ, Reisman M, Massaro J, Mauri L, Adams H, Albers GW, Felberg R, Herrmann H, Kar S, Landzberg M, Raizner A, Wechsler L and Investigators CI. Closure or medical therapy for cryptogenic stroke with patent foramen ovale. *N Engl J Med*. 2012;366:991-9.
76. Meier B, Kalesan B, Mattle HP, Khattab AA, Hildick-Smith D, Dudek D, Andersen G, Ibrahim R, Schuler G, Walton AS, Wahl A, Windecker S, Juni P and Investigators PCT. Percutaneous closure of patent foramen ovale in cryptogenic embolism. *N Engl J Med*. 2013;368:1083-91.
77. Barnett HJ, Taylor DW, Eliasziw M, Fox AJ, Ferguson GG, Haynes RB, Rankin RN, Clagett GP, Hachinski VC, Sackett DL, Thorpe KE, Meldrum HE and Spence JD. Benefit of carotid endarterectomy in patients with symptomatic moderate or severe stenosis. North American Symptomatic Carotid Endarterectomy Trial Collaborators. *N Engl J Med*. 1998;339:1415-25.
78. Bekwelem W, Jensen PN, Norby FL, Soliman EZ, Agarwal SK, Lip GY, Pan W, Folsom AR, Longstreth WT, Jr., Alonso A, Heckbert SR and Chen LY. Carotid Atherosclerosis and Stroke in Atrial Fibrillation: The Atherosclerosis Risk in Communities Study. *Stroke*. 2016;47:1643-6.
79. North American Symptomatic Carotid Endarterectomy Trial C, Barnett HJM, Taylor DW, Haynes RB, Sackett DL, Peerless SJ, Ferguson GG, Fox AJ, Rankin RN, Hachinski VC, Wiebers DO and Eliasziw M. Beneficial effect of carotid endarterectomy in symptomatic patients with high-grade carotid stenosis. *N Engl J Med*. 1991;325:445-53.
80. Halliday A, Harrison M, Hayter E, Kong X, Mansfield A, Marro J, Pan H, Peto R, Potter J, Rahimi K, Rau A, Robertson S, Streifler J, Thomas D and Asymptomatic Carotid Surgery Trial Collaborative G. 10-year stroke prevention after successful carotid endarterectomy for asymptomatic stenosis (ACST-1): a multicentre randomised trial. *Lancet*. 2010;376:1074-84.
81. Hart RG, Sharma M, Mundl H, Kasner SE, Bangdiwala SI, Berkowitz SD, Swaminathan B, Lavados P, Wang Y, Wang Y, Davalos A, Shamalov N, Mikulik R, Cunha L, Lindgren A, Arauz A, Lang W, Czlonkowska A, Eckstein J, Gagliardi RJ, Amarenco P, Ameriso SF, Tatlisumak T, Veltkamp R, Hankey GJ, Toni D, Bereczki D, Uchiyama S, Ntaios G, Yoon BW, Brouns R, Endres M, Muir KW, Bornstein N, Ozturk S, O'Donnell MJ, De Vries Basson MM, Pare G, Pater C, Kirsch B, Sheridan P, Peters G, Weitz JI, Peacock WF, Shoamanesh A, Benavente OR, Joyner C, Themeles E, Connolly SJ and Investigators NE. Rivaroxaban for Stroke Prevention after Embolic Stroke of Undetermined Source. *N Engl J Med*. 2018;378:2191-2201.

82. Diener HC, Sacco RL, Easton JD, Granger CB, Bernstein RA, Uchiyama S, Kreuzer J, Cronin L, Cotton D, Grauer C, Brueckmann M, Chernyatina M, Donnan G, Ferro JM, Grond M, Kallmunzer B, Krupinski J, Lee BC, Lemmens R, Masjuan J, Odinak M, Saver JL, Schellinger PD, Toni D, Toyoda K, Committee R-SES and Investigators. Dabigatran for Prevention of Stroke after Embolic Stroke of Undetermined Source. *N Engl J Med*. 2019;380:1906-1917.
83. Ntaios G, Swaminathan B, Berkowitz SD, Gagliardi RJ, Lang W, Siegler JE, Lavados P, Mundl H, Bornstein N, Meseguer E, Amarenco P, Cucchiara B, Camps-Renom P, Makaritsis K, Korompoki E, Papavasileiou V, Marti-Fabregas J, Milionis H, Vemmos K, Connolly SJ, Hart RG and Investigators NE. Efficacy and Safety of Rivaroxaban Versus Aspirin in Embolic Stroke of Undetermined Source and Carotid Atherosclerosis. *Stroke*. 2019;50:2477-2485.
84. Perera KS, Ng KKH, Nayar S, Catanese L, Dyal L, Sharma M, Connolly SJ, Yusuf S, Bosch J, Eikelboom JW and Hart RG. Association Between Low-Dose Rivaroxaban With or Without Aspirin and Ischemic Stroke Subtypes: A Secondary Analysis of the COMPASS Trial. *JAMA Neurol*. 2019.
85. Elkind MS. Stroke Etiologic Classification-Moving From Prediction to Precision. *JAMA Neurol*. 2017;74:388-390.
86. Longstreth WT, Jr., Kronmal RA, Thompson JL, Christenson RH, Levine SR, Gross R, Brey RL, Buchsbaum R, Elkind MS, Tirschwell DL, Seliger SL, Mohr JP and deFilippi CR. Amino terminal pro-B-type natriuretic peptide, secondary stroke prevention, and choice of antithrombotic therapy. *Stroke*. 2013;44:714-9.
87. Zannad F, Anker SD, Byra WM, Cleland JGF, Fu M, Gheorghiade M, Lam CSP, Mehra MR, Neaton JD, Nessel CC, Spiro TE, van Veldhuisen DJ, Greenberg B and Investigators CH. Rivaroxaban in Patients with Heart Failure, Sinus Rhythm, and Coronary Disease. *N Engl J Med*. 2018;379:1332-1342.
88. Kamel H and Healey JS. Cardioembolic Stroke. *Circulation Research*. 2017;120:514-526.
89. Watson T, Shantsila E and Lip GYH. Mechanisms of thrombogenesis in atrial fibrillation: Virchow's triad revisited. *The Lancet*. 2009;373:155-166.
90. Watson T, Shantsila E and Lip GY. Mechanisms of thrombogenesis in atrial fibrillation: Virchow's triad revisited. *Lancet*. 2009;373:155-66.
91. Hamatani Y, Ogawa H, Takabayashi K, Yamashita Y, Takagi D, Esato M, Chun Y-H, Tsuji H, Wada H, Hasegawa K, Abe M, Lip GYH and Akao M. Left atrial enlargement is an independent predictor of stroke and systemic embolism in patients with non-valvular atrial fibrillation. *Scientific Reports*. 2016;6:31042.
92. Tiwari S, Løchen ML, Jacobsen BK, Hopstock LA, Nyrnes A, Njølstad I, Mathiesen EB and Schirmer H. CHA2DS2-VASc score, left atrial size and atrial fibrillation as stroke risk factors in the Tromsø Study. *Open Heart*. 2016;3:e000439.
93. Benjamin Emelia J, D'Agostino Ralph B, Belanger Albert J, Wolf Philip A and Levy D. Left Atrial Size and the Risk of Stroke and Death. *Circulation*. 1995;92:835-841.
94. Lai CL, Chien KL, Hsu HC, Su TC, Chen MF and Lee YT. Left atrial dimension and risk of stroke in women without atrial fibrillation: the Chin-Shan Community Cardiovascular Cohort study. *Echocardiography*. 2011;28:1054-60.

95. Bouzas-Mosquera A, Broullon FJ, Alvarez-Garcia N, Mendez E, Peteiro J, Gandara-Sambade T, Prada O, Mosquera VX and Castro-Beiras A. Left atrial size and risk for all-cause mortality and ischemic stroke. *CMAJ*. 2011;183:E657-64.
96. Pierdomenico SD, Pierdomenico AM, Di Carlo S, Di Tommaso R and Cuccurullo F. Left atrial enlargement and risk of ischemic stroke in elderly treated hypertensive patients. *Am J Hypertens*. 2014;27:1179-84.
97. Di Tullio MR, Sacco RL, Sciacca RR and Homma S. Left atrial size and the risk of ischemic stroke in an ethnically mixed population. *Stroke*. 1999;30:2019-24.
98. Kim BS, Lee HJ, Kim JH, Jang HS, Bae BS, Kang HJ, Lee BR and Jung BC. Relationship between left atrial size and stroke in patients with sinus rhythm and preserved systolic function. *Korean J Intern Med*. 2009;24:24-32.
99. Piotrowski G, Banach M, Gerdts E, Mikhailidis DP, Hannam S, Gawor R, Stasiak A, Rysz J and Gawor Z. Left atrial size in hypertension and stroke. *J Hypertens*. 2011;29:1988-93.
100. Azemi T, Rabdiya VM, Ayirala SR, McCullough LD and Silverman DI. Left Atrial Strain Is Reduced in Patients with Atrial Fibrillation, Stroke or TIA, and Low Risk CHADS2 Scores. *Journal of the American Society of Echocardiography*. 2012;25:1327-1332.
101. Leung M, van Rosendael PJ, Abou R, Ajmone Marsan N, Leung DY, Delgado V and Bax JJ. Left atrial function to identify patients with atrial fibrillation at high risk of stroke: new insights from a large registry. *European Heart Journal*. 2017;39:1416-1425.
102. Ciuffo L, Inoue YY, Tao S, Gucuk Ipek E, Balouch M, Lima JAC, Nazarian S, Spragg DD, Marine JE, Berger RD, Calkins H and Ashikaga H. Mechanical dyssynchrony of the left atrium during sinus rhythm is associated with history of stroke in patients with atrial fibrillation. *European Heart Journal - Cardiovascular Imaging*. 2017;19:433-441.
103. Inoue YY, Alissa A, Khurram IM, Fukumoto K, Habibi M, Venkatesh BA, Zimmerman SL, Nazarian S, Berger RD, Calkins H, Lima JA and Ashikaga H. Quantitative tissue-tracking cardiac magnetic resonance (CMR) of left atrial deformation and the risk of stroke in patients with atrial fibrillation. *J Am Heart Assoc*. 2015;4.
104. Chimowitz MI, DeGeorgia MA, Poole RM, Hepner A and Armstrong WM. Left atrial spontaneous echo contrast is highly associated with previous stroke in patients with atrial fibrillation or mitral stenosis. *Stroke*. 1993;24:1015-9.
105. Leung DY, Black IW, Cranney GB, Hopkins AP and Walsh WF. Prognostic implications of left atrial spontaneous echo contrast in nonvalvular atrial fibrillation. *J Am Coll Cardiol*. 1994;24:755-62.
106. Zhao Y, Ji L, Liu J, Wu J, Wang Y, Shen S, Guo S, Jian R, Chen G, Wei X, Liao W, Kutty S, Liao Y and Bin J. Intensity of Left Atrial Spontaneous Echo Contrast as a Correlate for Stroke Risk Stratification in Patients with Nonvalvular Atrial Fibrillation. *Sci Rep*. 2016;6:27650.
107. Transesophageal echocardiographic correlates of thromboembolism in high-risk patients with nonvalvular atrial fibrillation. The Stroke Prevention in Atrial Fibrillation Investigators Committee on Echocardiography. *Ann Intern Med*. 1998;128:639-47.

108. Sadanandan S and Sherrid MV. Clinical and echocardiographic characteristics of left atrial spontaneous echo contrast in sinus rhythm. *J Am Coll Cardiol*. 2000;35:1932-8.
109. Taina M, Sipola P, Muuronen A, Hedman M, Mustonen P, Kantanen AM, Jäkälä P and Vanninen R. Determinants of left atrial appendage volume in stroke patients without chronic atrial fibrillation. *PLoS One*. 2014;9:e90903.
110. Kimura T, Takatsuki S, Inagawa K, Katsumata Y, Nishiyama T, Nishiyama N, Fukumoto K, Aizawa Y, Tanimoto Y, Tanimoto K, Jinzaki M and Fukuda K. Anatomical characteristics of the left atrial appendage in cardiogenic stroke with low CHADS2 scores. *Heart Rhythm*. 2013;10:921-925.
111. Basu-Ray I, Sudhakar D, Schwing G, Monlezun D, Zhang L, Shah SK, Pujara D, Ting K, Rafeh NA, Ali G, Cassidy M, Ellenbogen K, Levine G, Lam W, Mathuria N, Saeed M, Bunch J, Martin-Schild S, Gold M, Aryana A, Razavi M and Rasekh A. Complex Left Atrial Appendage Morphology Is an Independent Risk Factor for Cryptogenic Ischemic Stroke. *Frontiers in Cardiovascular Medicine*. 2018;5.
112. Goldman ME, Pearce LA, Hart RG, Zabalgoitia M, Asinger RW, Safford R and Halperin JL. Pathophysiologic correlates of thromboembolism in nonvalvular atrial fibrillation: I. Reduced flow velocity in the left atrial appendage (The Stroke Prevention in Atrial Fibrillation [SPAF-III] study). *J Am Soc Echocardiogr*. 1999;12:1080-7.
113. Lee JM, Shim J, Uhm JS, Kim YJ, Lee HJ, Pak HN, Lee MH and Joung B. Impact of increased orifice size and decreased flow velocity of left atrial appendage on stroke in nonvalvular atrial fibrillation. *Am J Cardiol*. 2014;113:963-9.
114. Di Biase L, Mohanty S, Trivedi C, Romero J, Natale V, Briceno D, Gadiyaram V, Couts L, Gianni C, Al-Ahmad A, Burkhardt JD, Gallinghouse GJ, Horton R, Hranitzky PM, Sanchez JE and Natale A. Stroke Risk in Patients With Atrial Fibrillation Undergoing Electrical Isolation of the Left Atrial Appendage. *J Am Coll Cardiol*. 2019;74:1019-1028.
115. Ozer N, Tokgözoğlu L, Ovünç K, Kabakçi G, Aksöyek S, Aytemir K and Kes S. Left atrial appendage function in patients with cardioembolic stroke in sinus rhythm and atrial fibrillation. *J Am Soc Echocardiogr*. 2000;13:661-5.
116. Lee JM, Shim J, Uhm J-S, Kim YJ, Lee H-J, Pak H-N, Lee M-H and Joung B. Impact of Increased Orifice Size and Decreased Flow Velocity of Left Atrial Appendage on Stroke in Nonvalvular Atrial Fibrillation. *The American Journal of Cardiology*. 2014;113:963-969.
117. Zuo K, Sun L, Yang X, Lyu X and Li K. Correlation between cardiac rhythm, left atrial appendage flow velocity, and CHA2DS2-VASc score: Study based on transesophageal echocardiography and 2-dimensional speckle tracking. *Clinical Cardiology*. 2017;40:120-125.
118. King JB, Azadani PN, Suksaranjit P, Bress AP, Witt DM, Han FT, Chelu MG, Silver MA, Biskupiak J, Wilson BD, Morris AK, Kholmovski EG and Marrouche N. Left Atrial Fibrosis and Risk of Cerebrovascular and Cardiovascular Events in Patients With Atrial Fibrillation. *J Am Coll Cardiol*. 2017;70:1311-1321.
119. Tandon K, Tirschwell D, Longstreth WT, Jr., Smith B and Akoum N. Embolic stroke of undetermined source correlates to atrial fibrosis without atrial fibrillation. *Neurology*. 2019;93:e381-e387.

120. Kim Y, Kim TJ and Lee SH. Cardiac wall motion abnormality as a predictor for undetermined stroke with embolic lesion-pattern. *Clin Neurol Neurosurg*. 2020;191:105677.
121. Di Tullio MR, Qian M, Thompson JL, Labovitz AJ, Mann DL, Sacco RL, Pullicino PM, Freudenberger RS, Teerlink JR, Graham S, Lip GY, Levin B, Mohr JP, Buchsbaum R, Estol CJ, Lok DJ, Ponikowski P, Anker SD, Homma S and Investigators W. Left Ventricular Ejection Fraction and Risk of Stroke and Cardiac Events in Heart Failure: Data From the Warfarin Versus Aspirin in Reduced Ejection Fraction Trial. *Stroke*. 2016;47:2031-7.
122. Hays Allison G, Sacco Ralph L, Rundek T, Sciacca Robert R, Jin Z, Liu R, Homma S and Di Tullio Marco R. Left Ventricular Systolic Dysfunction and the Risk of Ischemic Stroke in a Multiethnic Population. *Stroke*. 2006;37:1715-1719.
123. Seo JY, Lee KB, Lee JG, Kim JS, Roh H, Ahn MY, Park BW and Hyon MS. Implication of left ventricular diastolic dysfunction in cryptogenic ischemic stroke. *Stroke*. 2014;45:2757-61.
124. Ishikawa S, Sugioka K, Sakamoto S, Fujita S, Ito A, Norioka N, Iwata S, Nakagawa M, Takagi M, Miki Y, Ueda M and Yoshiyama M. Relationship between tissue Doppler measurements of left ventricular diastolic function and silent brain infarction in patients with non-valvular atrial fibrillation. *Eur Heart J Cardiovasc Imaging*. 2017;18:1245-1252.
125. Blomstrand P, Engvall M, Festin K, Lindstrom T, Lanne T, Maret E, Nystrom FH, Maret-Ouda J, Ostgren CJ and Engvall J. Left ventricular diastolic function, assessed by echocardiography and tissue Doppler imaging, is a strong predictor of cardiovascular events, superior to global left ventricular longitudinal strain, in patients with type 2 diabetes. *Eur Heart J Cardiovasc Imaging*. 2015;16:1000-7.
126. de Bruijn RF, Portegies ML, Leening MJ, Bos MJ, Hofman A, van der Lugt A, Niessen WJ, Vernooij MW, Franco OH, Koudstaal PJ and Ikram MA. Subclinical cardiac dysfunction increases the risk of stroke and dementia: the Rotterdam Study. *Neurology*. 2015;84:833-40.
127. Verdecchia P, Porcellati C, Reboldi G, Gattobigio R, Borgioni C, Pearson TA and Ambrosio G. Left ventricular hypertrophy as an independent predictor of acute cerebrovascular events in essential hypertension. *Circulation*. 2001;104:2039-44.
128. Di Tullio MR, Zwas DR, Sacco RL, Sciacca RR and Homma S. Left ventricular mass and geometry and the risk of ischemic stroke. *Stroke*. 2003;34:2380-4.
129. Costanzo P, Savarese G, Rosano G, Musella F, Casaretti L, Vassallo E, Paolillo S, Marsico F, Rengo G, Leosco D and Perrone-Filardi P. Left ventricular hypertrophy reduction and clinical events. A meta-regression analysis of 14 studies in 12,809 hypertensive patients. *Int J Cardiol*. 2013;167:2757-64.
130. Bluemke DA, Kronmal RA, Lima JA, Liu K, Olson J, Burke GL and Folsom AR. The relationship of left ventricular mass and geometry to incident cardiovascular events: the MESA (Multi-Ethnic Study of Atherosclerosis) study. *J Am Coll Cardiol*. 2008;52:2148-55.
131. Bouzas-Mosquera A, Broullon FJ, Alvarez-Garcia N, Peteiro J, Mosquera VX and Castro-Beiras A. Association of left ventricular mass with all-cause mortality, myocardial infarction and stroke. *PLoS One*. 2012;7:e45570.

132. Thomas L and Abhayaratna WP. Left Atrial Reverse Remodeling: Mechanisms, Evaluation, and Clinical Significance. *JACC Cardiovasc Imaging*. 2017;10:65-77.
133. Delgado V, Di Biase L, Leung M, Romero J, Tops LF, Casadei B, Marrouche N and Bax JJ. Structure and Function of the Left Atrium and Left Atrial Appendage: AF and Stroke Implications. *Journal of the American College of Cardiology*. 2017;70:3157-3172.
134. Leung DY, Boyd A, Ng AA, Chi C and Thomas L. Echocardiographic evaluation of left atrial size and function: Current understanding, pathophysiologic correlates, and prognostic implications. *American Heart Journal*. 2008;156:1056-1064.
135. Hoit BD. Left Atrial Size and Function: Role in Prognosis. *Journal of the American College of Cardiology*. 2014;63:493-505.
136. Habibi M, Samiei S, Ambale Venkatesh B, Opdahl A, Helle-Valle TM, Zareian M, Almeida AL, Choi EY, Wu C, Alonso A, Heckbert SR, Bluemke DA and Lima JA. Cardiac Magnetic Resonance-Measured Left Atrial Volume and Function and Incident Atrial Fibrillation: Results From MESA (Multi-Ethnic Study of Atherosclerosis). *Circ Cardiovasc Imaging*. 2016;9.
137. Gan GCH, Ferkh A, Boyd A and Thomas L. Left atrial function: evaluation by strain analysis. *Cardiovasc Diagn Ther*. 2018;8:29-46.
138. Siebermair J, Kholmovski EG and Marrouche N. Assessment of Left Atrial Fibrosis by Late Gadolinium Enhancement Magnetic Resonance Imaging: Methodology and Clinical Implications. *JACC: Clinical Electrophysiology*. 2017;3:791-802.
139. Akoum N, Fernandez G, Wilson B, McGann C, Kholmovski E and Marrouche N. Association of atrial fibrosis quantified using LGE-MRI with atrial appendage thrombus and spontaneous contrast on transesophageal echocardiography in patients with atrial fibrillation. *J Cardiovasc Electrophysiol*. 2013;24:1104-9.
140. Yaghi S, Song C, Gray WA, Furie KL, Elkind MSV and Kamel H. Left Atrial Appendage Function and Stroke Risk. *Stroke*. 2015;46:3554-3559.
141. Sadanandan S and Sherrid MV. Clinical and echocardiographic characteristics of left atrial spontaneous echo contrast in sinus rhythm. *Journal of the American College of Cardiology*. 2000;35:1932-1938.
142. Ammash N, Konik EA, McBane RD, Chen D, Tange JI, Grill DE, Herges RM, McLeod TG, Friedman PA and Wysokinski WE. Left atrial blood stasis and Von Willebrand factor-ADAMTS13 homeostasis in atrial fibrillation. *Arterioscler Thromb Vasc Biol*. 2011;31:2760-6.
143. Black IW, Chesterman CN, Hopkins AP, Lee LC, Chong BH and Walsh WF. Hematologic correlates of left atrial spontaneous echo contrast and thromboembolism in nonvalvular atrial fibrillation. *J Am Coll Cardiol*. 1993;21:451-7.
144. Fatkin D, Loupas T, Low J and Feneley M. Inhibition of red cell aggregation prevents spontaneous echocardiographic contrast formation in human blood. *Circulation*. 1997;96:889-96.
145. Briley DP, Giraud GD, Beamer NB, Spear EM, Grauer SE, Edwards JM, Clark WM, Sexton GJ and Coull BM. Spontaneous echo contrast and hemorheologic abnormalities in cerebrovascular disease. *Stroke*. 1994;25:1564-9.

146. Zotz RJ, Muller M, Genth-Zotz S and Darius H. Spontaneous echo contrast caused by platelet and leukocyte aggregates? *Stroke*. 2001;32:1127-33.
147. Fatkin D, Kelly RP and Feneley MP. Relations between left atrial appendage blood flow velocity, spontaneous echocardiographic contrast and thromboembolic risk in vivo. *J Am Coll Cardiol*. 1994;23:961-9.
148. Thomas L, Marwick TH, Popescu BA, Donal E and Badano LP. Left Atrial Structure and Function, and Left Ventricular Diastolic Dysfunction: JACC State-of-the-Art Review. *Journal of the American College of Cardiology*. 2019;73:1961-1977.
149. Markl M, Carr M, Ng J, Lee DC, Jarvis K, Carr J and Goldberger JJ. Assessment of left and right atrial 3D hemodynamics in patients with atrial fibrillation: a 4D flow MRI study. *Int J Cardiovasc Imaging*. 2016;32:807-15.
150. Kilner PJ, Yang GZ, Wilkes AJ, Mohiaddin RH, Firmin DN and Yacoub MH. Asymmetric redirection of flow through the heart. *Nature*. 2000;404:759-61.
151. Yazdani A, Li H, Humphrey JD and Karniadakis GE. A General Shear-Dependent Model for Thrombus Formation. *PLoS Comput Biol*. 2017;13:e1005291.
152. Gulan U, Saguner A, Akdis D, Gotschy A, Manka R, Brunckhorst C, Holzner M and Duru F. Investigation of Atrial Vortices Using a Novel Right Heart Model and Possible Implications for Atrial Thrombus Formation. *Sci Rep*. 2017;7:16772.
153. Son JW, Park WJ, Choi JH, Houle H, Vannan MA, Hong GR and Chung N. Abnormal left ventricular vortex flow patterns in association with left ventricular apical thrombus formation in patients with anterior myocardial infarction: a quantitative analysis by contrast echocardiography. *Circ J*. 2012;76:2640-6.
154. Biasetti J, Hussain F and Gasser TC. Blood flow and coherent vortices in the normal and aneurysmatic aortas: a fluid dynamical approach to intra-luminal thrombus formation. *J R Soc Interface*. 2011;8:1449-61.
155. Garcia J, Sheitt H, Bristow MS, Lydell C, Howarth AG, Heydari B, Prato FS, Drangova M, Thornhill RE, Nery P, Wilton SB, Skanes A and White JA. Left atrial vortex size and velocity distributions by 4D flow MRI in patients with paroxysmal atrial fibrillation: Associations with age and CHA2 DS2 -VASc risk score. *Journal of magnetic resonance imaging : JMRI*. 2019.
156. Lip GY. The CHA(2)DS(2)-VASc score for stroke risk stratification in patients with atrial fibrillation: a brief history. *Eur Heart J*. 2015;36:2880-5.
157. Wijesurendra RS, Liu A, Eichhorn C, Ariga R, Levelt E, Clarke WT, Rodgers CT, Karamitsos TD, Bashir Y, Ginks M, Rajappan K, Betts T, Ferreira VM, Neubauer S and Casadei B. Lone Atrial Fibrillation Is Associated With Impaired Left Ventricular Energetics That Persists Despite Successful Catheter Ablation. *Circulation*. 2016;134:1068-1081.
158. Truong VT, Palmer C, Wolking S, Sheets B, Young M, Ngo TNM, Taylor M, Nagueh SF, Zareba KM, Raman S and Mazur W. Normal left atrial strain and strain rate using cardiac magnetic resonance feature tracking in healthy volunteers. *Eur Heart J Cardiovasc Imaging*. 2019.
159. Gong IY, Ong G, Brezden-Masley C, Dhir V, Deva DP, Chan KKW, Graham JJ, Chow CM, Thavendiranathan P, Dai D, Ng MY, Barfett JJ, Connelly KA and Yan AT. Early diastolic strain rate measurements by cardiac MRI in breast cancer patients treated with trastuzumab: a longitudinal study. *Int J Cardiovasc Imaging*. 2019;35:653-662.
160. Chirinos JA, Sardana M, Ansari B, Satija V, Kuriakose D, Edelstein I, Oldland G, Miller R, Gaddam S, Lee J, Suri A and Akers SR. Left Atrial Phasic Function by

Cardiac Magnetic Resonance Feature Tracking Is a Strong Predictor of Incident Cardiovascular Events. *Circ Cardiovasc Imaging*. 2018;11:e007512.
161. Norris DG and Hutchison JM. Concomitant magnetic field gradients and their effects on imaging at low magnetic field strengths. *Magn Reson Imaging*. 1990;8:33-7.
162. Purvis LAB, Clarke WT, Biasiolli L, Valkovic L, Robson MD and Rodgers CT. OXSA: An open-source magnetic resonance spectroscopy analysis toolbox in MATLAB. *PLoS One*. 2017;12:e0185356.
163. Loecher M, Schrauben E, Johnson KM and Wieben O. Phase unwrapping in 4D MR flow with a 4D single-step laplacian algorithm. *Journal of magnetic resonance imaging : JMRI*. 2016;43:833-42.
164. A Caprihan SAA, E Benitez-Read. Flow-velocity imaging from linear regression of phase images with techniques for reducing eddy-current effects. *Journal of Magnetic Resonance*. 1990;90:71-89.
165. Bustamante M, Gupta V, Carlhall CJ and Ebbers T. Improving visualization of 4D flow cardiovascular magnetic resonance with four-dimensional angiographic data: generation of a 4D phase-contrast magnetic resonance CardioAngiography (4D PC-MRCA). *J Cardiovasc Magn Reson*. 2017;19:47.
166. Elbaz MS, Calkoen EE, Westenberg JJ, Lelieveldt BP, Roest AA and van der Geest RJ. Vortex flow during early and late left ventricular filling in normal subjects: quantitative characterization using retrospectively-gated 4D flow cardiovascular magnetic resonance and three-dimensional vortex core analysis. *J Cardiovasc Magn Reson*. 2014;16:78.
167. Suwa K, Saitoh T, Takehara Y, Sano M, Nobuhara M, Saotome M, Urushida T, Katoh H, Satoh H, Sugiyama M, Wakayama T, Alley M, Sakahara H and Hayashi H. Characteristics of intra-left atrial flow dynamics and factors affecting formation of the vortex flow - analysis with phase-resolved 3-dimensional cine phase contrast magnetic resonance imaging. *Circ J*. 2015;79:144-52.
168. Eriksson J, Carlhall CJ, Dyverfeldt P, Engvall J, Bolger AF and Ebbers T. Semi-automatic quantification of 4D left ventricular blood flow. *J Cardiovasc Magn Reson*. 2010;12:9.
169. Fyrenius A, Wigstrom L, Ebbers T, Karlsson M, Engvall J and Bolger AF. Three dimensional flow in the human left atrium. *Heart*. 2001;86:448-55.
170. Ong F, Uecker M, Tariq U, Hsiao A, Alley MT, Vasanawala SS and Lustig M. Robust 4D flow denoising using divergence-free wavelet transform. *Magn Reson Med*. 2015;73:828-42.
171. Pal P ZZ, Lin BA, Dione D, Sinusas AJ, Sampath S. . Flow vortex quantification in the left atrium. *J Cardiovasc Magn Reson* 2012;14(Suppl 1):W23
172. Kim WY, Walker PG, Pedersen EM, Poulsen JK, Oyre S, Houlind K and Yoganathan AP. Left ventricular blood flow patterns in normal subjects: a quantitative analysis by three-dimensional magnetic resonance velocity mapping. *J Am Coll Cardiol*. 1995;26:224-38.
173. Feigin VL, Norrving B and Mensah GA. Global Burden of Stroke. *Circ Res*. 2017;120:439-448.
174. Handke M, Harloff A, Hetzel A, Olschewski M, Bode C and Geibel A. Left atrial appendage flow velocity as a quantitative surrogate parameter for thromboembolic risk: determinants and relationship to spontaneous echocontrast

and thrombus formation--a transesophageal echocardiographic study in 500 patients with cerebral ischemia. *J Am Soc Echocardiogr*. 2005;18:1366-72.
175. Stoddard MF, Dawkins PR, Prince CR and Ammash NM. Left atrial appendage thrombus is not uncommon in patients with acute atrial fibrillation and a recent embolic event: a transesophageal echocardiographic study. *J Am Coll Cardiol*. 1995;25:452-9.
176. Dyverfeldt P, Bissell M, Barker AJ, Bolger AF, Carlhall CJ, Ebbers T, Francios CJ, Frydrychowicz A, Geiger J, Giese D, Hope MD, Kilner PJ, Kozerke S, Myerson S, Neubauer S, Wieben O and Markl M. 4D flow cardiovascular magnetic resonance consensus statement. *J Cardiovasc Magn Reson*. 2015;17:72.
177. Healey JS, Alings M, Ha A, Leong-Sit P, Birnie DH, de Graaf JJ, Freericks M, Verma A, Wang J, Leong D, Dokainish H, Philippon F, Barake W, McIntyre WF, Simek K, Hill MD, Mehta SR, Carlson M, Smeele F, Pandey AS, Connolly SJ and Investigators A-I. Subclinical Atrial Fibrillation in Older Patients. *Circulation*. 2017;136:1276-1283.
178. Wijesurendra RS, Liu A, Notaristefano F, Ntusi NAB, Karamitsos TD, Bashir Y, Ginks M, Rajappan K, Betts TR, Jerosch-Herold M, Ferreira VM, Neubauer S and Casadei B. Myocardial Perfusion Is Impaired and Relates to Cardiac Dysfunction in Patients With Atrial Fibrillation Both Before and After Successful Catheter Ablation. *J Am Heart Assoc*. 2018;7:e009218.
179. Bhuva N, Bulluck H, Captur G, Treibel A, Augusto B, Knott D, Seraphim A, Hughes D, Moon C, Manisty H, Lau C, Davies H, Ye Y, Culotta V, Petersen E, Rueckert D, Bai W, McAlindon E, Bucciarelli-Ducci C, Swoboda P, Greenwood P, Cole D and Edwards C. A Multicenter, Scan-Rescan, Human and Machine Learning CMR Study to Test Generalizability and Precision in Imaging Biomarker Analysis. *Circ Cardiovasc Imaging*. 2019;12:e009214.
180. Stoll VM, Loudon M, Eriksson J, Bissell MM, Dyverfeldt P, Ebbers T, Myerson SG, Neubauer S, Carlhall CJ and Hess AT. Test-retest variability of left ventricular 4D flow cardiovascular magnetic resonance measurements in healthy subjects. *J Cardiovasc Magn Reson*. 2018;20:15.
181. Nolan SP, Dixon SH, Jr., Fisher RD and Morrow AG. The influence of atrial contraction and mitral valve mechanics on ventricular filing. A study of instantaneous mitral valve flow in vivo. *Am Heart J*. 1969;77:784-91.
182. Skinner NS, Jr., Mitchell JH, Wallace AG and Sarnoff SJ. Hemodynamic Effects of Altering the Timing of Atrial Systole. *Am J Physiol*. 1963;205:499-503.
183. Harrison MR, Clifton GD, Pennell AT and DeMaria AN. Effect of heart rate on left ventricular diastolic transmitral flow velocity patterns assessed by Doppler echocardiography in normal subjects. *Am J Cardiol*. 1991;67:622-7.
184. Ishida Y, Meisner JS, Tsujioka K, Gallo JI, Yoran C, Frater RW and Yellin EL. Left ventricular filling dynamics: influence of left ventricular relaxation and left atrial pressure. *Circulation*. 1986;74:187-96.
185. Iliceto S, D'Ambrosio G, Marangelli V, Amico A, Di Biase M and Rizzon P. Echo-Doppler evaluation of the effects of heart rate increments on left atrial pump function in normal human subjects. *Eur Heart J*. 1991;12:345-51.
186. Martin RI, Pogoryelova O, Koref MS, Bourke JP, Teare MD and Keavney BD. Atrial fibrillation associated with ivabradine treatment: meta-analysis of randomised controlled trials. *Heart*. 2014;100:1506-10.

187. Koki Nakanishi MRDT, Min Qian, John L.P, Thompson, Arthur J. Labovitz, Douglas L. Mann, Ralph L. Sacco, Patrick M. Pullicino, Ronald S. Freudenberger, John R. Teerlink, Susan Graham, Gregory Y.H. Lip, Bruce Levin, Jay P. Mohr, Richard Buchsbaum, and Conrado J. Estol DJL, Piotr Ponikowski, Stefan D. Anker, Shunichi Homma, WARCEF Investigators Resting Heart Rate and Ischemic Stroke in Patients with Heart Failure *Cerebrovasc Dis 2017;44:43–50*. 2017.
188. Markl M, Lee DC, Ng J, Carr M, Carr J and Goldberger JJ. Left Atrial 4-Dimensional Flow Magnetic Resonance Imaging: Stasis and Velocity Mapping in Patients With Atrial Fibrillation. *Invest Radiol*. 2016;51:147-54.
189. Van Gelder IC, Healey JS, Crijns H, Wang J, Hohnloser SH, Gold MR, Capucci A, Lau CP, Morillo CA, Hobbelt AH, Rienstra M and Connolly SJ. Duration of device-detected subclinical atrial fibrillation and occurrence of stroke in ASSERT. *Eur Heart J*. 2017;38:1339-1344.
190. Lau DH, Nattel S, Kalman JM and Sanders P. Modifiable Risk Factors and Atrial Fibrillation. *Circulation*. 2017;136:583-596.
191. Khan IA. Atrial stunning: basics and clinical considerations. *International Journal of Cardiology*. 2003;92:113-128.
192. Romero J, Cao JJ, Garcia MJ and Taub CC. Cardiac imaging for assessment of left atrial appendage stasis and thrombosis. *Nature Reviews Cardiology*. 2014;11:470.
193. Tatu L, Moulin T, Bogousslavsky J and Duvernoy H. Arterial territories of the human brain: cerebral hemispheres. *Neurology*. 1998;50:1699-708.
194. Petersen SE, Aung N, Sanghvi MM, Zemrak F, Fung K, Paiva JM, Francis JM, Khanji MY, Lukaschuk E, Lee AM, Carapella V, Kim YJ, Leeson P, Piechnik SK and Neubauer S. Reference ranges for cardiac structure and function using cardiovascular magnetic resonance (CMR) in Caucasians from the UK Biobank population cohort. *J Cardiovasc Magn Reson*. 2017;19:18.
195. Arvidsson PM, Kovacs SJ, Toger J, Borgquist R, Heiberg E, Carlsson M and Arheden H. Vortex ring behavior provides the epigenetic blueprint for the human heart. *Sci Rep*. 2016;6:22021.
196. O'Brien JR. Shear-induced platelet aggregation. *Lancet*. 1990;335:711-3.
197. Taka T, Okano E, Seki J and Yamamoto J. Effects of clopidogrel on platelet activation and coagulation of non-anticoagulated rat blood under high shear stress. *Haemostasis*. 1999;29:189-96.
198. Jing J, Meng X, Zhao X, Liu L, Wang A, Pan Y, Li H, Wang D, Johnston SC, Wang Y and Wang Y. Dual Antiplatelet Therapy in Transient Ischemic Attack and Minor Stroke With Different Infarction Patterns: Subgroup Analysis of the CHANCE Randomized Clinical Trial. *JAMA Neurol*. 2018;75:711-719.
199. Soppitt GD and Mitchell JR. The effect of colchicine on human platelet behaviour. *J Atheroscler Res*. 1969;10:247-52.
200. Tardif JC, Kouz S, Waters DD, Bertrand OF, Diaz R, Maggioni AP, Pinto FJ, Ibrahim R, Gamra H, Kiwan GS, Berry C, Lopez-Sendon J, Ostadal P, Koenig W, Angoulvant D, Gregoire JC, Lavoie MA, Dube MP, Rhainds D, Provencher M, Blondeau L, Orfanos A, L'Allier PL, Guertin MC and Roubille F. Efficacy and Safety of Low-Dose Colchicine after Myocardial Infarction. *N Engl J Med*. 2019;381:2497-2505.
201. Chen Z, Venkat P, Seyfried D, Chopp M, Yan T and Chen J. Brain-Heart Interaction: Cardiac Complications After Stroke. *Circ Res*. 2017;121:451-468.

202. Al-Khaled M and Eggers J. MRI findings and stroke risk in TIA patients with different symptom durations. *Neurology*. 2013;80:1920-6.
203. Berg DD, Ruff CT, Jarolim P, Giugliano RP, Nordio F, Lanz HJ, Mercuri MF, Antman EM, Braunwald E and Morrow DA. Performance of the ABC Scores for Assessing the Risk of Stroke or Systemic Embolism and Bleeding in Patients With Atrial Fibrillation in ENGAGE AF-TIMI 48. *Circulation*. 2019;139:760-771.
204. Benjamin EJ, D'Agostino RB, Belanger AJ, Wolf PA and Levy D. Left atrial size and the risk of stroke and death. The Framingham Heart Study. *Circulation*. 1995;92:835-41.
205. Yaghi S, Moon YP, Mora-McLaughlin C, Willey JZ, Cheung K, Di Tullio MR, Homma S, Kamel H, Sacco RL and Elkind MS. Left atrial enlargement and stroke recurrence: the Northern Manhattan Stroke Study. *Stroke*. 2015;46:1488-93.
206. Jordan K, Yaghi S, Poppas A, Chang AD, Mac Grory B, Cutting S, Burton T, Jayaraman M, Tsivgoulis G, Sabeh MK, Merkler AE, Kamel H, Elkind MSV, Furie K and Song C. Left Atrial Volume Index Is Associated With Cardioembolic Stroke and Atrial Fibrillation Detection After Embolic Stroke of Undetermined Source. *Stroke*. 2019;50:1997-2001.
207. Yaghi S, Song C, Gray WA, Furie KL, Elkind MS and Kamel H. Left Atrial Appendage Function and Stroke Risk. *Stroke*. 2015;46:3554-9.